1-1-2014

A Bottom-Up Assembly Of Vascularized Bioartificial Constructs Using Ecm Based Microscale Modules

Ramkumar Tiruvannamalai Annamalai
Wayne State University,

A BOTTOM-UP ASSEMBLY OF VASCULARIZED BIOARTIFICIAL CONSTRUCTS USING ECM BASED MICROSCALE MODULES

by

RAMKUMAR TIRUVANNAMALAI ANNAMALAI

DISSERTATION

Submitted to the Graduate School of

Wayne State University,

Detroit, Michigan

in partial fulfillment of the requirements

for the degree of

DOCTOR OF PHILOSOPHY

2014

MAJOR: BIOMEDICAL ENGINEERING

Approved By:

Advisor **Date**

ACKNOWLEDGMENTS

I would like to express my deepest appreciation to Dr. Matthew for all the supervision, support and mentorship he has shown during my graduate school days. He has taught me the meaning of being an independent researcher. I would like to express my gratitude to Dr. Grimm, Dr. Ren, and Dr. Armant, for their time and suggestions in the preparation of this dissertation. I would also like to thank Dr. Berkowitz and Dr. Kamir of MICR who have provided great insight into the in-vitro and in-vivo imaging for my research. I believe their comments and advice will determine the direction of my future research. In addition a special thanks to Dr. Kavdia, Dr. Cavanaugh, Dr. Vande Vord, Ms. Murthy and all the other faculty members of the biomedical department for providing me with financial assistance and moral support during my graduate years.

I'd like to thank all my friends and colleagues in the Dr. Matthew's research group, especially Dr. Therese Bou-Akl, for all the help and support. I am thankful to my parents, and my family especially Sukanya Srinivasan for making me the person I am today. Also, I would like to acknowledge funding provided by National Science Foundation and Wayne State DIRCTR Award during my work.

TABLE OF CONTENTS

LIST OF TABLES

LIST OF FIGURES

CHAPTER: 1

1.1 Introduction

Tissue engineering (TE) aims to resolve the technical difficulties associated with the regeneration, repair or replacement of damaged organs and tissues. A primary goal of tissue engineering is to fabricate a 3D construct that can promote cell-cell interaction, extra cellular matrix (ECM) deposition and tissue level organization (Langer and Vacanti 1993). Accomplishing these prerequisites with the currently available conventional scaffolds and fabrication techniques still remains a challenge. Some of the tissue types that have been successfully engineered include skin (MacNeil 2007), bone (Zhang, Venugopal et al. 2008, Jones and Yang 2011, Hammouche, Hammouche et al. 2012) and cartilage (Vinatier, Bouffi et al. 2009, Hammouche, Hammouche et al. 2012, LaPorta, Richter et al. 2012). Significant success has also been achieved in nerve regeneration (Cunha, Panseri et al. 2011), corneal construction (Germain, Carrier et al. 2000, Lawrence, Marchant et al. 2009, Paquet, Larouche et al. 2010) and vascular tissue engineering (Ravi and Chaikof 2010); However, the success rate has been relatively low in engineering complex tissue types such as liver, lung, and kidney due to their complex architectures and metabolic activities.

1.2 Statement of Problem:

In conventional preformed scaffolds, the cell viability depends on diffusion of oxygen, nutrients and growth factors from the surrounding host tissues, and it is limited to 100-200 microns thickness at cell densities comparable to that of normal tissues (Carmeliet and Jain 2000). Hence in constructs with larger dimensions, efficient mass transfer and subsequent cell survival can be

achieved only by significantly reducing cell densities or by tolerating hypoxic conditions. Moreover, in a porous scaffold, uniform distribution throughout the construct is difficult to achieve, and the seeded cells will stay on the peripheral surface of the construct forming a thin peripheral layer. In addition, these scaffolds cannot facilitate incorporation of multiple cell types in a controlled manner. Hence the slow vascularization, mass transfer limitation, low cell density and non-uniform cell distribution, limits conventional methods from engineering large and more complex organs. Therefore, an innate structure that supports functional vascularization is imperative for engineering large tissues grafts.

1.3 Long Term Goal

Many strategies have been proposed to incorporate vascular structure that includes creating endothelial microchannels inside scaffolds (Hahn, Taite et al. 2006, Leslie-Barbick, Moon et al. 2009), surface modification and/or controlled releasing of pro-vasculogenic growth factor and cytokines (Nillesen, Geutjes et al. 2007, Chiu and Radisic 2010, Miyagi, Chiu et al. 2011), coculturing vascular cell types for microvessel formation (Jain 2003) etc. Despite their limited success, none of these approaches is able to incorporate an extensive vasculature as seen in natural organs. We propose to develop an advanced and efficient method for fabricating vascularized tissue constructs by assembling ECM based microscale modules. The long term goal of the project is to engineer functional tissues by establishing a technology foundation for subsequent rapid assembly of three-dimensional, tissue density constructs.

CHAPTER: 2

2.1 Relevant background:

Tissue Engineered Scaffolds: A TE construct consists of different combinations of various components broadly classified into biological components, material components and chemical factors. The biological component constitutes the cells that are the functional components of a tissue. The material component includes hydrogels and polymeric scaffolding materials like fibers, plastics and natural biomaterials. The material component guides various cellular functions such as cell growth, attachment, proliferation, differentiation etc., and it also provides the required mechanical stability for the construct. The chemical factors assist the biological components to perform the desired biological activity. Langer and Vacanti summarized the different strategies in engineering tissues into three broad categories (Langer and Vacanti 1993, Langer 2000) as follows:

1. *Cell substitutes:* This strategy involves replacement of non-functional cells in a defective host with healthy cells to perform essential functions. The transplanted cells can be from the same host (autogeneic), from a different host of the same species (allogeneic) or from a different species (xenogeneic) depending on the application. Even though this strategy can avoid invasive surgeries, immune rejection and poor cell performance limit its potential.
2. *Materials for autologous cell colonization:* This strategy involves transplantation of tissue growth inducing biomaterials to provide space for cell-based tissue regeneration, and controlled release of signaling molecules. The success of this strategy depends on the selection of suitable biomaterial, the development of fabrication techniques and the production of purified signaling molecules.

3. *Cell Seeded scaffolds and tissue models*: This strategy involves transplantation of in-vitro matured tissue constructs made by seeding healthy therapeutic cells in scaffolds. The cell-material construct can be extensively cultured in bioreactors under dynamic conditions. The scaffolding materials of constructs are made up of biocompatible natural materials like collagen, chitosan and hyaluronan and synthetic polymers like polylactic acid or polyglycolic acid (Hunt and Grover 2010). These tissue constructs apart from host implantation can also be used as extracorporeal devices.

The above-mentioned strategies can be employed alone or in combinations to achieve specific goals in various applications.

2.2 Specific Goals of Tissue Engineering:

TE is an alternative approach for organ transplantation and has the ability to control and accelerate the wound healing process by combining materials and cells that can support cell migration, growth factors release, cell activation etc. Defective and degenerating tissues can also be repaired or replaced with the help of TE. The other specific goal of TE is to deliver drugs to specific targets; for example, hormones such as insulin/glucagon can be released in the body in a controlled fashion using TE scaffolds, as a potential treatment for diabetes. Temporary substitution for specific functions of organs like kidney and liver can be achieved using TE. This has been a lifesaving tool for patients waiting for organ donors. Models of tissues, organs or any systems in our body can be manipulated in-vitro using TE, and this has led to quick and more accurate drug testing and toxicity analysis. The goals of TE along with some specific examples are summarized in Table 1.

TABLE 1: Goals of Tissue Engineering

S.NO	SPECIFIC GOALS	APPLICATION
1	Organ transplant alternative	Kidney, Liver, Bone, Urinary bladder
2	Wound Healing	Cornea, Skin, tendons
3	Replacing defective tissues	Substantia nigra in Parkinson's disease and other neurodegenerative diseases
4	Drug delivery	Diabetes (Insulin), Bronchitis (Bronchodilator)
5	Temporary organ substitutes	Liver, kidney (dialyzers)
6	In-vitro models	Drug testing, Toxicology analysis

2.3 Conventional Methods of Tissue Engineering

Conventional TE involves seeding healthy therapeutic cells in porous scaffolds to form tissue constructs (Langer and Vacanti 1993). The scaffolding material is biodegradable, and the cells are cultured in these preformed scaffolds that eventually degrade the material forming engineered tissues. The conventional tissue engineering method usually involves the following steps:

1. The suitable cell source has to be identified and expanded to a clinically significant number.
2. The suitable material (synthetic or natural) must be identified to serve as a tissue substrate; then, the material should be isolated, purified and molded for specific application.

3. The cells are later seeded into the substrates, and they can be cultured under dynamic or static conditions. The cell distribution in the scaffold has to be uniform in order to achieve optimal performance.
4. The construct is then implanted in-vivo. Depending on the metabolic rate of the cells and diffusion conditions, vascularization may be mandatory in some applications for tissue survival.

2.4 Current status of conventional tissue engineering:

Tissues and organs of almost every part of the human body has been attempted to engineer using this technology. Significant success has been achieved in many applications; for example, nerve regeneration and their functional recovery have been achieved using various TE strategies (Cunha, Panseri et al. 2010). Electrospun nano-scaffolds made of natural materials like chitosan and laminin, polyesters like PLA and PGS has been successfully employed to aid nerve regeneration (Cunha, Panseri et al. 2010). Human corneal reconstruction using tissue engineering is in final stages for human implantation (Germain, Carrier et al. 2000, Lawrence, Marchant et al. 2009, Paquet, Larouche et al. 2010). Several studies have also been focusing on tissue engineered heart valves, large blood vessels like aorta and smaller blood vessels. Seeding smooth muscle cells and endothelial cells in carefully designed scaffolds, and culturing them in pulsatile flow conditions have made tremendous progress in vascular TE (Ravi and Chaikof 2010, Villalona, Udelsman et al. 2010, Zhu, Cao et al. 2010).

Much effort has also been focused on engineering bone and cartilages for different parts of the skeletal system including hip, knee and facial bone and cartilage. Osteoblasts and chondrocytes seeded on different natural and synthetic scaffolds have shown to promote deposition of

extracellular matrix (ECM) components like glycosaminoglycans and collagen thereby improving the mechanical properties of the implant (Wang, He et al. 2010, Yang, Yin et al. 2010). Limited success has also been achieved in creating tissue-engineered tendons, liver, pancreas and other vital organs.

2.5 Disadvantages of conventional scaffolds:

In almost all the above mentioned applications, the cell viability solely depends on the diffusion of oxygen, nutrients and growth factors from the surrounding host tissues. Mass transfers in these engineered tissue constructs are limited to a thickness of 100-200 microns at cell densities comparable to that of normal tissues (Carmeliet and Jain 2000) (Refer Fig. 1). In tissue constructs with larger dimensions, efficient mass transfer and subsequent cell survival can be achieved only by significantly reducing cell densities or by tolerating hypoxic conditions. This has been a major cause for the failure in engineering larger tissues like liver and pancreas using conventional methods. Moreover, in a conventional scaffold, uniform distribution throughout the construct cannot be achieved. Usually the seeded cells will stay on the peripheral surface of the construct (Zhang and Suggs 2007) forming a thin peripheral layer, and it can prevent the infusion of cells from the surrounding host after implantation; furthermore, these scaffolds cannot facilitate incorporation of multiple cell types in a controlled manner.

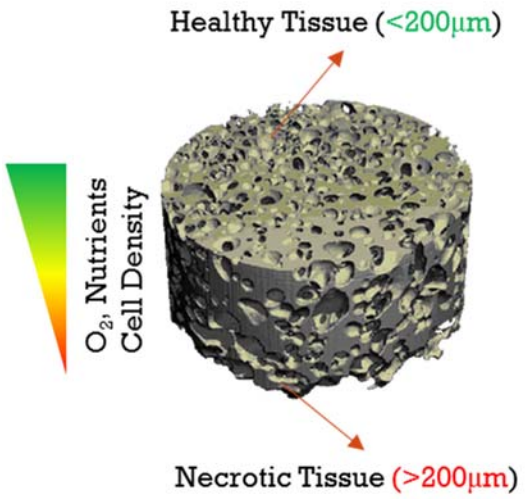

Figure 1: The Challenge: Assembling 3D Tissue.

Many studies have shown that the controlled co-culturing of multiple cell types can benefit each other in growth and cell regulation through endocrine and paracrine interactions (Cucina, Borrelli et al. 2003). However, this strategic multi layers cannot be implemented in a conventional scaffold. Hence, the slow vascularization, mass transfer limitation, low cell density and non-uniform cell distribution limit conventional methods from engineering large and more complex organs. A potential solution to these drawbacks can be attained through a modular tissue engineering approach.

2.6 Modular Tissue Engineering

Modular TE is a scalable strategy of assembling tissue constructs from microscale modules containing both parenchymal and vascular components (McGuigan and Sefton 2006). This approach enables fabrication of the vascularized 3D construct with uniform cell densities and also can incorporate multiple cell types. Using this modular approach one can achieve the common

goals of TE mentioned earlier and avoid the common limitations of conventional scaffolds and fabrication techniques.

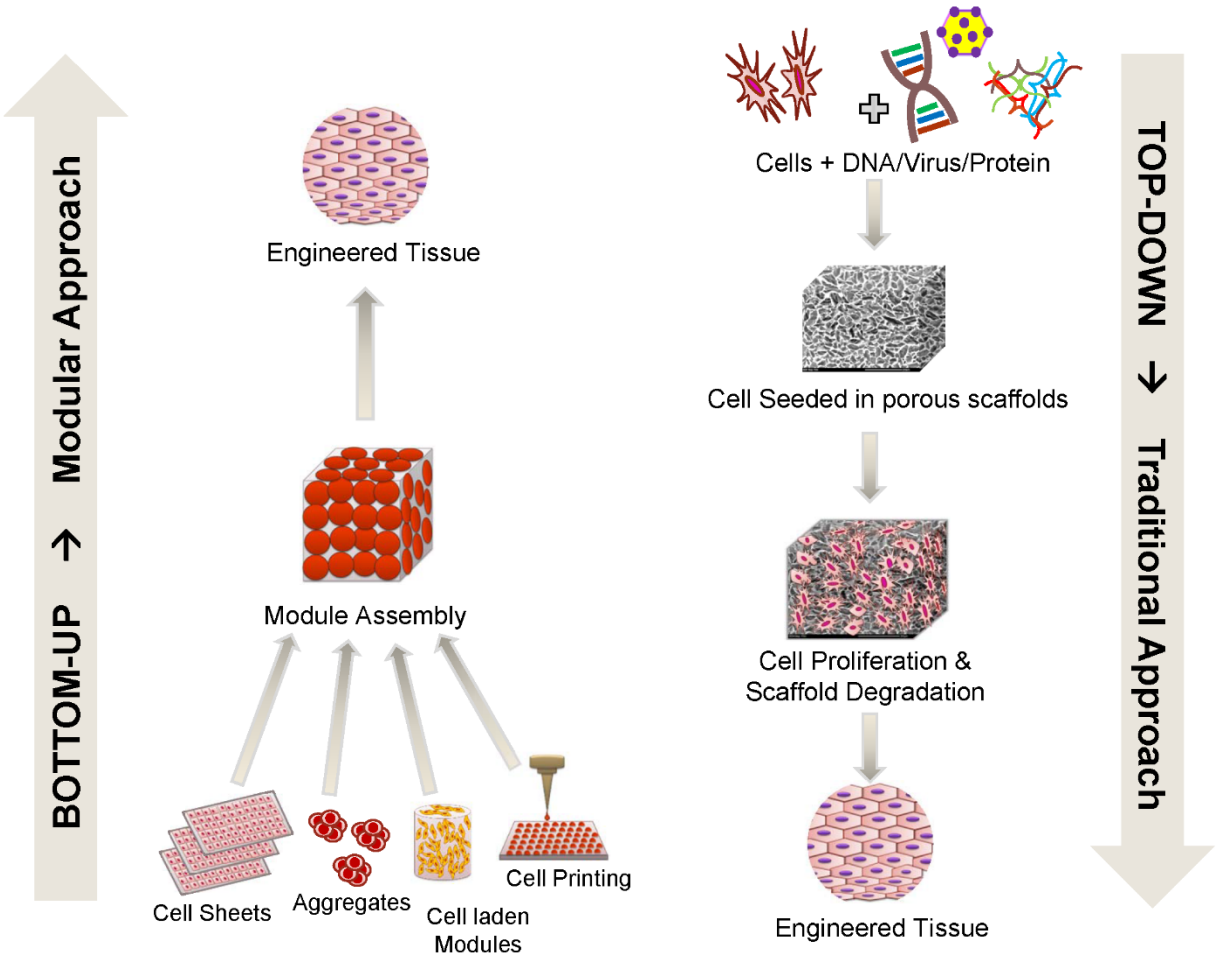

Figure 2: Modular Tissue Engineering.

A bio-inspired scalable strategy of assembling tissue systems from discrete modules containing parenchymal and vascular components. (Tiruvannamalai-Annamalai, Armant et al. 2014).

Current Modular scaffolding methods and fabrication techniques

Complex structures assembled from microscale modular components are seen widely in nature; for example, the kidney is made up of discrete modular components called the nephrons,

and the organ of liver is made up of numerous lobules. Based on this natural principle, complex tissues and organs can be engineered efficiently from microscale modules. This approach is called the bottom up approach as opposed to the top down approach of conventional scaffolds (Nichol and Khademhosseini 2009). Many techniques have been currently developed using this bottom up approach, and some of them are discussed below.

1. *Cells embedded in collagen modules*: This modular approach has been aimed at creating capillary channels through random package of cylindrical collagen modules (McGuigan and Sefton 2006, Leung and Sefton 2010). The parenchymal cells were first mixed with cold collagen, and they were cut into cylindrical modules after the gelation of collagen. These modules can also be coated on the outside surface with endothelial cells to promote vascularization. Modules are then randomly assembled in a tubular structure to form a packed bed like arrangement. Culture medium or blood can be perfused in this packed bed assembly to form a mini vascularized tissue. Even though this method has the potential to eliminate the mass transfer limitation, they have not been able to produce self-supported and mechanically stable structure comparable to that of a native tissue. The other shortcoming is that the cell densities in the modules are not enough to match with the native tissues. Significant development is required to achieve higher cell densities and mechanical strength of modules.

2. *Directed assembly of hydrogel modules:* This modular approach utilizes the surface tension characteristics of hydrogel modules to assemble them to form complex structures (Du, Lo et al. 2008). Modules of specific dimensions are made by controlled photopolymerization of hydrogels, and these hydrophilic structures are then dumped into mineral oil of specific viscosity. The hydrophobicity of oil causes the modules to aggregate and thus form tissue constructs of various desired shapes and sizes. They have also demonstrated a lock and key type of directed assembly

by varying the aspect ratios of the microscale modules. This versatile technique has the potential to eliminate the complicated assembly procedures involved in making a tissue construct. However, there are shortcomings in this method that can limit the maximum achievable size of tissue constructs. Uncontrolled random assembly of modules is another limitation that needs to be addressed before one can promote this technique to clinical applications.

3. Cell sheet technology: This modular approach is capable of producing tissue constructs with mechanical properties comparable to that of native tissues (L'heureux, Paquet et al. 1998, L'Heureux, McAllister et al. 2007, See, Toh et al. 2010). This has been made possible by growing the cells in sheets, thereby allowing cells to deposit sufficient extracellular matrix materials that eventually strengthen the construct. More than a decade ago, this technology was pioneered by creating a multiple cell type laden vascular graft (L'heureux, Paquet et al. 1998). Human trials have also shown promising results (L'Heureux, McAllister et al. 2007). Although this technology produces scaffolds with mechanical properties close to native tissues, they are limited to possible shapes and structures. Moreover, leaking between different cell layers is another potential drawback of this technique. However, this method has been a better choice for highly proliferative cell types that can deposit sufficient extracellular matrix components.

4. Cell printing technology: This has been one of the latest and more promising methods of fabrication that can produce rapid vascularized constructs. This method utilizes a traditional printer, replacing ink with cell matrix and cell suspension, creating 2D cell arrays that can be laid one over the other to make a 3D construct (Mironov, Boland et al. 2003, Fedorovich, De Wijn et al. 2008). Controlled patterning of cell arrays and matrix can be achieved through computer aided designing. Vascular network or anastomosis has been manipulated in 3D hydrogel layers by these organ printers (Wu and Ringeisen 2010). Using this method one can also make porous scaffolds

alone, with desired porosity, microstructure and mechanical properties. One potential limitation of this technique is low cell viability due to time elapse between laying subsequent layers of cells and matrix. Moreover, attachment between the layers has been difficult to achieve in some cases.

5. *Others modular strategies*: Various other modular approaches have been tested by various groups to overcome the disadvantages of conventional scaffolds. Toroid shaped modules have been generated using agarose gels, and cells cultured in these modules showed predictable changes. These modules have also shown to assemble along their lumens in specific conditions (Livoti and Morgan 2010). Poor mechanical properties and complex assembly techniques has been some of the shortcomings of this approach. Similarly cardiac tissues have been engineered by assembling mechanically conditioned cell laden microscale units under serum free conditions (Naito, Melnychenko et al. 2006). This method also has the advantage of reducing immunogenicity upon implantation as they have been made under serum-free and ECM-free conditions. Micro-molds made up of agarose has been shown to make controlled cell aggregates which serve as modules for 3D constructs (Nelson and Chen 2003). However, this system only has limited ability to produce desired mechanical stability. A comparison of major aspects of modular and traditional scaffolds is summarized in Table: 2 and schematically represented in Figure: 2.

The major challenge to advance this modular approach has been to improve or develop new methods for assembling modules in a more precise and controlled manner. The other challenge has been to improve the resolution of the assembled 3D constructs by making better reproducible modules of even smaller dimensions. The mechanical properties of the modular scaffolds can be improved by more conventional methods like introducing fibers or membranes to support the modular constructs.

TABLE: 2 Conventional vs. Modular scaffolds

S.N	Aspects	Conventional scaffolds	Modular Scaffolds
1	Distribution of cells	Non-uniform	Uniform
2	Tissue cell densities	Less than native tissues	Comparable to native tissues
3	Multi cellular structure	Uncontrolled	Can be achieved easily
4	Vascularization	Limited	Extensive
	Mass transfer and diffusion	<100-200μm	>200μm can be achieved
5	Mechanical Properties	Comparable to native tissues	Poorer than conventional scaffolds

2.7 Principle Materials:

In our study we mainly used chitosan and GAG proteoglycans for generating microcapsules. Our choice of biomaterial has been significantly driven by the charge the biomaterial carries and their role in regulating cellular activities. Some important characteristics of chitosan and GAGs are discussed below.

2.7.1 Chitosan:

Chitosan is a deacetylated form of chitin, a naturally available biopolymer. It is soluble in most organic solvents and its crystallinity and degradability depends upon its degree of deacetylation. Its molecular structure has a repeated N-acetyl-D-glucosamine and D-glucosamine

units (Lindahl and Hook 1978) which makes other compounds like GAGs to be covalently linked through the amine group. It is biocompatible, biodegradable and has been shown to have anti-microbial properties. It can accelerate wound healing directly and indirectly and thus a promising biomaterial for cell-based transplantation, non-viral vector based gene therapy and in regenerative medicine (Shi, Zhu et al. 2006). Hence, it can be a suitable material for our modular scaffolds both in the short term and the long term.

2.7.2 Glycosaminoglycans (GAGs):

Proteoglycans are proteins with one are more GAG chains attached to them, predominantly found in connective tissues, cell surfaces and in intracellular and extracellular matrices (Kolset, Prydz et al. 2004, Iozzo 2005, Sasisekharan, Raman et al. 2006, Couchman and Pataki 2012). The GAGs are complex carbohydrates of 10-100kDa molecular mass and participate in wide range of biological functions. There are seven commonly recognized types of GAGs. Six of them have a similar carbohydrate backbone and hexosamine residues. Hyaluronic acid, dermatan sulphate, heparin, heparan sulphate, chondroitin sulfate and keratan sulfate are the six major classes of GAGs (Lin and Perrimon 2002, Kolset, Prydz et al. 2004, Iozzo 2005, Ferdous and Grande-Allen 2007, Theocharis, Skandalis et al. 2008, Couchman and Pataki 2012). With the exception of hyaluronic acid all others are sulfated, with heparin being the most highly sulfated GAG of all. The criteria that distinguish the GAG types are the type of monomer, the position of glycosidic linkages and the amount of sulfation. All GAGs are negatively charged due to the presence of acidic sulphate and/or acid groups (COO-)(Gandhi and Mancera 2008). The GAGs are widely distributed in animals and are essential for maintaining the integrity of connective tissues.

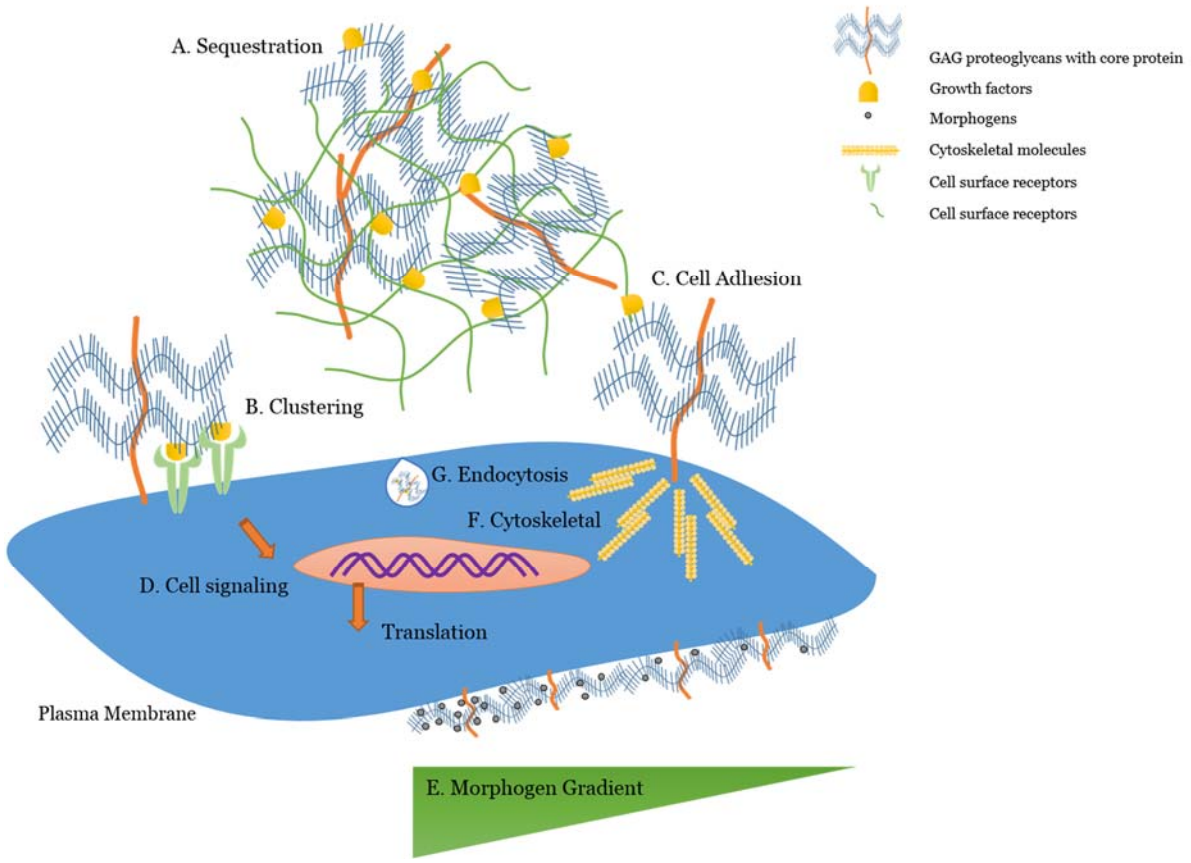

Figure 3: Glycosaminoglycans and their functions

They are highly viscous and have low compressibility; hence, they function as a lubricating agent in articulating joints (Gandhi and Mancera 2008). They support the structural integrity of cells inside tissues and facilitate their migration by interacting with a wide range of macromolecules (ref. fig.:3). In our study various types of GAGs and GAG like biomaterials were tested for cell viability, proliferation, differentiation, mechanical strength, permeability, etc. Optimal formulations were chosen for various cell types. Combination of GAGs were also used to reproduce specific characteristics.

CHAPTER: 3

3.1 CENTRAL HYPOTHESIS AND SPECIFIC AIMS

Our modular tissue engineering strategy involves the use of a polysaccharide microcapsule. The wall of the microcapsule is made out of GAG-chitosan polyelectrolyte complex and the capsules are hollow, which gives us room for tuning the interior environment. The size of the capsules can be achieved from 200-2000μm in diameter during the encapsulation process. The capsule wall permeability, thickness and strength are tunable via the molecular weight of its material components. The capsules are completely biodegradable and the rate is dependent on its material composition. These capsules serve as the building blocks of our modular constructs.

.

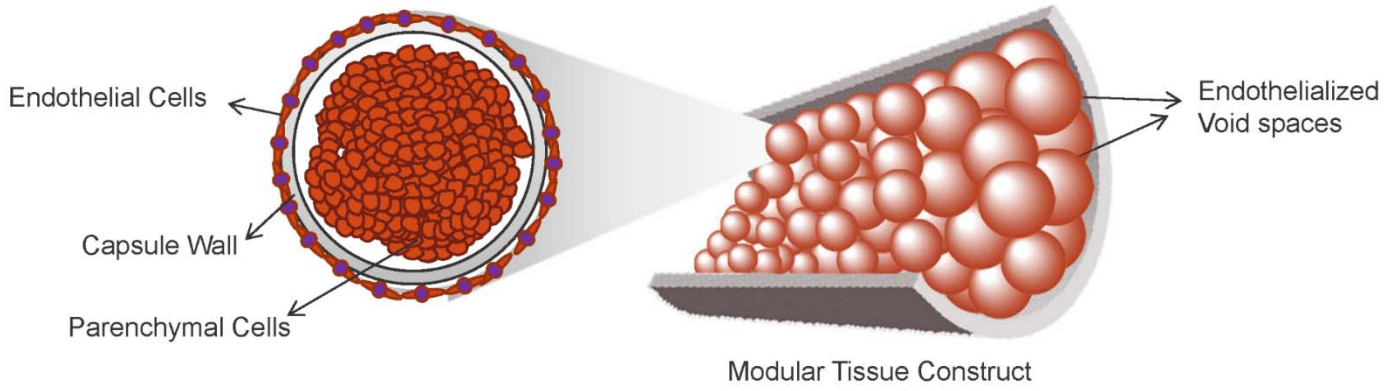

Figure 4: Central Hypothesis: Modular constructs assembled from micro scale modules permeated by a network of interconnected, endothelial cell-lined channels can facilitate extensive vascularization and mass transport.

These capsules are seeded with parenchymal cells on the inside and endothelial cells on the outside. The ***central hypothesis*** to be tested is that, once these cell laden capsules are fused

together it will form a 3D modular construct permeated by a network of interconnected, endothelial cell-lined channels (ref. fig.: 4), that can facilitate rapid and extensive vascularization upon implantation or perfusion

The ***specific aims*** of the proposal are:

1. To characterize different GAGs and develop tools and methods for tuning internal microcapsule environment to accommodate parenchymal cells.
2. To characterize capsule physical properties and mechanical stability.
3. To modify the outside surface of capsules to accommodate endothelial cells.
4. To develop tools and methods for assembling individual modules into 3D constructs with interconnected channels.
5. To develop design parameters for maintaining hepatocyte and endothelial cells in perfused modular constructs.
6. To determine the effects of module endothelialization on vascularization of constructs in vivo.

3.2 Overall research design:

The overall plan to test my central hypothesis is schematically represented in figure 4. First the internal microenvironment of the microcapsules were optimized to accommodate the parenchymal component. Secondly, the outside surface was tuned for endothelial cell seeding. Then suitable method for fusing the capsules were formulated and finally the construct was tested both in-vitro dynamic cultures and in-vivo studies.

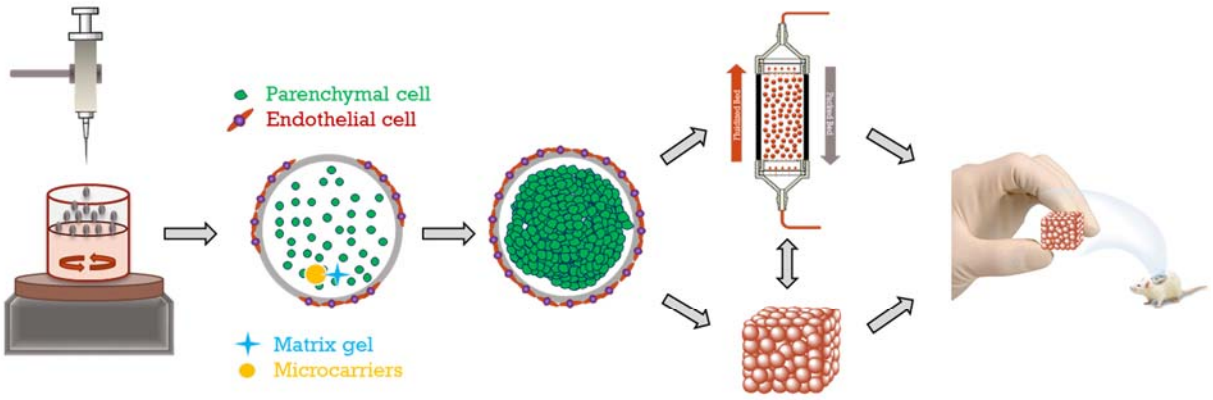

A. Encapsulation	B. Outer cell seeding	C. Tissue density capsules	D. Assembly & In-vitro remodeling	E. In-vivo
Cells + Matrix + Microcarriers	Endothelial cells	Maturation: Static culture	Fabrication: Ionic, Photopolymerization	SCID Mice

Figure 5: Overall research design. The internal microenvironment and outside surface were optimized, then a suitable method for fusing the capsules was formulated and finally the construct was tested both in-vitro dynamic cultures and in-vivo studies.

3.3 Significance and Rationale

Modular tissue engineering has great potential in engineering more advanced tissues and organs thereby advancing the field of tissue engineering. Some of the modular strategies have been well studied and documented, yet the method of assembling tissue constructs from microscale modules is relatively new. This strategy is very significant because of its ability to reproduce the full functionality of tissues by mimicking the innate architecture and complexity of natural tissues. It has the capability to reproduce complex cellular mechanisms that are the hallmark of the complex tissues and organs.

Our microencapsulation technique makes this modular strategy even more efficient by its simple and versatile nature. GAG based microenvironment has been shown to regulate a wide spectrum of biological activities and hence compared to other modular techniques our capsule system has the capability to mimic a wide range of microenvironments. The hollow nature of the capsules makes it more advantageous for fine tuning, and most of the capsule formulations are fully biodegradable by cells. Hence our study is very significant and promising in producing functional bioartificial tissue constructs. Integrating this modular approach and the traditional approach of engineering tissues can also lead to creation of even more advanced scaffolds and fabrication techniques in the future. Hence our research has immense potential in promoting the field of TE and regenerative medicine to the next level of more advanced, optimized tissue and organ systems.

CHAPTER: 4

TISSUE DENSITY CULTURES

4.1 Introduction:

The first step in fabricating a modular construct is to develop suitable methods for tissue density cultures. This is one of the defining features of a modular construct, thru which we can efficiently pack cells with clinically significant cell density in a relatively small construct volume without losing cell performance. In this chapter, methods to develop tissue density cultures were explored by characterizing different GAGs and various ways to tune the internal microenvironment were investigated. This chapter also details different methods to optimize the capsule system, depending on the type of cells and its behavior in the GAG microenvironment.

4.2 Aim and Rationale:

The main specific aim of this chapter is to develop tissue density cultures using our GAG based encapsulation methods. The rationale for this aim is that by developing tissue density cultures with cell densities comparable to that of the natural organs and tissues, we can fabricate larger tissues without compromising its overall performance. The significance of this objective is that it will help overcome the common diffusion limitation across a given module and a more uniform cell microenvironment can be maintained across a tissue construct. These tissue density capsules unlike porous scaffolds will enable us to reproduce the full functionality of the organ of interest in the long term.

4.3 Experimental Approach:

Study 1: Cells were encapsulated in different GAG microcapsules and evaluated.

Optimal capsule formulation was identified by encapsulating primary and undifferentiated cells in microcapsules made up of different types of GAGs and GAG like biomaterials and monitoring cell viability, growth, proliferation and differentiation.

Study 2: Microcarriers were co-encapsulated to provide surface for adhesion.

Additional optimization was performed for adhesion dependent cells by co-encapsulating surface providing microcarriers made of suitable biomaterial including ECM biopolymers like collagen, serum proteins etc. This step was particularly helpful for adhesion dependent cells.

Study 3: Self-contracting capsules were made by utilizing cell mediated contraction of collagen matrix.

For cells that have low proliferation rates, self-contracting thin walled and matrix rich capsules were made by incorporating more collagen inside capsules. The cell mediated contraction of the encapsulated collagen matrix yielded tissue density capsules in short term cultures. This also reduced the culture durations, for cells that won't tolerate GAG rich microenvironments for longer durations.

4.4 Materials and Methods:

Briefly, in all the above mentioned studies, encapsulated cells were evaluated for morphology, distributions, cell viability, proliferation and differentiation. Cell viability was

monitored using Calcein AM/Ethidium Homodimer live/dead fluorescence assay. Proliferation of cells was quantified using Hoechst DNA quantification assays. Differentiation of cells was monitored using immunohistochemistry of cell specific markers. General morphology of cells, aggregates and their distribution was monitored using phase contrast and confocal microscopy, H&E and Masson's Trichrome assay. Detailed materials and methods are discussed below.

4.4.1 Cell culture conditions

All chemical and culture reagents were purchased from Sigma-Aldrich unless mentioned otherwise. The human trophoblast cell line HTR-8/SVneo (Graham, Hawley et al. 1993) (HTBs) was used as the model cell type for some studies due to their high proliferative capacity and ability to form dense, tissue-like aggregates. The cells were cultured in 10 cm tissue culture dishes, using F12/DMEM supplemented with 5% fetal bovine serum (FBS), 50 mg/ml gentamycin and 2.5 mg/L Amphotericin-B.

For co-culture studies, vascular smooth muscle cells (SMCs) were isolated from rat aorta and endothelial cells (AECs) were isolated from sheep aorta using established enzymatic procedures (Christen, Bochaton-Piallat et al. 1999, Butcher and Nerem 2004, MacNeil 2007). Sheep aortas were procured from a slaughterhouse under an educational license (Wolverine Packing Company, Detroit, MI). Aortas were obtained within 2 hours of slaughter and used for AEC isolation immediately. Human umbilical vein endothelial cells (HUVECs) obtained from ATCC (Manassas, VA) were also used as vascular component. Primary cells were used from passages 3 to 6. SMCs and AECs were maintained in DMEM supplemented with 10% FBS, 50 mg/ml gentamycin, and 2.5 mg/L Amphotericin-B. In addition, SMC cultures were supplemented with 2 ng/ml fibroblast growth factor 2 and AECs with 50 ng/ml of epidermal growth factor. For

HUVECs, MCDB 131 medium supplemented with Endothelial Cell Growth Kit-VEGF (ATCC) was used. During co-cultures of parenchymal and vascular components, a 50-50 mixture of the respective culture media was used. Primary hepatocytes were isolated from Sprague dawley rats weighing 250-450 g by the two-step collagenase perfusion technique described by Seglen (Seglen 1979) and modified by Dunn (Dunn, Yarmush et al. 1989, Dunn, Tompkins et al. 1991). Cell viability averaged 90-95%, as assessed by trypan blue exclusion, and the average yield was $4x10^8$ viable cells per liver. Type I collagen was isolated from Sprague dawley rat tail tendons as previous described (Dunn, Tompkins et al. 1991) and used for hepatocyte collagen sandwich cultures. Hepatocyte culture medium consisted of high glucose DMEM medium supplemented with 10% fetal bovine serum (FBS), 0.5 U/mL insulin, 7 ng/mL glucagon, 20 ng/mL epidermal growth factor, 7.5 μg/mL hydrocortisone, 100 mg/L gentamycin and 2.5 mg/L amphotericin B. Culture medium was collected and analyzed for albumin and urea synthesis using established methods (Matthew, Sternberg et al. 1996, Surapaneni, Pryor et al. 1997). All dish cell cultures were maintained at 37ºC in a 5% CO2/95% air humidified incubator.

4.4.2 Biopolymer Materials

The materials used in preparing our microcapsules and modular scaffolds were: chitosan from crab shells, molecular weight ~600 kDa (Sigma); chondroitin 4-sulfate sodium salt from bovine trachea, molecular weight ~50-100 kDa (Sigma); hyaluronic acid sodium salt from *Streptococcus equii*, molecular weight 1500-1800 kDa (Sigma); dextran sulfate sodium salt, molecular weight ~500 kDa (SCBT); heparin sodium salt from porcine intestinal mucosa, molecular weight 17-19 kDa (Celsus); carboxymethylcellulose sodium salt, molecular weight 250 kDa (Sigma); polygalacturonic acid sodium salt (Sigma) and collagen type-I isolated from Sprague Dawley rat tail tendons (Invitrogen).

Aqueous solutions of the polyanions (chondroitin 4-sulfate (CSA), carboxymethylcellulose (CMC), hyaluronic acid (HA), polygalacturonic acid (PGA)) were prepared in a HEPES-sorbitol buffer containing: 0.4 g/L KC1, 0.5 g/L NaC1, 3.0 g/L HEPES-sodium salt, and 36 g/L sorbitol, pH 7.3. Polyanion solutions were sterilized by autoclaving at 121°C. The two formulations of polyanionic solutions studied for capsule formation were: (a) 4 wt% CSA/1.5 wt% CMC and (b) 1.0 or 1.5 wt% HA. To prepare the polycationic solution, chitosan powder was suspended in water (3 g in 250 ml) and autoclaved at 121° C. Under sterile conditions, 0.6 ml of glacial acetic acid was added to the aqueous suspension and stirred for 4 hours to partially dissolve the chitosan. Likewise, 19 g of sorbitol was autoclaved in 250 ml of water and then mixed with the chitosan solution. Undissolved chitosan was removed by centrifugation at 500 G. PGA (0.1 wt%) in HEPES-sorbitol buffer was used for surface stabilization of capsules. For capsule experiments employing collagen, cold collagen-I solution was diluted to 2 mg/ml in 1 mM HCl, and then neutralized with 10X DMEM (9:1 ratio). Normal saline (0.9 wt% NaCl) was used for capsule washing immediately after formation.

4.4.3 Cell encapsulation

Cells were encapsulated in microcapsules produced by polyelectrolyte complexation between cationic chitosan and polyanions as described in detail previously (Matthew, Salley et al. 1993, Lin and Matthew 2002). In brief, the 5-10 million cells were suspended in 1 ml of a polyanionic solution (either 4 wt% CSA/1.5 wt% CMC, or 1.5 wt% HA). Droplets of the cell suspension (~0.8 mm diameter) were dispensed into 30 ml of stirred chitosan solution containing 2-3 drops of Tween 20. A 24 gauge Teflon catheter was used to generate droplets and filtered air was blown coaxially to shear away the droplets at a suitable size. Care was taken during encapsulation process to ensure uniform droplet size. Capsule membranes were formed almost

instantaneously by ionic complexation between the oppositely charged polymers. Capsules were allowed to mature for ~1 min in the stirred chitosan, followed by two washes with normal saline and surface stabilization by washing with 0.1% PGA solution. Microcapsules were subsequently equilibrated with culture medium for ~60 min and then transferred to suitable culture conditions (Figure 5).

The interior environment of the capsules could be enhanced with collagen gel or adhesion surface-providing microcarriers when desired. For capsules with an internal collagen matrix, chilled Type I collagen solution (1 mg/ml in 1 mM HCL) was neutralized with 10X DMEM in a 9:1 ratio, and mixed with an equal volume of double strength polyanionic solution (e.g. 8% CSA/3% CMC). Cells were then suspended in this mixture instead of the regular polyanion solution, and capsules were made as described previously. For microcarrier co-encapsulation, PBS swelled microcarriers were suspended along with cells in normal strength polyanionic solution at a volume ratio of 0.5:1 (packed cells+microcarriers:polyanion solution). The suspension was then dispensed as droplets to generate capsules as described above. Capsules enhanced with interior collagen or microcarriers were subjected to similar washing and surface stabilization steps as described above prior to culture.

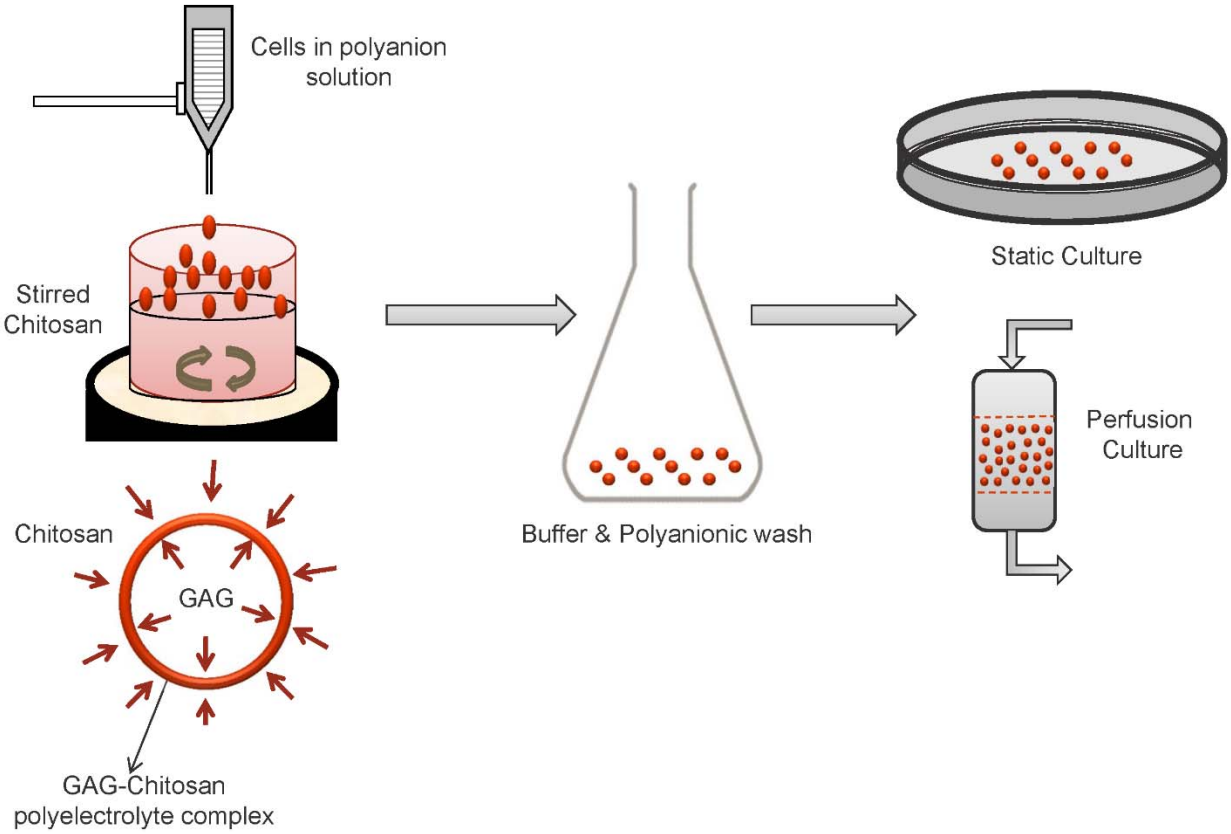

Figure 5: Microencapsulation through complex coacervation. Droplets of cells suspended in a polyanionic solution were dispensed into a stirred chitosan solution. Ionic interactions between the oppositely charged polymers formed an insoluble ionic complex membrane at the droplet-solution interface, thus encapsulating the suspended cells.

4.4.4 Evaluation of cell proliferation inside capsules

Cell proliferation inside capsules was characterized using either a Hoechst DNA quantification assay (Gallagher and Desjardins 2001) or an MTT assay. Briefly, 30 capsules were distributed into each well of a 24 well plate. Capsules were maintained under standard culture conditions, and one well was sacrificed at each time point. The capsules were gently ruptured using a fire-polished Pasteur pipette, and the cell aggregates within were lysed using cell lysis buffer

(0.1% SDS, 10 mM Tris-HCl, 1 mM EDTA) to extract whole DNA. To an aliquot of this extract was added an equal volume of Hoechst 33258 dye dissolved at 1 mg/ml in TNE buffer (50 mM Tris-HCL, 100 mM NaCl, 0.1 mM EDTA). Fluorescence of the mixture was then measured (EX/EM 350/450 nm). A calf thymus DNA standard curve was used to determine the total DNA concentration. For the MTT proliferation assay, capsules were washed in PBS and suspended in phenol red free DMEM containing 2 mg/ml MTT. After incubation for 4 hours at 37°C, the solution was aspirated and 150 µL of DMSO was added to extract the formazan crystals. After 10 mins of rotary agitation, the absorbance of the DMSO extract was measured at 540 nm using a spectrophotometer. Exponential cell growth was assumed and the specific growth rate was determined by fitting the following equation to the absorbance reading:

$$\ln\left(\frac{A}{A_0}\right) = \mu\left(t - t_0\right)$$

Where A_0 and A are initial and final absorbance or fluorescence readings respectively, t_0 and t are initial and final time points, and µ is the specific growth rate in $time^{-1}$.

4.4.5 Cell viability imaging and histology

Cell viability was assessed using Calcein-AM and ethidium homodimer (Cytotoxicity Kit L3224, Invitrogen). The cell laden capsules were washed with PBS and incubated in serum free DMEM containing 4 µM Calcein-AM and 4 µM ethidium homodimer for 20 min at 37ºC. For long-term tracking of HUVECs on capsules and fused capsule constructs, CellTracker™ Green CMFDA (Invitrogen) was used. Briefly, adherent cells were rinsed with PBS and incubated in a serum free culture medium containing 5 µM CellTracker Green probe for 45-60 min. After the incubation the medium was replaced with pre-warmed normal medium and incubated for another

30 min for the dye to undergo modification due to intracellular esterases. The cells were then trypsinized and seeded onto capsule outer surface. Cell fluorescence was then observed using wide-field fluorescence microscopy and laser scanning confocal microscopy (Zeiss LSM-410).

The distribution and organization of cells and matrix inside the encapsulated cultures were investigated by histology. Cell laden individual capsules and fused capsule constructs were washed in PBS, fixed in 10% buffered formalin, dehydrated in an ethanol series, paraffin embedded, sectioned (4-6 μm) and stained using Hematoxylin and Eosin (H&E) or Masson's trichrome stains (Sigma-Aldrich). The stained sections were observed using bright field microscopy.

4.5 Results:

4.5.1 Characteristics of different GAG based microcapsules and their properties:

A model system was designed to study the influence of different GAGs on microcapsule properties including wall thickness, strength, rate of degradation and invasiveness of cells to capsule wall. Human trophoblast cell line HTR-8/SVneo (HTBs) was chosen as the model cell type due to their high proliferative capacity and tolerance to hypoxic conditions. These HTBs were encapsulated in different GAG based microcapsules and phase contrast images were captured at different time intervals. HTBs grew rapidly and formed spheroids in all test formulations. By day 30, HTBs filled the capsules in all formulations. However, the growth pattern of HTBs and capsule integrity differed between formulations.

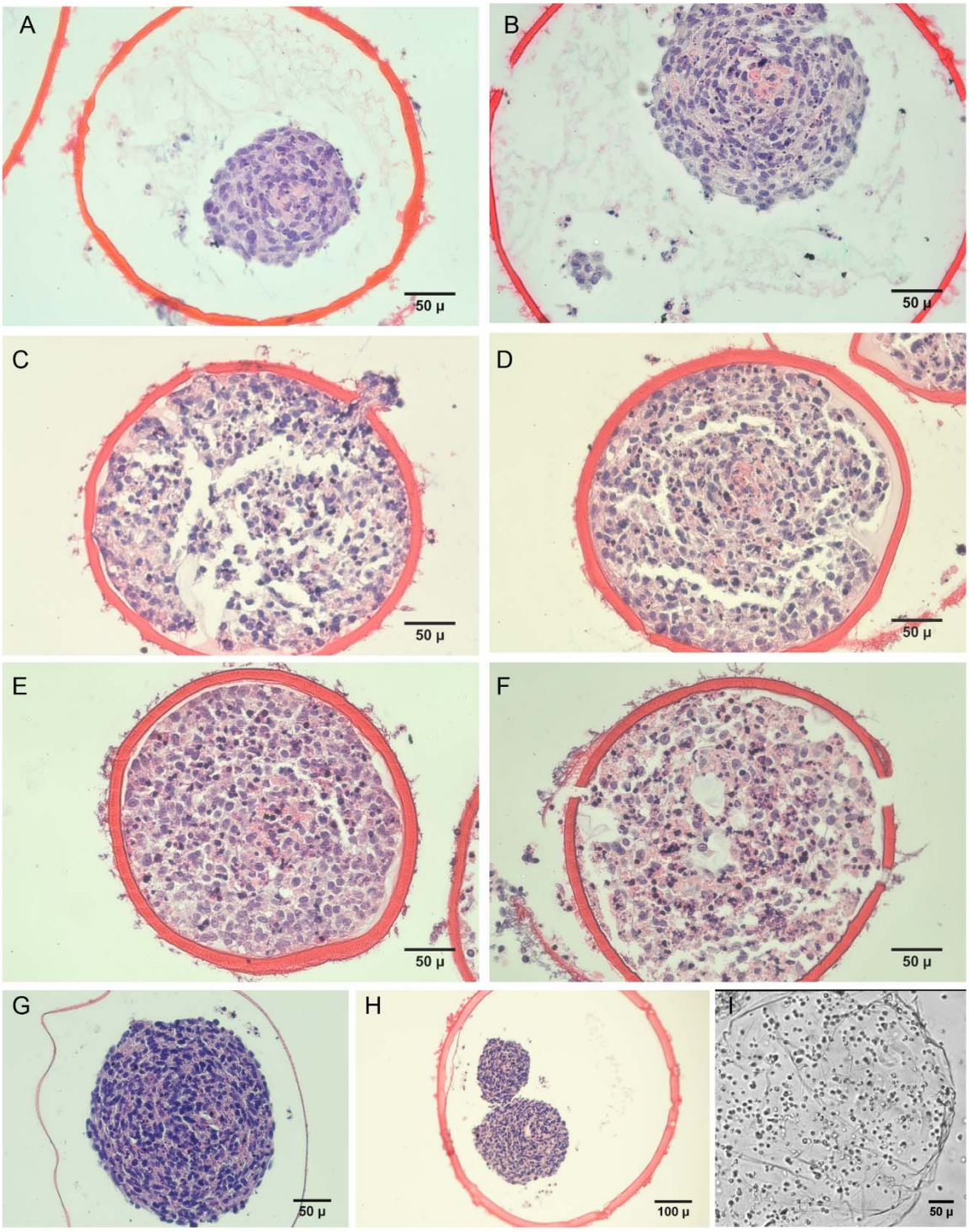

Figure 7: Histology of microencapsulated culture es of human trophoblasts (HTBs) in various GAG-chitosan capsule formulations. HTBs in CSA/CMC capsules on days (A) 5, (B)

10, (C) 15, (D) 20, (E) 25, (F) 30. (G) Hyaluronan/CMC capsules. (H) HA capsules. (I) Dextran sulfate/CMC capsules quickly ruptured due to osmotic swelling.

Compact spherical aggregates were seen in CSA capsules (Fig. 7A-F) while the aggregates were irregular and significantly dispersed when an internal collagen matrix was included (Fig.8A, B). HA/CMC formed very thin walled capsules, many of which collapsed after a week of culture (Fig. 7G). Capsule wall thickness increased, and the integrity of the capsule was compromised in the HA formulation due to rapid HTB invasion into the capsule wall (Fig. 7C). Notably, the CSA/CMC microcapsules were more intact and the HTBs were found to be less invasive in this formulation. Capsules made with Dextran sulfate (DXS) and mCMC (4%DXT and 3% mCMC) ruptured rapidly due to swelling (Fig 7I).

4.5.2 Tuning the inner environment of the microcapsules with matrix proteins and Microcarriers:

The hollow nature of the GAG based microcapsule enables us to tune the inner microenvironment efficiently. Here we investigated the effect of collagen matrix and surface providing microcarriers on cell microenvironment by encapsulating them in microcapsules along with cells. When collage matrix is included along with the HTBs, the aggregates are loosely distributed inside the CSA capsules (Fig 8A, B) but the cell invasion into the walls remained the same. The other attempt to tune the inner environment is by providing a solid surface for the cells to attach by encapsulating microcarriers along with cells. We investigated the effect of gelatin coated dextran microcarriers (Cytodex-3) encapsulated in high molecular weight HA, on aortic smooth muscle cells (SMCs) proliferation and viability. The Live/Dead assay using Calcein AM and Ethidium Homodimer showed that encapsulation of microcarriers along with the cells

increased the viability and proliferation of SMCs. Similar results were not observed with microcarriers made of dextran only instead there was a decrease in total number of viable cells. This method can be very productive especially with adhesion dependent cells.

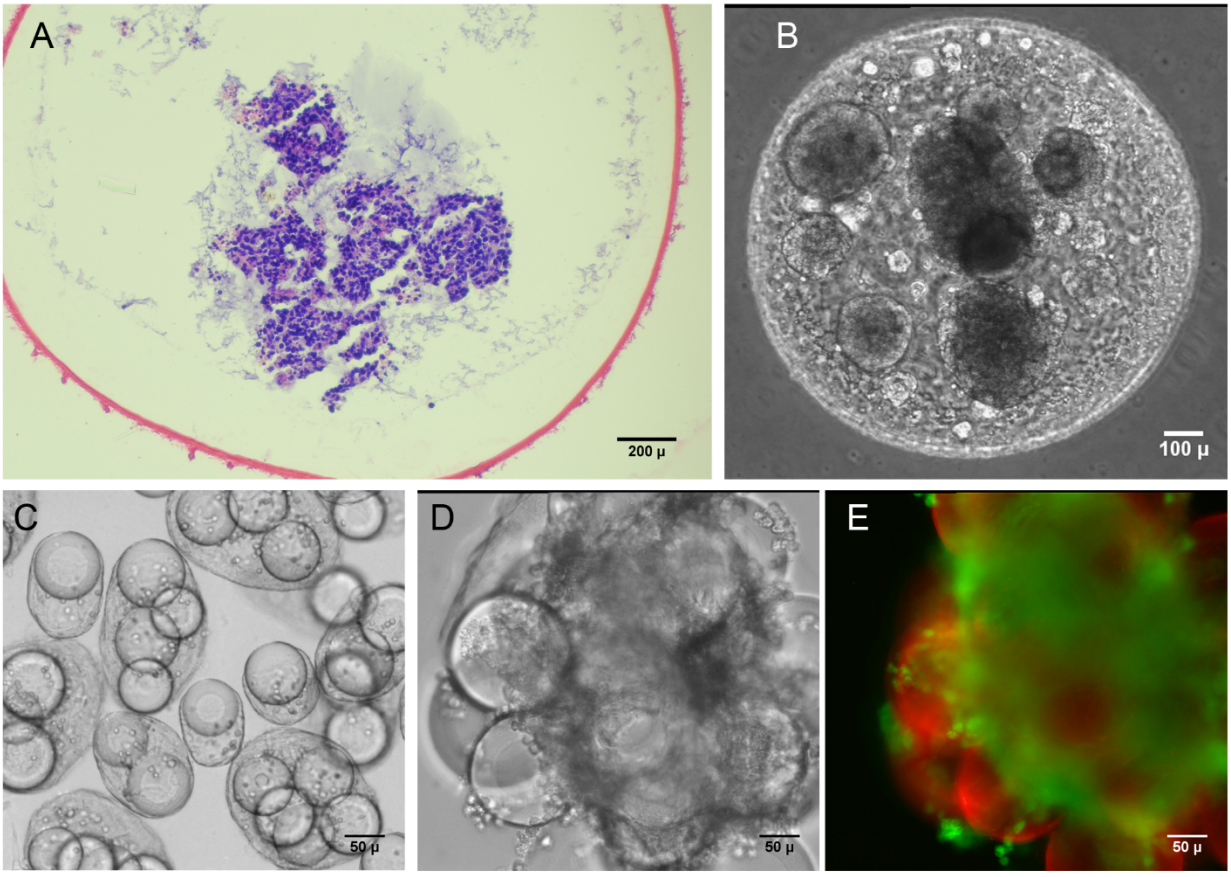

Figure 8. Tuning the inner capsule microenvironment with a collagen gel matrix and microcarriers. (A-B) HTBs in CSA/CMC capsules with a collagen type-I gel after one week of static culture. (A) H&E histology. (B) Phase contrast image. (C-E) SMCs co-encapsulated with gelatin coated dextran (Cytodex-3) microcarriers in HA capsules. (C) 60 min after encapsulation. (D) Day 14 of culture. (E) Calcein-AM stained fluorescence images on day 14 (green = live cells, red = microcarriers).

4.5.3 High density encapsulated cell cultures

The major shortcoming in traditional scaffolds is their inability to achieve cell density comparable to that of a native tissue. We investigated the ability of GAG-based microcapsules to maintain clinically significant cell density needed to fabricate a tissue contract of implantable size. HTBs were encapsulated in CSA-capsules and were cultured for at least 45 Days in static conditions. Encapsulated HTBs grew rapidly, eventually filling the capsules, and most cells appeared viable with a distinct nucleus up to at least day 30 (Figure 7A-F). This indicated that the capsule wall was sufficiently permeable to nutrients to allow maintenance of a dense, tissue-like cell mass. The estimated capsule cell density (~$6x10^7$ cells/cm^3, assessed via image analysis) at day-30 was high enough to replicate the cell density in many tissues. By the end of week-3, HTBs had invaded the capsule wall as seen in Figure 8C. This in vitro invasion suggests that the capsule materials may be degraded within a relatively short time frame upon implantation in vivo. No necrotic core was observed within the encapsulated cell mass at least until 45 days of static culture.

4.5.4 Collagen contracted capsules for non-proliferative cells and short time cultures:

Due to their high proliferative capability, we used HTB cell line as our model system for our previous studies to characterize the capsule system. However, not all the cells grow well in our capsule system and hence attaining cell growth with higher tissue densities is a challenge. To overcome this, we developed a method of contracting the initial volume of cells encapsulated to a clinically significant density, using collagen. Here we investigated the ability of collagen to contract the capsules by encapsulating them at different mass ratios with GAG solution, along with cells.

SMCs in CSA/CMC capsules with collagen matrix: Initially when collagen was encapsulated along with HTBs in CSA/CMC capsules at a final concentration of 1.5 mg/ml, the aggregates became loosely packed with healthy cells as mentioned before. When collagen of same concentration was encapsulated along with SMCs in CS/CMC capsules, the cells were initially fairly dispersed inside the capsules. However, within 24hrs the cells contracted the collagen matrix and formed a denser mass of cells and matrix as shown (Fig 9A-C). Even though the internal matrix had contracted, the walls of the CSA capsules were unyielding and retained their spherical shape as shown below. Since, SMCs didn't proliferate well in CSA we also investigated the ability of HA capsules to collagen contraction.

SMCs in HA capsules with collagen matrix: We experimented different concentrations of HA and collagen to maximize the contraction of capsules and increase the cell density while retaining the integrity of the capsules. Maximal contraction was achieved using formulations containing 0.5-0.7 g/ml of HA and 1.0- 1.2 mg/ml of collagen as shown (Fig 9). Unlike CSA/CMC capsules, this formulation yielded good viability of SMCs in both short term and long term cultures as evident from the live/dead staining (Fig 9D). Optimization of capsule formulation maybe required for other cell types to attain maximal growth and proliferation. Hence this method can be a potential tool to make tissue density capsules with cells that normally do not proliferate well in-vitro.

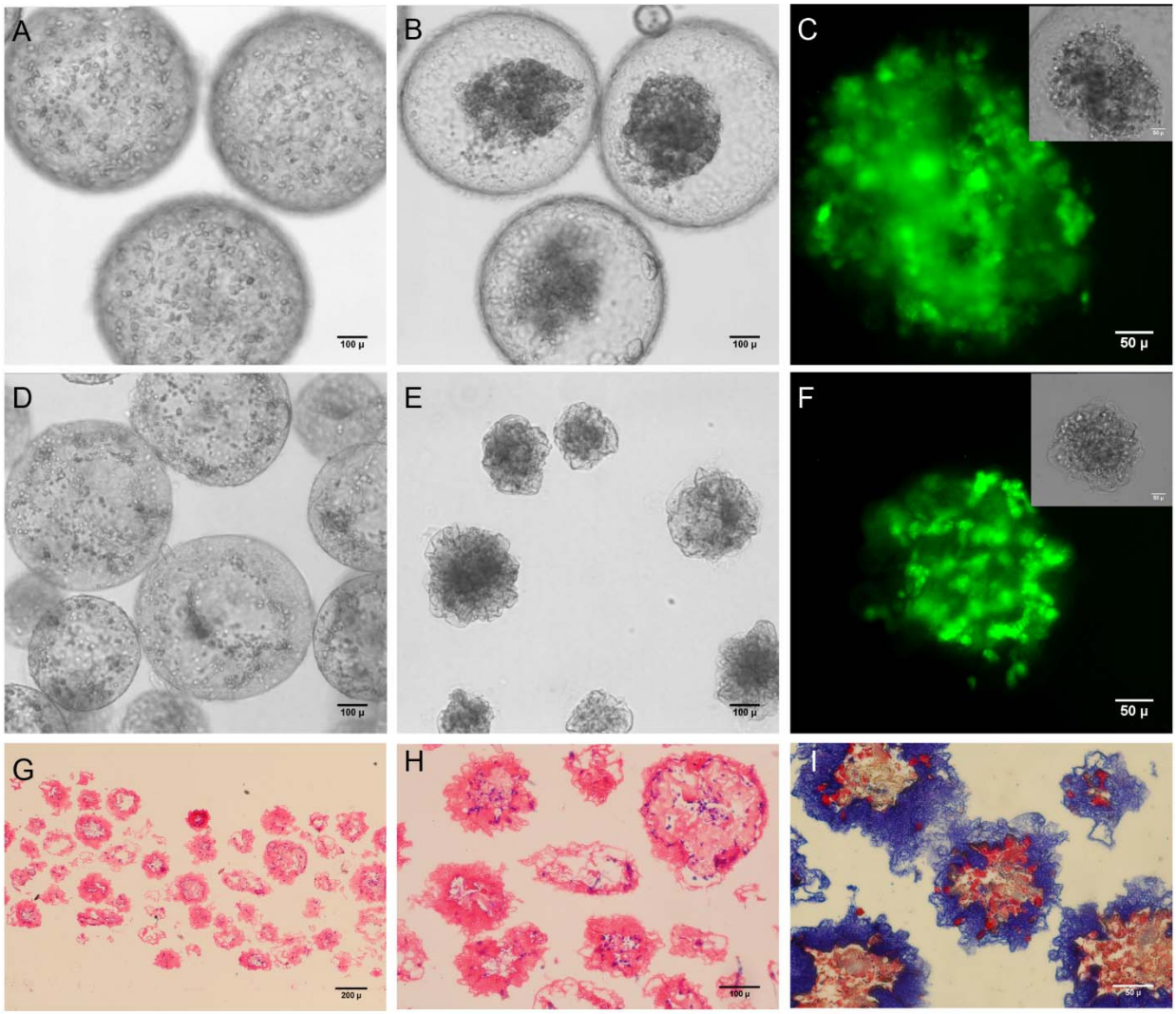

Figure 9. Vascular smooth muscle cells in collagen-containing capsules.

(A-C) SMCs in CSA/CMC capsules with a 1 mg/ml collagen gel. (A) 60 min after encapsulation, SMCs are well dispersed in the internal collagen matrix. (B) After 24 hours of culture, the cells had contracted the internal collagen gel and formed a dense cell-matrix mass. (C) Calcein-AM fluorescence of contracted cell mass. Inset shows phase contrast image. **(D-F)** SMC encapsulated in HA capsules with 1 mg/ml collagen-I gel. (D) 60 min after encapsulation, cells are well dispersed in the internal collagen matrix. (E) After 24 hours of culture, the cells contracted the internal collagen gel, simultaneously collapsing the entire capsule structure to form a denser

module with a convoluted surface membrane. (F) Calcein-AM fluorescence of contracted cell mass. Inset shows phase contrast image. (G-I) Histology of contracted capsules. H&E (G,H) staining showing compacted capsule structure with minimal void volume. (I) Masson's Trichrome staining of contracted capsule, showing the distribution of collagen (blue) within the structure.

A quantitative analysis reveals a 70-80% reduction in total volume of capsules within 24 hours (Fig 10). Hence this enables us to achieve tissue densities very fast. This will be very useful mainly in case of low proliferative cells and cells that can't grow fast in GAG based microenvironment. Moreover, this can also reduce diffusion limitations by reducing the diameter of the capsules.

A)

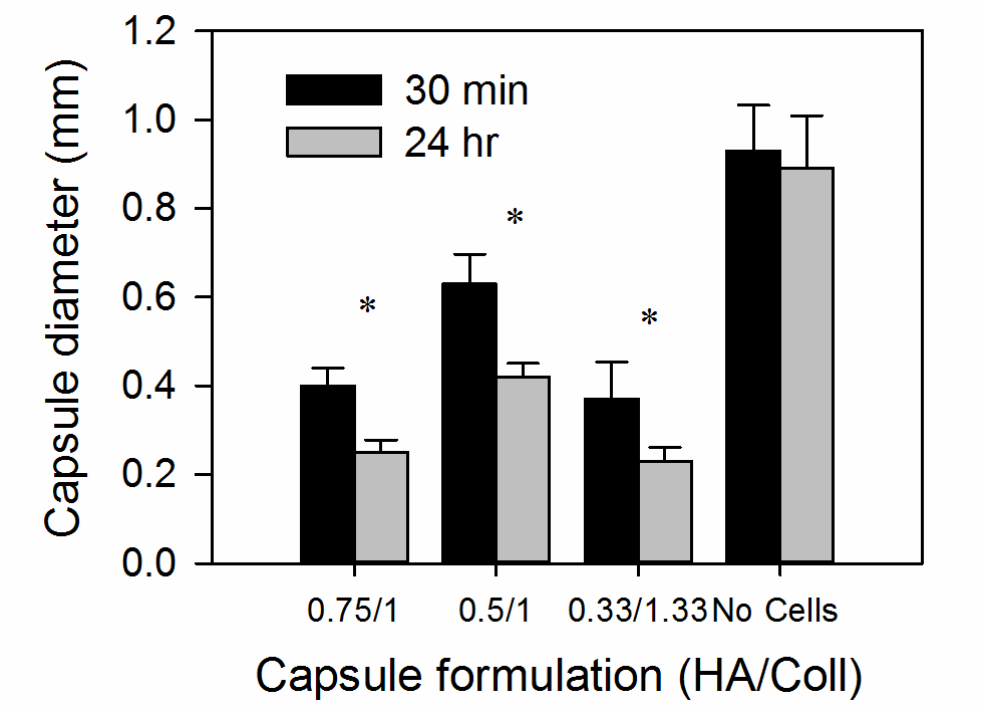

B)

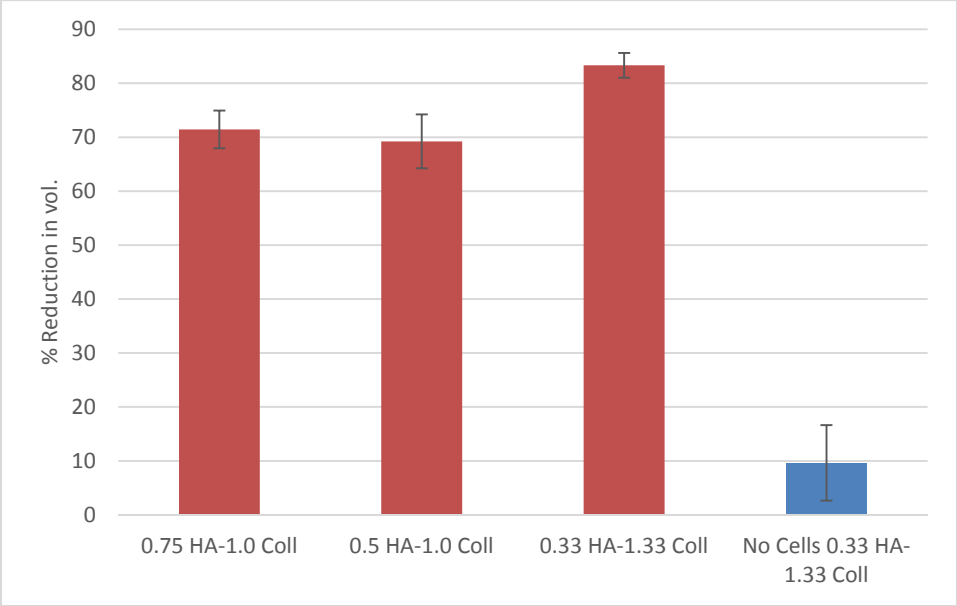

Figure 10: Percent decrease in dimensions of collagen contracted capsules. (A) Decrease in diameter of the capsules. (B) Decrease in the total volume of the capsules.

Other cell types:

We also encapsulated Rhesus monkey embryonic stem cells in our capsule systems and maintained them for two weeks in MEF monolayers. After a week of culturing, the stem cells formed embryoid bodies (Figure 11). At the end of week two, the embryoid bodies formed distinct compartments with different cell morphologies (Figure 12). The cell layers that are close to the capsule wall showed distinct cell nucleus whereas the cell layers farthest from the wall showed condensed chromatin fragments in H&E staining. This might be due to growth factor binding capabilities of the GAGs in the capsule wall that are close to one side of the embryoid bodies. The diffusion gradient across the length of the capsule might also have contributed to this difference in morphology. Cell encapsulated capsules that are cultured under feeder free conditions were also seen healthy and viable at the end of day-4 (Figure: 13). Further rigorous analysis is needed to

report solid claims about the status of pluripotency and self-renewal of stem cells cultured in our capsule system. Overall, we believe that GAG based culture systems possess superior properties in delivering growth factors and providing biochemical cues and can be advantageous in stem cell maintenance and differentiation.

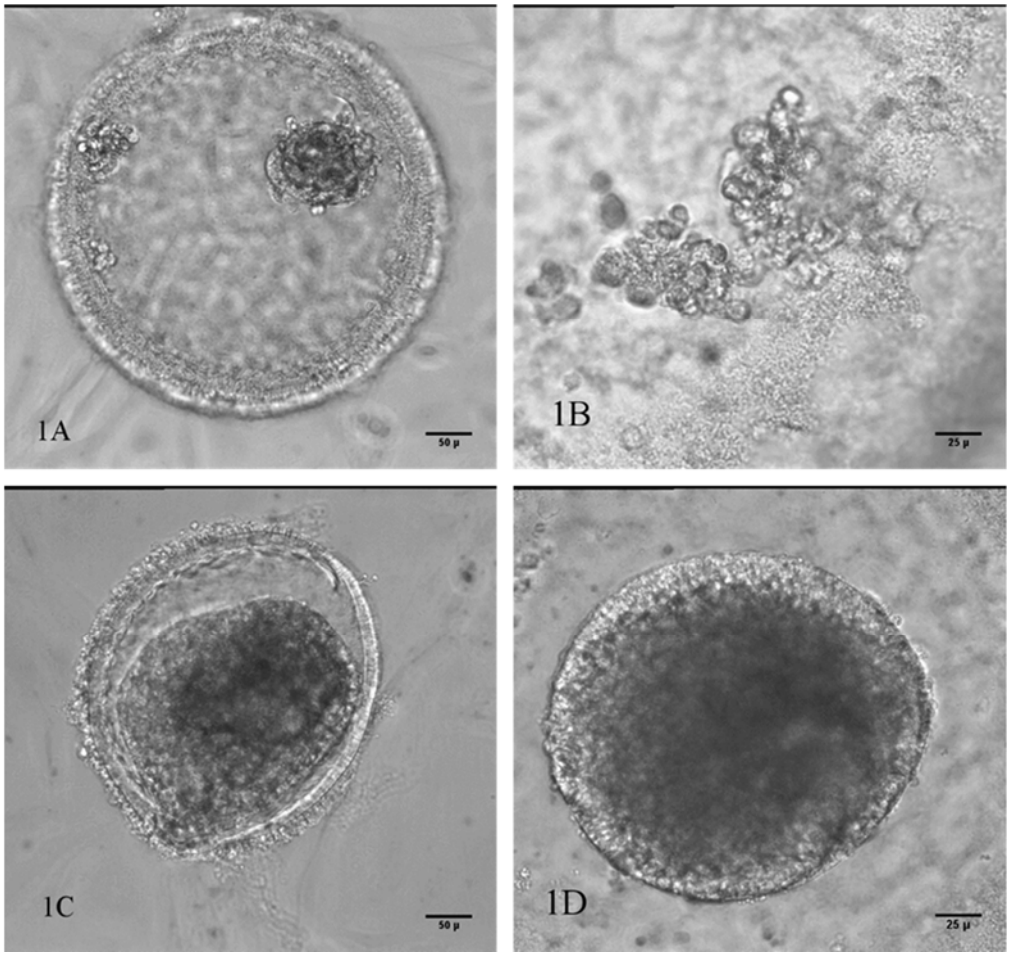

Figure 11: Bright field Images (4% Chondroitin Sulfate-A/1.5% Carboxymethyl Cellulose capsules with ES cells in MEF Monolayer); A,B: 24 hours after encapsulation shows smaller and loosely packed cell aggregates; C, D: Day-10 images show embryoid bodies formation which occupies most of the capsule volume.

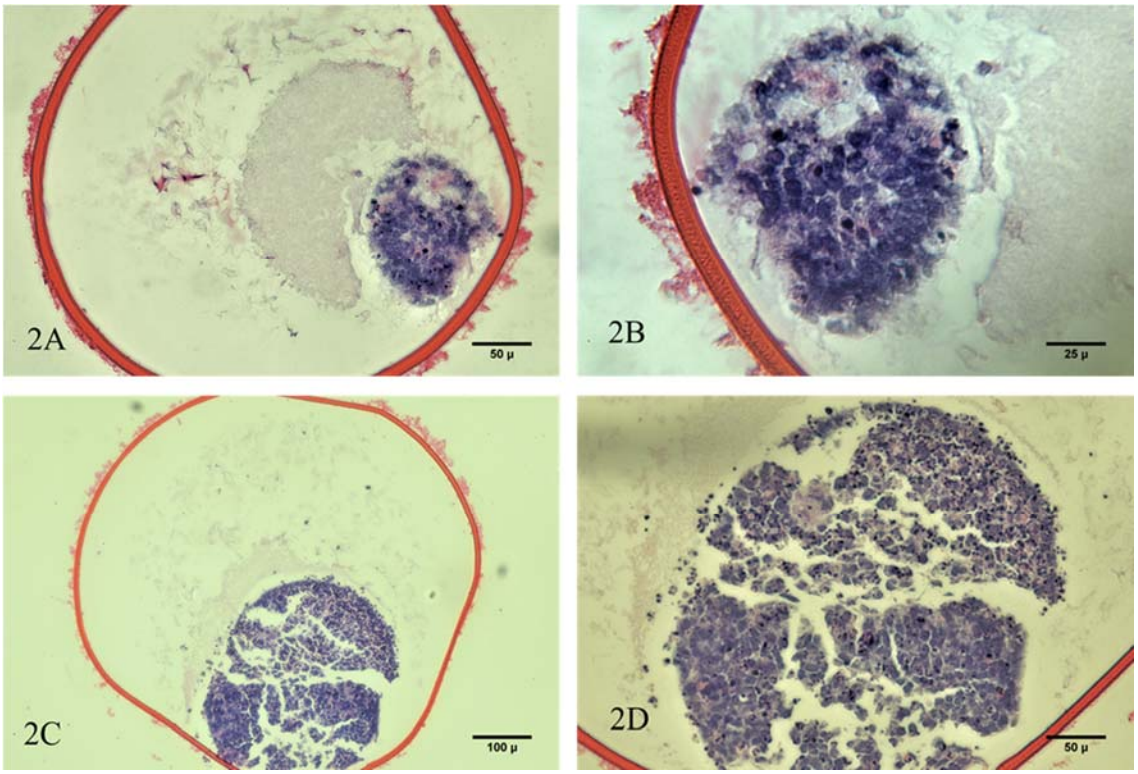

Figure 12: Rhesus monkey ES cells in MEF Monolayer (Co-culture); Hematoxylin and Eosin staining of (4%Chondroitin Sulfate-A/1.5%Carboxymethyl cellulose) capsule sections; A, B: Day-7 of encapsulated culture shows smaller aggregate with distinct nucleus; C,D: Day-14 of encapsulated culture shows embryoid bodies with distinct compartments showing different cell morphologies.

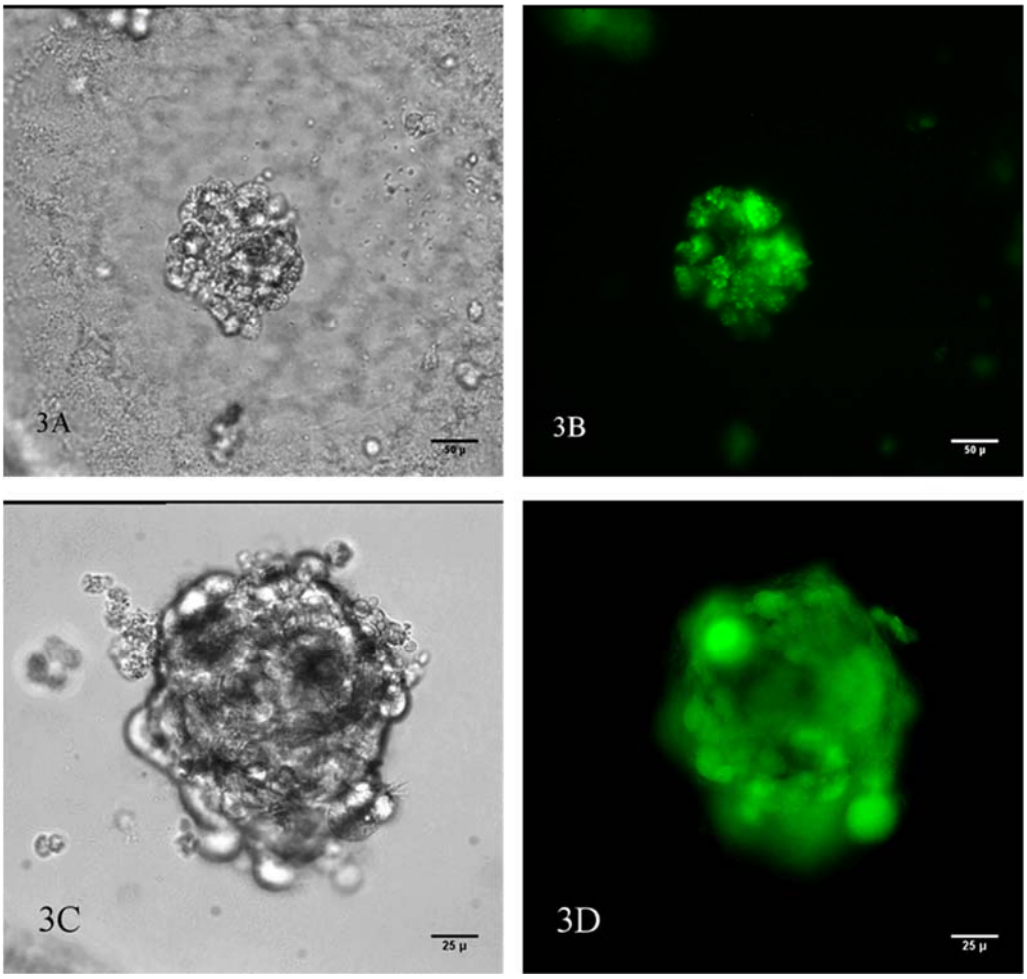

Figure 13: Calcein AM -Fluorescent Images-Cells Seeded: Rhesus monkey ES cells; A,C: Bright field images and B,D: respective fluorescent images; ES cells encapsulated and maintained on feeder layer free conditions show good viability during the first week of culture.

4.5.5 Growth rates of encapsulated smooth muscle cells

Sheep aortic smooth muscle cells were encapsulated for purposes of evaluating the performance of a normal parenchymal cell type. Use of these cells also allowed indirect evaluation of their interaction with endothelial cells in a subsequent study. SMC specific growth rate data showed that the cells proliferated significantly better in HA than in CSA/CMC capsules ($p<0.05$)

during the first 36 hours of culture (Figure 14). However, differences between the formulations were less pronounced after 36 hours ($p<0.10$). The difference in cell proliferation might be attributable to hyaluronan-specific signaling through CD44 cell surface receptors (Jain, He et al. 1996). Alternatively, CSA, a sulfated GAG, may have bound and partially sequestered growth factors necessary for SMC growth. In addition, the HA capsules appeared to support slightly better cell attachment to the internal surface than CSA/CMC, thereby promoting formation of several small aggregates rather than the single large spheroid typically seen in CSA/CMC capsules. . Smaller aggregates are less likely to be adversely affected by diffusion limitations and may thus exhibit higher growth rates in the early stages than larger aggregates.

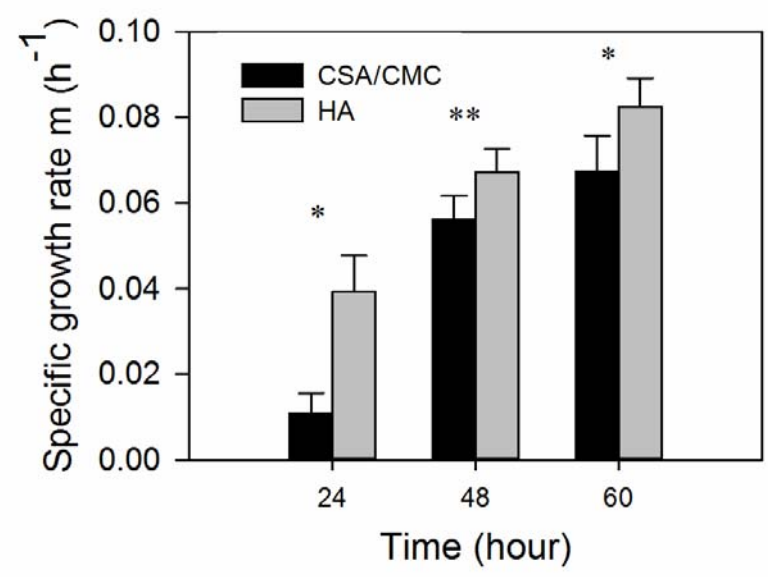

Figure 14. Specific growth rates of aortic smooth muscle cells in HA and CSA/CMC capsules. Specific growth rates were calculated using DNA measurements. Error bars represent standard deviations of 3-5 independent measurements. Significant differences are denoted by single or double asterix (* = $p<0.05$; ** = $p<0.10$).

Specific growth rate of VICs vs. SMCs. In order to study the proliferation pattern of different cell types, MTT assay was employed in our capsules system seeded with different cell types. Porcine smooth muscle (SMCs) cells and valvular interstitial cells (VICs) were seeded in HA and CSA capsules respectively and their specific growth rate were calculated.

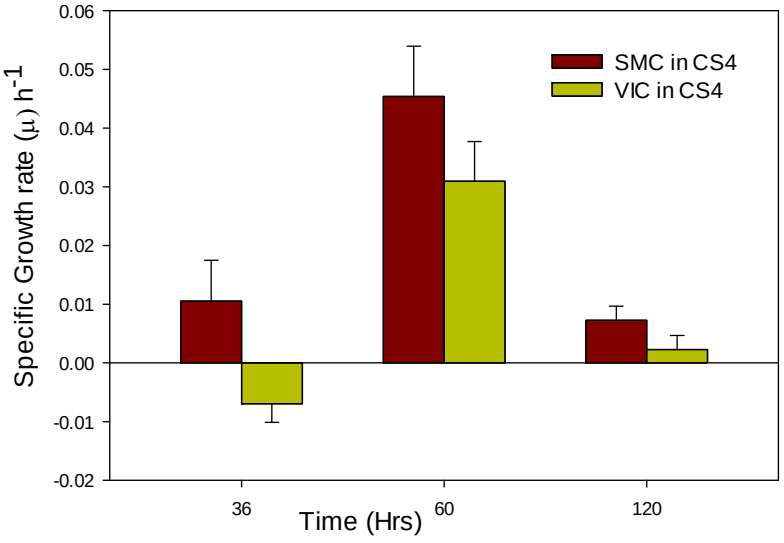

Figure 15: Proliferation of SMCs and VICs in CSA/CMC capsules

Both the cell types followed a similar pattern of growth in CSA/CMC capsules. There was a slow growth initially followed by an exponential increase and finally a lag phase. The initial lag in the growth can be attributed to the initial adaptation time required for the newly seeded cells in our GAG microcapsules. Once the cells overcome the initial shock, they show an exponential increase in the growth rates and that leads to the formation of larger aggregates. The formation of larger aggregates introduces diffusion limitation in to the system that results in the decrease in the growth rates as seen in the charts.

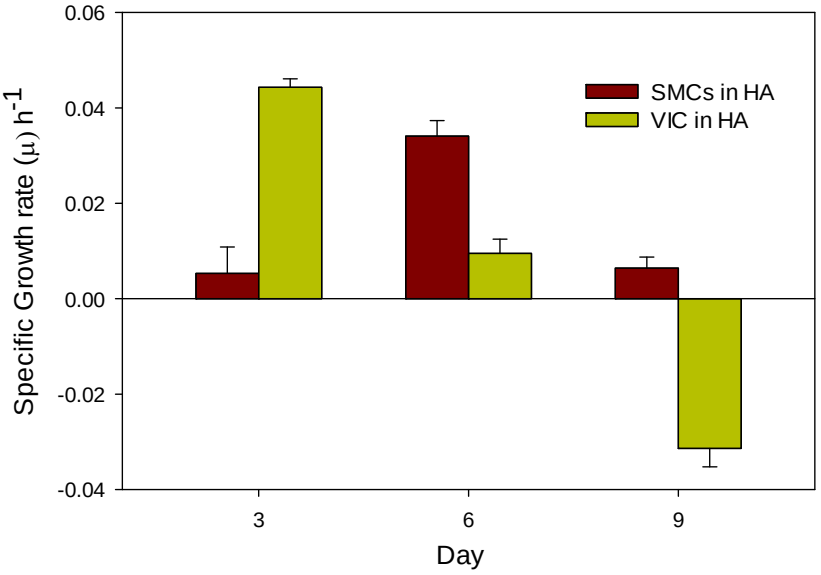

Figure 16: Proliferation of SMCs and VICs in HA capsules

However, the VICs behave differently in the HA capsules as explained previously. The VICs adapted quickly to the HA environment than the SMC and formed larger aggregates that resulted in the decrease of its specific growth rates. These growth patterns suggest the biological phenomenon that can be exploited in our modular systems to recapitulate the in-vivo patterns. We can also intervene in many ways as discussed earlier in the chapter by co-encapsulating collagen or microcarriers to change the growth dynamics of the cells inside the modules.

4.6 Summary and Discussions:

In summary, we have demonstrated the cell encapsulation in GAG-chitosan capsules with physical and biological properties tunable via composition; the capsules support high density cell growth and allow a range of options for adjusting the interior microenvironment; some formulations are fully cell-degradable and permeable to most growth factors and cytokines. The

GAG-based microcapsules described above allow efficient mass transfer, which is evident from the tissue-density cultures that were maintained for up to 45 days under static culture conditions. The diameter of the capsules can be easily controlled between 0.3 and 2.0 mm, and smaller diameters are achievable using more sophisticated droplet formation methods such as microfluidics. In addition, the cell-contractable capsule formulations provide an additional mechanism for modulating cell density within either the capsules or the fused construct. The high density trophoblast cultures were primarily intended to demonstrate the potential of the microcapsules with a highly proliferative human cell type. However, these cultures also provided direct evidence of both the degradability of the GAG-chitosan materials, and the ability of cells to invade the capsule wall.

The trophoblast cell line maintains some characteristics of human trophoblasts, in particular the ability to tolerate hypoxic conditions and to invade tissue rapidly. Both characteristics are presumably related to its original, placenta-formation function (Chang and Vivian Yang 2013) and may be mediated by focal expression of MMPs, GAG lyases or other matrix degrading enzymes. Wall invasion and cell escape in these trophoblast cultures was evident after week 2 of culture and was clearly captured in histological sections. This phenomenon strongly suggests that implanted capsules would present only a temporary barrier to integration of encapsulated cells with adjacent tissues. Coupled with the known pro-angiogenic effects of GAG-based materials (Black, Hudon et al. 1999, Ferretti, Boschi et al. 2003, Mathieu, Chevrier et al. 2013), these results further suggest that rapid vascularization is a likely outcome after transplantation of capsule-based constructs.

CHAPTER: 5

PHYSICAL PROPERTIES OF MODULES

5.1 Introduction

The physical properties of the capsules, especially the wall permeability and capsule integrity is essential to ensure that our modular construct design is non-diffusion limited. In this chapter capsules made out of our stable formulations HA and CSA/CMC representing soft and hard tissue applications respectively were studied to quantify membrane permeability and capsule wall integrity. Establishing the relation between the capsule material properties such as molecular weight and their physical properties, enables us to customize our modular system for specific applications.

5.2 Aim and Rationale

The specific aim of this chapter is to quantify the physical properties of the individual modules that is relevant to ensure a non-diffusion limiting design. In a conventional preformed scaffold, there is a 200μm limit above which the cells are usually subjected to reduced nutrient and gaseous exchange. In our modular design, in order to make sure that each module provides a microenvironment for the encapsulated cells that is not subjected to the 200μm limit, we design the system with minimal resistance to diffusion. This optimization is done without compromising their other key features especially mechanical integrity. In this chapter we studied the capsule wall permeability and wall mechanical integrity to achieve our specific aim.

5.3 Experimental design

Study 1: In the first phase, a suitable biomolecule was chosen (globular protein albumin) to study its diffusion across the capsule membrane. The capsules were loaded with fluorescently tagged albumin and its diffusion across the membrane was fluorometrically quantifies. Modelling was done to calculate membrane permeability from the rate of diffusion curve of albumin.

Study 2: In the second phase, an agitation system was designed to study the capsule wall integrity. A suitable power was fed to the system containing capsules suspended in an aqueous medium using a turbine agitator. The total number of unbroken capsules was then counted at regular time intervals. Using this technique, specific material components with higher influence over the other material components of the capsule wall were identified.

5.4 Material and Methods

5.4.1 Evaluation of capsule wall permeability

The permeability of capsule walls was studied fluorometrically by measuring the rate of diffusion of tetramethylrhodamine-labelled bovine serum albumin (BSA-TMR) from the capsules, as detailed before (Crooks, Douglas et al. 1990, Matthew, Salley et al. 1993, Lin and Matthew 2002). The rate was used to calculate an overall mass transfer coefficient for the capsule wall membrane under mixing conditions.

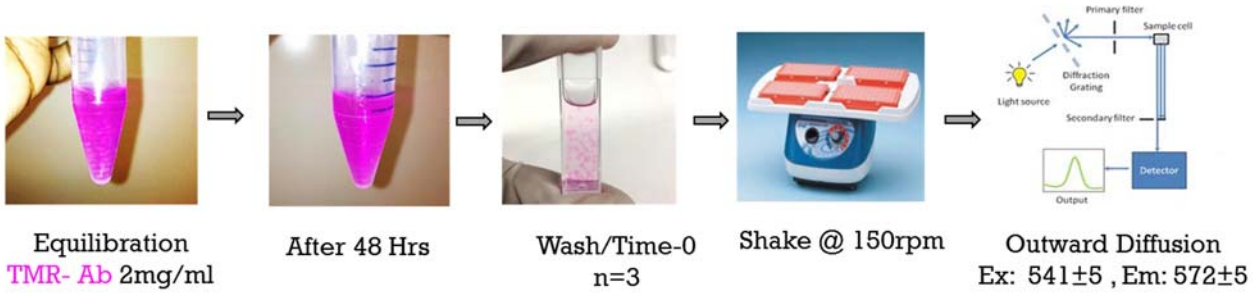

Figure 17: Rate of diffusion of albumin across capsule membrane.

A precise number of capsules (100-150 per sample, n=3) of similar size from each formulation were counted out and equilibrated in HBSS (pH 7.4) containing 2.5 mg/ml BSA (13% TMR-labeled. The equilibration saturated all the BSA binding sites of the capsule wall and efficiently loaded BSA into the capsules. After washing and resuspension in fresh HBSS, the capsules were redistributed into three fluorescence cuvettes (4 ml volume, 1 cm light path) at 35-50 capsules per cuvette. The HBSS volume was made up to 3 ml and the cuvettes were sealed and mixed horizontally on a linear shaker at 100 rpm. The outward diffusion of BSA was followed by measuring the fluorescence of the external HBSS at exitation/emission wavelengths of 541/572 nm at regular time intervals for 3 h. The BSA concentration was determined using a standard curve covering the range of 0-50 μg/mL total albumin. The overall mass-transfer coefficient for diffusion across the capsule wall (K) was calculated by solving the differential equation obtained through an unsteady state mass balance on the external solution (Matthew, Salley et al. 1993).

$$V\frac{dC}{dt} = KA(C_C - C) \tag{1}$$

$$NC_C V_C + VC = NC_\infty V_C + VC_0 = M \tag{2}$$

Where: K is the overall mass transfer coefficient for membrane diffusion; M is the total mass of solute present in the cuvette ($M = C_r(V+NV_c)$); V and V_c are the volume of external solution and volume of capsules, respectively; N is the number of capsules; A is the total surface area (A = N*surface area of single capsule); C is the concentration of solute in external solution; C_o is the initial extracapsular concentration; C_c is the concentration of solute in the capsules; C_∞ is the initial

intracapsule concentration; C_r is the final concentration after end of 3 hours; and t is time. The solution to the equations 1 and 2 yields,

$$\ln(Q) = \left(\frac{KA(V + NV_C)}{NVV_C} \right) t \tag{3}$$

Where Q is a dimensionless concentration-dependent parameter defined as

$$Q = \frac{M - (V + NV_C)C_0}{M - (V + NV_C)C} \tag{4}$$

The overall mass-transfer coefficient for transmembrane diffusion, K, was determined by plotting ln(Q) vs. time and determining the slope of the linear portion of the curve by linear regression. The intrinsic permeability, P, of each capsule wall was determined from the relation:

$$K = \frac{P}{\delta} \tag{5}$$

Where δ is the thickness of the capsule wall.

5.4.2 Evaluation of mechanical integrity: Agitation

An agitation system was designed to study the capsule wall integrity. A suitable power was fed to the system containing capsules suspended in an aqueous medium using a turbine agitator. The total number of unbroken capsules was then counted at regular time intervals. Using this technique, specific material components with higher influence over the other material components of the capsule wall were identified. The figure below shows the agitation system setup. We used a turbine agitator and accordingly the power number for the calculation are used.

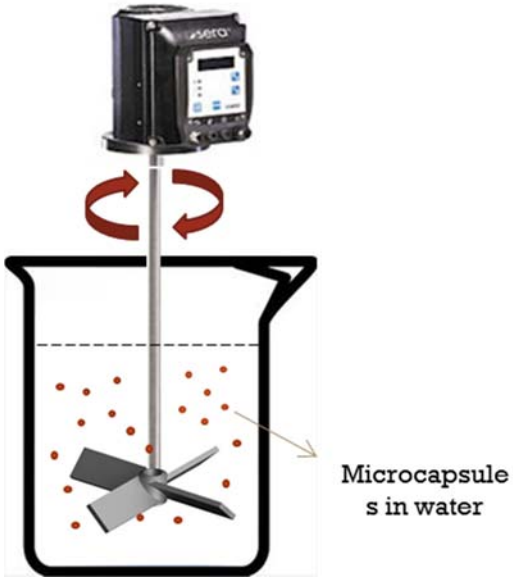

Figure 18: Agitation system setup for capsule wall integrity.

The formula used to calculate the total power fed was as follows:

Power Analysis: $P = N_p {D_a}^5 n^3 \rho$

N_{Re} (Reynolds Number)= 300 $N_{Re} = \frac{{D_a}^2 n \rho}{\mu}$

D_a(Diameter of propeller)= 0.05 m

ρ (Fluid Density)= 1,000 kg/m^3

n = Rotations per sec (r/s)

μ (Fluid Viscosity)= 8.9 x 10^{-4} kg/ms

Np = Power number (Exp. values)

5.4.3 Methacrylation of HA

Hyaluronic acid is derivatized to make them photopolymerizable as described previously (Bencherif, Srinivasan et al. 2008). Briefly, 100X molar excess of glycidyl methacrylate

containing an epoxy ring was used to introduce unsaturated bonds in the hyaluronan chains in the presence of dimethylformamide (DMF) and triethylamine (TEA) (Figure:19). We were able to achieve 32% degree of Methacrylation.

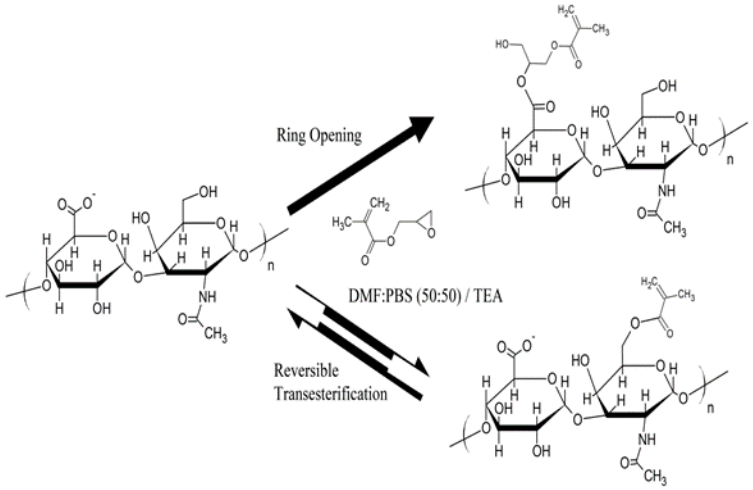

Figure 19: Methacrylation of Hyaluronan (HAGM – Hyaluronan-glycidyl methacrylate). **Image reference:** Bencherif et al. Biomaterials 29 (2008) 1739-49

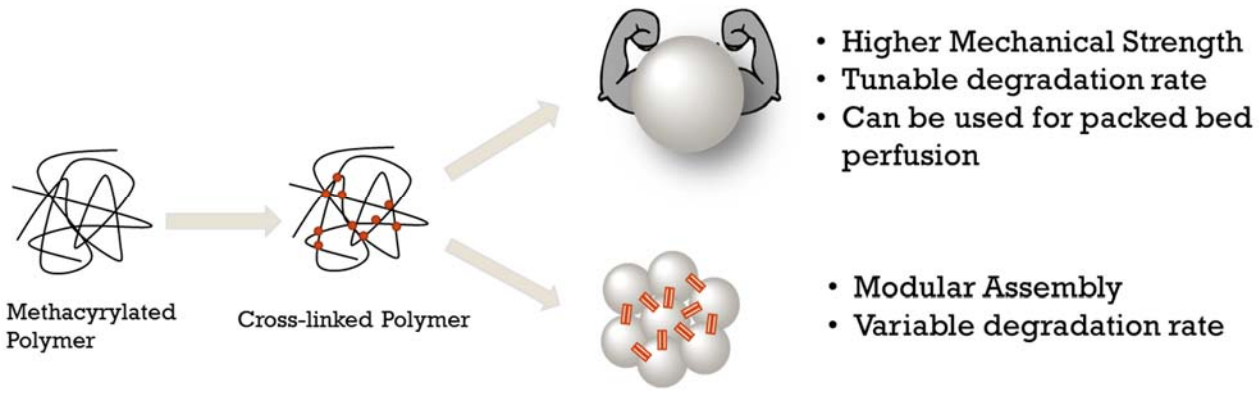

Figure 20: Photopolymerizable capsule materials.

These photopolymerizable capsule materials can be used to enhance the mechanical strength of individual capsules and to tune their rate of degradation in-vivo. They can also be used

as a tool to fuse the capsule during modular fabrication process (Figure: 20). This is particularly useful in applications that need a high mechanically stable structures.

5.5 Results

5.5.1 Capsule membrane permeability

Results of the diffusion studies on encapsulated BSA are shown in Figure 6. A typical plot of the dimensionless concentration factor ln (Q) vs. time, for three replicates runs of the CSA/CMC capsule formulation is shown in Figure 21. The higher slope of the curve observed at early time points, is likely due to the rapid desorption of weakly bound albumin from the capsule wall. For our diffusion calculations, only the slope of the later, linear portion of the curve was used. Figure 22 compares the values of the overall mass-transfer coefficient (K), permeability coefficient (P), and wall thickness (δ) for the two most stable capsule formulations (HA and CSA/CMC). As expected, the HA capsules exhibited ~3 fold higher permeability than CSA/CMC capsules due to the higher molecular mass of HA and its expected formation of a looser polyelectrolyte complex network with chitosan. However, the overall mass transfer coefficient which correlates directly with the overall rate of BSA diffusion from capsules was higher in the CSA/CMC capsules, mainly due to their thinner walls. Significant post-formation swelling was also observed in CSA/CMC capsules, which nearly doubled their initial diameter. No such swelling was observed with HA capsules. Overall, the results indicate that both capsule types are permeable to globular proteins of moderate size, and suggest that the permeability of the capsule wall might be further tunable via the molecular weight of the capsule materials.

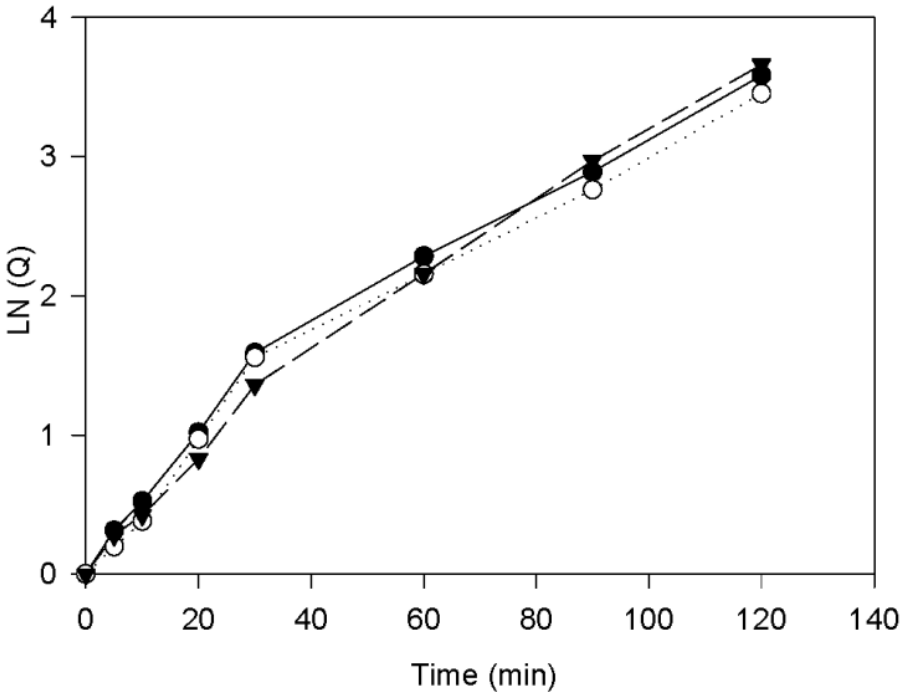

Figure 21: Albumin diffusion profile of CSA/CMC capsules. Representative plots of the concentration factor ln(Q) vs. time for three replicate runs with the CSA/CMC capsule formulation.

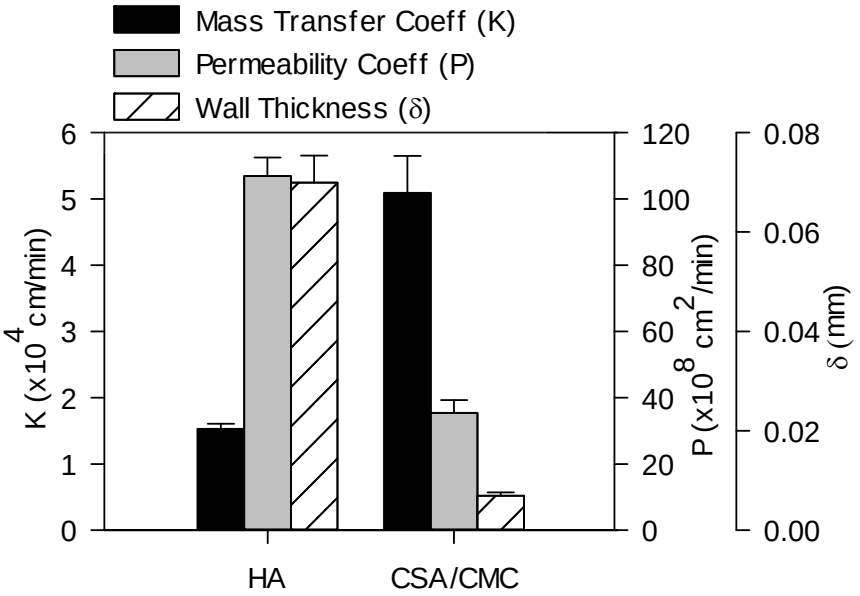

Figure 22: Mass transfer characteristics of HA and CSA/CMC capsules. Plots of permeability coefficient (P), overall mass transfer coefficient (K) and wall thickness (δ) for the HA and CSA/CMC capsule formulations. Error bars represent the standard deviation of three replicate measurements.

5.5.2 Capsule membrane mechanical Integrity

The mechanical integrity of four types of capsules were compared using our agitation system. Two molecular weight of CMC (mCMC: 250 kDa, hCMC : 700 kDa) and two molecular weights of chitosan were chosen (LC : 50-190 kDa,HC : >375 kDa) and four types of capsules were made using four possible combination of the materials. Capsules were carefully fed in to the agitation system and intact capsules were counted at 30 min time interval. The graphs were ploted as shown in figure 23. The results show that CMC has more influence over capsule integrity than chitosan, this shows that the molecular weight (MW) of the material components influence capsule mechanical strength. Therefore, MW helps to tune the physical and biological properties of a modular construct which makes our modular system very versatile.

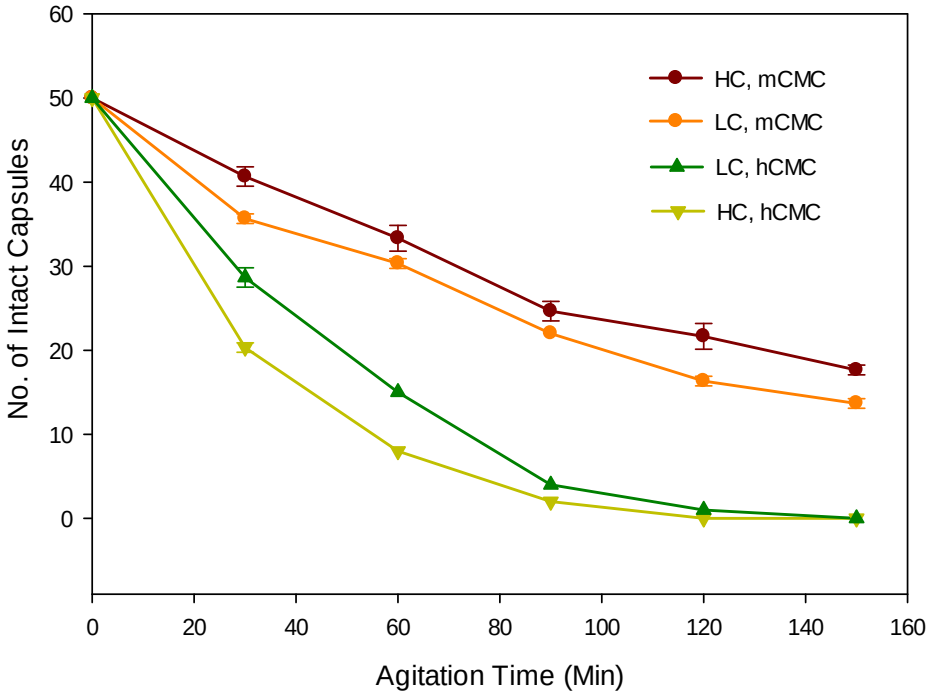

Figure 23: Capsule wall integrity. Low Vs. High MW of Chitosan and CMC

5.5.3 Photopolymerizable capsule materials

The capsules made out of HA and HAGM were subjected to mechanical agitation and total number of intact capsules were counted over time. As expected, the plots in figure 24 shows that photopolymerized HAGM stayed intact compared to normal HA.

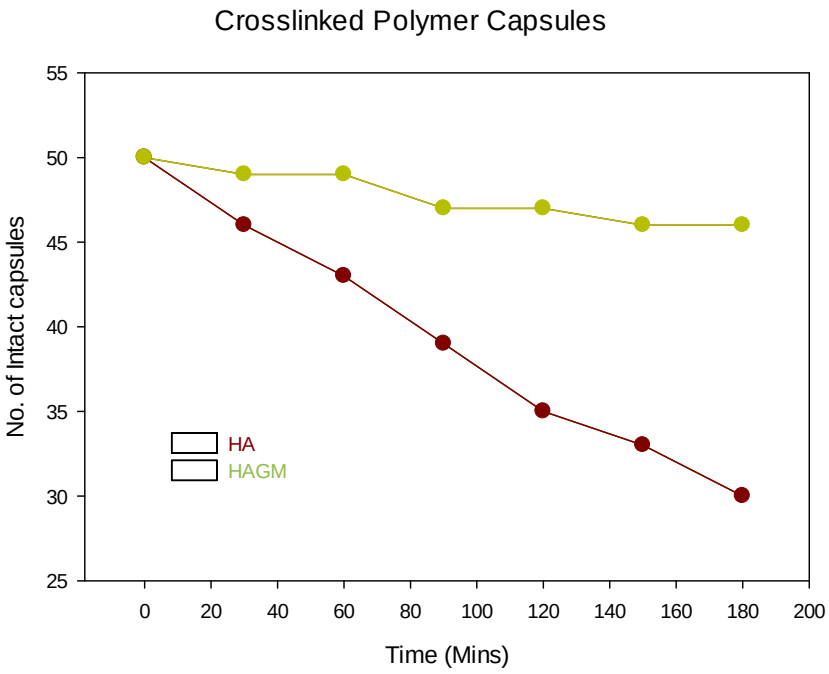

Figure 24: Capsule wall integrity. Ha vs. HAGM capsules

5.6 Summary and Discussions:

The GAG-based microcapsules described above allow efficient mass transfer, which is evident from the high mass-transfer rates. In principle, diffusion challenges can be minimized by choosing the right biopolymer with specific molecular weight to ensure an adequate supply of nutrients and oxygen to all regions of the cell mass. Diffusion inside capsules can be further modulated by controlling the extent of cell distribution and aggregation. Further, photopolymerizable capsule materials can be used to enhance the mechanical strength of individual capsules and to tune their rate of degradation in-vivo. They can also be used as a tool to fuse the capsule during modular fabrication process. This is particularly useful in applications that need high mechanically stable structures.

CHAPTER: 6

SEEDING CELLS ON OUTSIDE WALL FOR VASCULARIZATION

6.1 Introduction

The important step in fabricating a modular construct is to embed a network of inter-connected channels that can enable us to develop non-diffusion limited constructs. This is particularly helpful in case of thick constructs and constructs with high metabolic cells. In addition, the inter-connected channels can also be endothelialized to pre-vascularize the construct. Endothelialization of the channels can help promote rapid vascularization of the construct, upon transplantation in to a suitable host. This chapter details the process of rendering the outside surface of the capsules amenable for endothelial cell attachment and spreading. Simple ways to enhance the surface with receptors for endothelial cell attachment are discussed. The ability of seeded endothelial cells to form a monolayer and express tight junction proteins were also elucidated. Finally, the functional influence of the endothelial cells on the growth and proliferation of parenchymal cells on the inside of the capsules were also analyzed.

6.2 Aim and Rationale

The specific aim of this chapter is to modify the outside surface of capsules to accommodate endothelial cells. The rationale of this specific aim is that this will enable us to promote vascularization of the tissue constructs assembled using microcapsules and reduces thrombogenesis of blood contacting surfaces. This will enable us to achieve efficient diffusion and this can reduce necrosis in long term cultures. Regulatory mechanism and functional relationship between different cell types can also be reproduced by achieving this specific aim. This

prevascularization technique may also promote diffusion and nourishment by integrating with the host vasculature post implantation.

6.3 Experimental approach:

Study 1: Endothelial cells were seeded on outside capsule wall integrated with proteins. Endothelial cells were seeded on the outside wall of the microcapsules and cell adhesion, proliferation and migration were monitored using phase contrast microscopy, histology and immunohistochemistry.

Study 2: Endothelial cells were seeded on outside wall coated with collagen, and bovine serum proteins. The microcapsules were washed with ECM polymers like collagen or other cell adhesion supporting biopolymers like gelatin and endothelial cells were seeded on them. Cell adhesion, proliferation and migration were monitored over time using phase contrast microscopy, histology and immunohistochemistry.

6.4 Material and Methods

Cell adhesion, proliferation and migration were monitored over time using phase contrast microscopy, histology and immunohistochemistry.

6.4.1 Endothelial cell seeding on capsule surfaces

Capsules were coated with an adsorbed layer of Type I collagen prior to externally seeding endothelial cells. For coating collagen on the outer surface, non-surface stabilized capsules (i.e. capsules without a PGA final wash) were washed in dilute acidic collagen solution (0.2 mg/ml of collagen in 1 mM acetic acid) for 1-2 min and then equilibrated with culture medium for 30 mins.

Capsules that had been previously surface stabilized with PGA, were first washed with dilute chitosan solution (0.06% chitosan) prior to the dilute collagen wash. The equilibration culture medium was then removed and an endothelial cell suspension (HUVECs or AECs) in medium was added to settled capsules in a 50ml centrifuge tube. Cells were seeded at a density of 10^6 cells per ml of capsules and incubated at 37°C for 60 minutes with gentle resuspension every 10 min. After incubation, the seeded capsules were transferred to bioreactor chambers or tissue culture dishes for further experiments.

6.5 Results:

6.5.1 Endothelial cell growth on capsule surfaces

The growth of sheep aortic endothelial cells (AEC) and HUVECs was investigated by seeding these cells onto the outside surfaces of CSA/CMC capsules. Endothelial cells attached poorly to surface stabilized capsule surfaces. However, their attachment and growth greatly improved when type-I collagen was coated onto the outer surface of the CSA/CMC capsules. HUVECs seeded on the collagen coated CSA/CMC capsules attached well and formed a viable monolayer within 24 hours of seeding (Figure 25). SEM images of capsules fixed 1 hour post-seeding (Figure 26B) showed a continuous, but irregular monolayer of cells in varying stages of spreading. SEM images 24 hours after seeding showed a well spread and smooth endothelial monolayer, with few areas of exposed capsule surface (Figure 26C). This morphology was maintained for at least 14 days under static culture conditions.

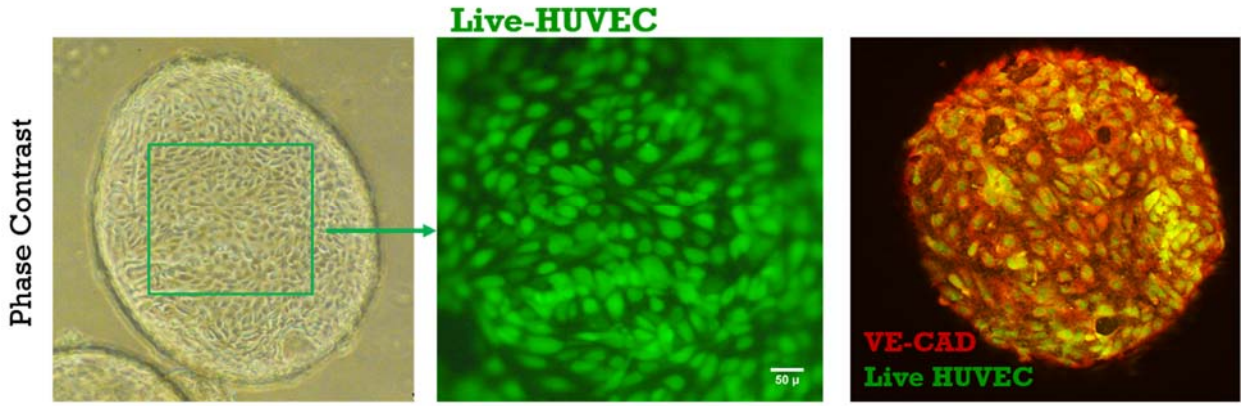

Figure 25: Capsules coated with collagen formed HUVEC monolayer with tight junctions.

This method has potential to vascularize the construct made by assembling these capsules. Although these EC layers didn't structurally match with the native vascular structure, they are expected to fasten the process of neovascularization and reduce thrombosis.

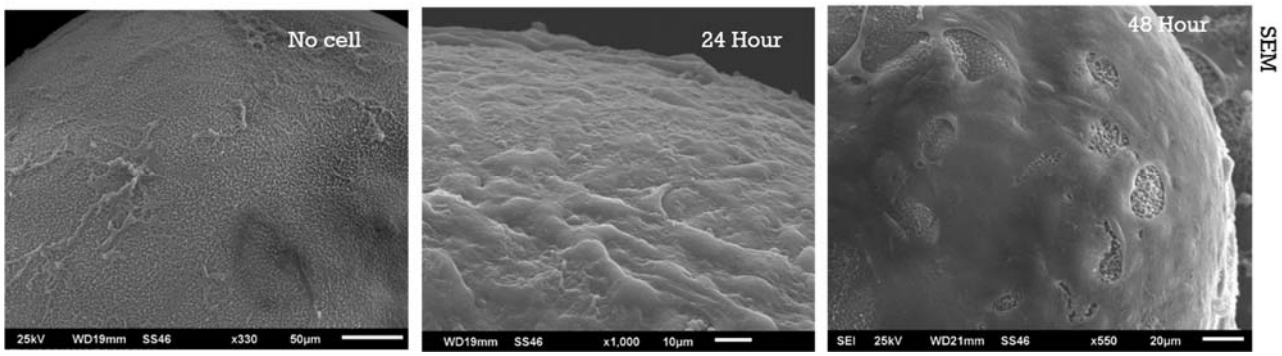

Figure 26: SME images of HUVEC monolayer with tight junctions.

6.5.2 Functional influence of endothelial on parenchymal cells

Regulatory mechanism: There are many studies explaining the regulatory mechanism and functional relationship that exist between different cell types especially between vascular and parenchymal cell types. Both proliferating and quiescent vascular endothelial cells (VECs) are shown to promote series of reactions that enhances SMC proliferation in a SMC/VES coculture system. Here we designed a similar coculture system using microcapsules, by encapsulating SMCs in HA capsules with collagen matrix and seeding VECs on the outside of the capsules. We compared these cocultured capsules with capsules that were seeded with SMCs on the inside but lacking VECs on the outside. After two days of culture, cocultured capsules had larger aggregates compared to those of the control system and this is more pronounced by the end of first week (Fig 27). This suggests that this method of coculturing of cells in the capsule system can be utilized to enhance SMC proliferation during maturation of modular constructs and simultaneously vascularize the construct after assembly

6.6 Summary and Discussions:

In summary, we have demonstrated that the outer surface of the capsule wall can be modified with collagen to provide suitable surface for endothelial cell to attach and proliferate. Washing the outer surface with collagen also enhanced cell adhesion and migration and resulted in the formation of an endothelial monolayer. Also the HUVEC monolayer exhibited tight junction markers as commonly exhibited by the endothelium of the blood vessels. This is essential to render the surface non-thrombogenic and simultaneously can accelerate vascularization in-vivo. Culturing SMCs with VEC also promoted SMC proliferation which is evident from larger aggregates and proliferation assays. This suggests that the capsule membrane is permeable and can

support paracrine signaling seen in vivo. Hence, the endothelial cells seeded on the modified outside surface has significant functions including endothelialization, enhanced perfusion, and functional influence on the encapsulated parenchymal cells.

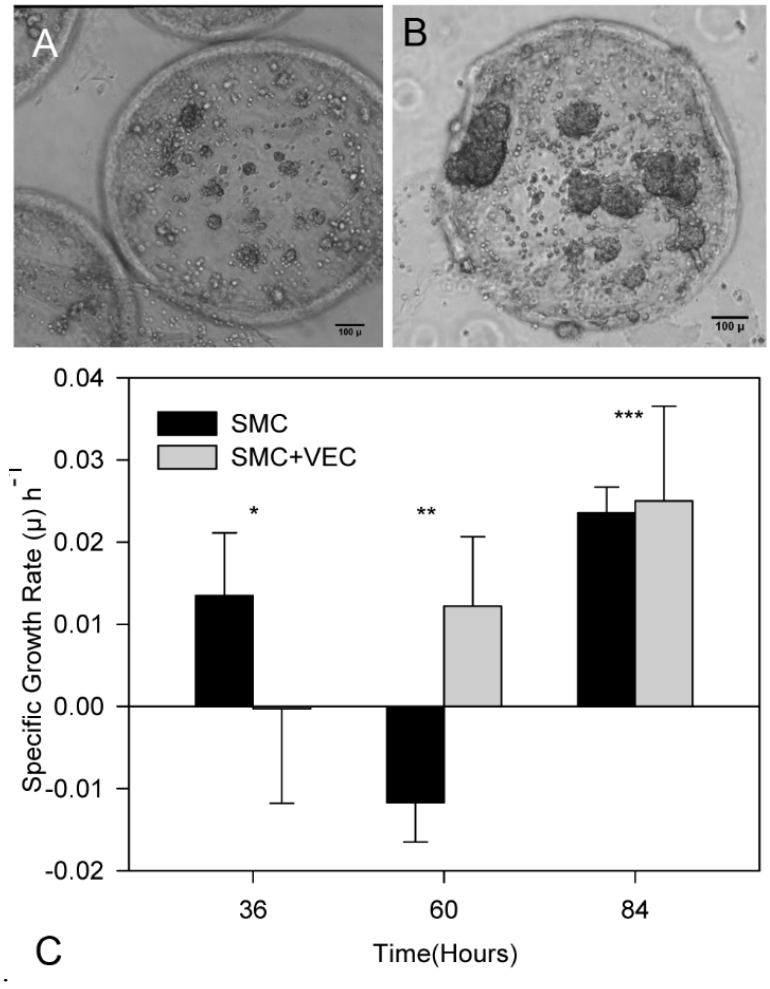

Figure 27: Cell growth in encapsulated cocultures of SMC and AEC. Cocultures of encapsulated SMCs with AECs on the external surfaces of HA/Collagen capsules exhibited increased SMC proliferation compared to encapsulated SMC monocultures. (A) Encapsulated SMCs only, day 7. (B) Encapsulated SMC with AECs, day 7.

CHAPTER: 7

MODULAR FABRICATION

7.1 Introduction:

The specific aim of this chapter is to develop methods for assembling 3D constructs. Compared to the conventional tissue engineering method, which is essentially a top-down approach, modular tissue engineering is a bottom-up approach, in which a tissue is fabricated by assembling discrete modules containing parenchymal and vascular components. This chapter explains the process and merits of this bottom-up assembly. The fabrication methods were developed to make self-supporting structures while keeping the inter-connected channels intact. Different ways to tune the inter-capsular spaces and overall cell density were also elucidated.

7.2 Aim and Rationale:

The objective of this specific aim is to develop methods for fabricating 3D constructs through the assembly of microcapsules. The rationale is that this modular fabrication strategy will recreate the modular architecture of natural organs that can facilitate optimal performance and development of the bioartificial construct by maintaining their native structure. This modular fabrication approach will also promote stability, reduce interdependency among different components of the construct and facilitate more control in engineering fine microstructure details of constructs.

7.3 Experimental approach:

Study 1: Self-supporting constructs were made by fusing microcapsules reloaded with biopolymer solution.

Microcapsules seeded with cells were reloaded with suitable anionic biocompatible polymer and fused with each other ionically using another cationic polymer like mild acidic chitosan to from a self-supporting construct. Histological analysis was performed to study porosity, capsule arrangement and strength of the construct was also determined.

Study 2: Chitosan membranes were used for capsule-fabrication to provide additional support.

Membranes made of chitosan with appropriate thickness may also be used as a means of support to fabricate constructs with desired structure. Histological analysis was performed to study porosity, capsule arrangement and strength of the construct was also determined.

7.4 Materials and Methods

Analysis criteria: Capsule arrangement in the fabricated construct, strength and porosity of the 3D construct were analyzed. Capsule arrangement and porosity is important to enable a network of interconnected, endothelial cell-lined channels to facilitate vascularization and mass transport. Histological evaluation were performed to analyze the above mention criteria. Scanning electron microscopy was also be used to determine the porosity and capsule arrangement.

7.4.1 Assembly of non-surface stabilized capsules

Individual capsules were fused into 3D constructs in one of the two ways. In the first method, freshly formed capsules were fused by allowing them to sit in contact with each other after the second saline wash, but before the surface stabilizing PGA wash. Freshly formed capsules were washed once with normal saline and then transferred in saline to a cylindrical mold with a 250 micron mesh at the base. Capsules were allowed to settle within the mold and held stationary for 2-3 minutes to allow inter-capsule adhesion. The excess saline was then drained and the capsule surfaces in the fused construct were then stabilized by briefly rinsing with saline, followed by a diluted polyanion solution (i.e. 0.1% PGA or 0.4% CSA/0.15% CMC), followed by a final PBS rinse.

7.4.2 Assembly of modular constructs by perfusion

In the second fusion method, previously stabilized and cultured capsules were first reloaded with a polyanion by incubation in a diluted polyanion solution (0.1% heparin or 0.4% CSA/0.15% CMC). The capsules were then transferred to a cylindrical mold with the mesh base. After draining excess polyanion solution, the mold with reloaded capsules was perfused with 0.06 wt% chitosan solution to ionically fuse the capsules. Excess chitosan solution was drained, the capsules were rinsed with normal saline and surface stabilized by a brief perfusion with a dilute polyanion solution. The fused modular construct was then removed from the mold for further culture or analysis.

7.4.3 Imaging of interconnected channels.

For long-term tracking of HUVECs on capsules and fused capsule constructs, CellTracker™ Green CMFDA (Invitrogen) was used. Briefly, adherent cells were rinsed with PBS and incubated in a serum free culture medium containing 5 μM CellTracker Green probe for 45-60 min. After the incubation the medium was replaced with pre-warmed normal medium and incubated for another 30 min for the dye to undergo modification due to intracellular esterases. The cells were then trypsinized and seeded onto capsule outer surface. Cell fluorescence was then observed using wide-field fluorescence microscopy and laser scanning confocal microscopy (Zeiss LSM-410).

7.5 Results:

7.5.1 Assembly of capsule modules

Assembly of capsules into three-dimensional modular constructs is a critical step in our modular tissue engineering approach to generate vascularized tissue. We investigated various methods for assembling larger 3D constructs from pre-cultured individual capsules. The most successful method involved reloading cultured capsules with a polyanion, followed by perfusion with a diluted polycation solution. Outward diffusion of reloaded GAG during the polycation perfusion step deposited a polyelectrolyte complex that effectively fused capsules together around points of contact. This method yielded self-supporting structures with interconnecting, perfusable spaces as shown.

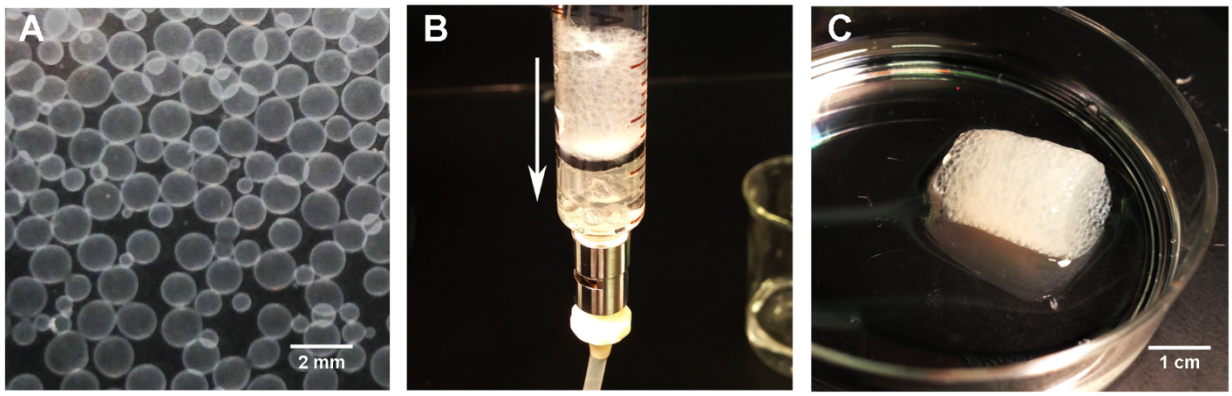

Figure 28: Modular assembly of GAG based microcapsules by fusion.

Modular constructs were fabricated by perfusing packed capsules in a chamber of desired dimensions with diluted polymer solutions. This method yielded self-supporting constructs with uniform porosity (Figure 28, 29). (A) Individual capsules in buffer solution before fusion. (B) Capsules being perfused with polymer solution in a perfusion chamber. Arrow indicates direction of flow. (C) Fused construct after removal from perfusion chamber.

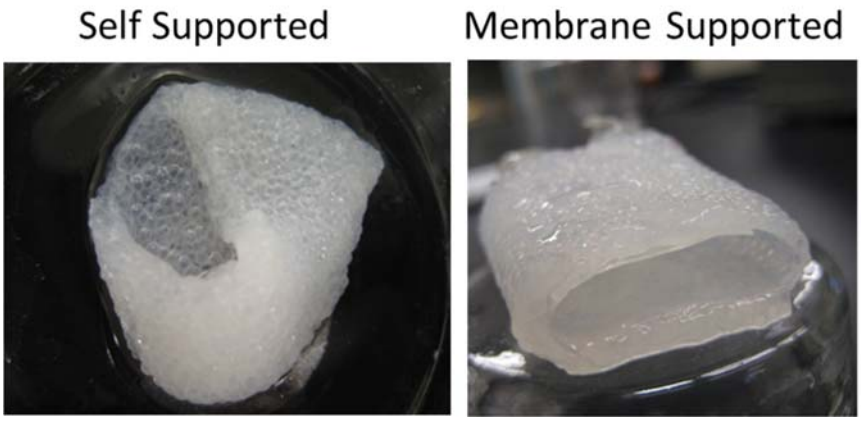

Figure 29: Self supported and Membrane supported structures

The capsules formed self-supporting stable modular structure and no structural deformation were seen at least for 24 hours (Fig 29). The modular constructs made with additional support from chitosan membranes were more stable with a smooth lumen (29).

Capsules that were surface-seeded with HUVECs and subsequently fused showed well endothelialized, interconnected channels as seen in phase contrast (Figure 30A) and confocal images (Figure 30B). SEM imaging of an axial section through a fused construct shows the interconnected channels more clearly (Figure 30C).

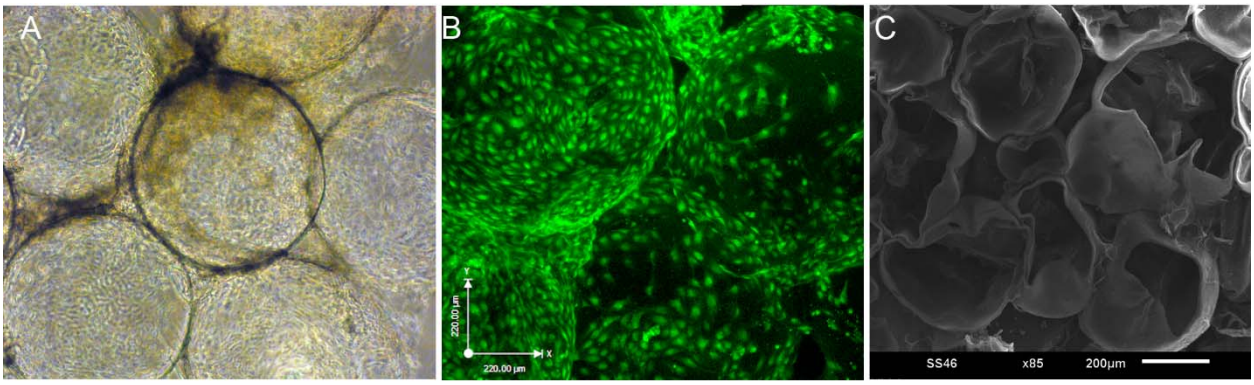

Figure 30: Endothelialized, interconnected channels in a fused modular construct.

(A) Phase contrast image of CSA/CMC capsules, seeded externally with HUVECs and fused 48 hours after seeding. (B) Combined confocal image stack of the modular construct shown in A with HUVECS visualized via CellTracker Green staining. (C) SEM image of an axially sectioned, modular construct assembled from fused empty capsules showing interconnected channels.

7.5.2 Tuning Cell density and inter-capsule space

In a modified procedure, fusion-based assembly of high cell density capsules was explored by encapsulating primary rat hepatocytes in HA-collagen capsules at a density of $10x10^6$ cells/ml of the HA/collagen solution, followed by heparin reloading, and centrifugation for 10 seconds at

50G to expel excess intracapsular liquid. H&E stained sections of the resulting construct showed a dense cell mass (~$5x10^7$ cells/cm^3, estimated via image analysis) with reduced, but still significant intercapsule spaces (Figure 31 A-B). Encapsulated hepatocyte constructs assembled without centrifugation showed a much less dense cellular construct (estimated at $9x10^6$ cells/cm^3 via image analysis) with more and larger intercapsule spaces (Figure 31 C-D). These results demonstrate that additional physical processing methods can be used to further adjust the effective cell density and perfusable void space within these modular constructs.

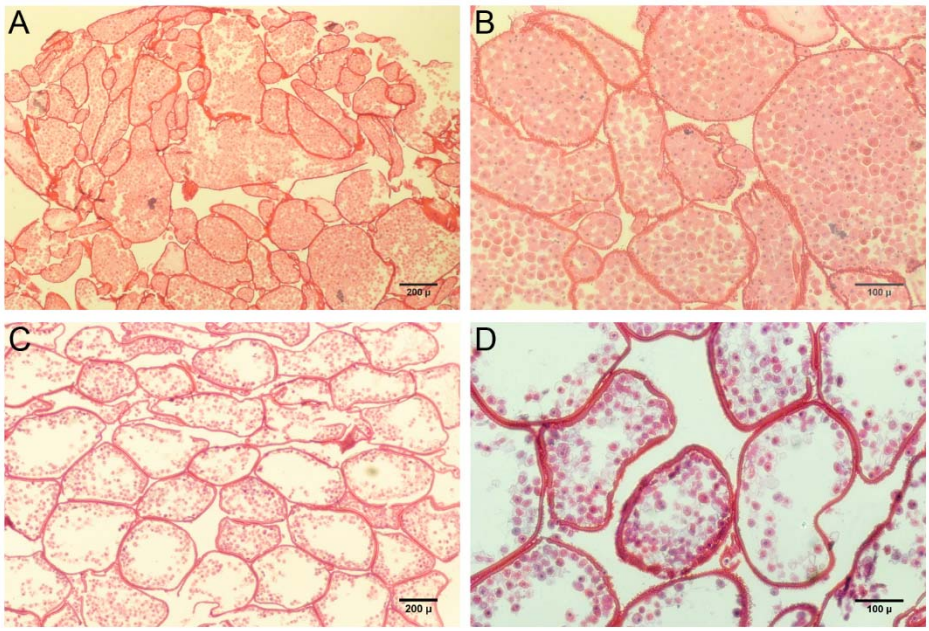

Figure 31: H&E staining of modular constructs based on hepatocytes in HA/collagen capsules. (A, B). Fused construct with reduced fluid volume and porosity due to centrifugation of capsules during the fusion process. (C, D) Construct formed by fusion of capsules settled under unit gravity, resulting in significantly greater fuid volume inside capsules and larger intercapsular spaces suitable for perfusion culture.

7.6 Summary and Discussion:

In summary, we have demonstrated that capsules can be fused to form stable 3D structures with or without membrane support. Fusion of the endothelialized capsules generated 3D constructs with an embedded network of interconnected, endothelialized channels that can support long-term perfusion in vitro and vascularization in vivo. After the fusion of the capsules, the endothelial cell layer on the outside of the capsules stayed intact and all the endothelial cells remained viable. The interconnected channels in the 3D construct also remained open after the fusion that involved reloading and perfusion of GAG and chitosan respectively.

The long term effects due to acidic chitosan wash, on the performance of the endothelial cells still need to be studied. The state of the endothelial monolayer after fusion, also need to be investigated as quiescent phenotype is more preferred for vascularizing our constructs and a proliferative phenotype may lead to pathophysiology. The SEM and histological data suggest that the inter-capsular space is available in our fused constructs for perfusion of medium or blood. The fusion protocol can also be used to control the cell packing density in our constructs. We have demonstrated that our fusion protocol can be modified to pack the capsules at higher cell densities that can be of clinical significance. Overall our fusion protocol yielded stable 3D constructs with tunable intercapsular space and cell densities.

CHAPTER: 8

IN-VITRO PERFUSION CULTURES

8.1 Introduction

Microvasculature of native tissues exhibit well defined structures such as basement membrane, lumen and functional biomarkers that are presented in a spatial architecture that supports tissue function. Traditional methods for recreating this microarchitecture fall short of the aforementioned basic requirements, as attempts to seed endothelial cells on the open channels in scaffolds resembles very less of the native vessel structure, and diffuse seeding of endothelial cell suspension enable limited interconnected vessel formation. Hence, there is a need for technologies to embed an intrinsic vasculature in an engineered tissue to enhance cell viability and tissue functionality.

Our goal is to improve the viability and thereby the functionality of an engineered tissue by enhancing its vasculature. We relied upon microfabrication techniques developed in our lab to fabricate tissue constructs with interconnected channels that resembles spatial architecture of native tissue vasculature. Perfusion bioreactors enable us to overcome the diffusion limitations associated with the preformed porous scaffolds. In addition, the flow mediated shear can induce mechanical stimuli that have functional consequences. For instance, the hydrodynamic shear at physiological range can render the endothelial cells non-thrombogenic and hence enhance its functionality as flow channels for blood. We proposed a method of fabricating vascularized constructs by fusing cell laden microcapsules as described in the previous chapters (Tiruvannamalai-Annamalai, Armant et al. 2014). Here, we analyzed various controllable

parameters experimentally and analytically with the aim of predicting the usable limits of our modular scaffolds in maintaining tissue density cultures.

8.2 Aim and rationale:

The specific aim of this chapter is to develop design parameters for maintaining hepatocyte and endothelial cells in perfused modular constructs by testing our cell seeded 3D fused modules with their interconnected channels for long-term perfusion. The hypothesis is that these interconnected channels can increase the perfusion of blood or medium which in turn will enhance the efficiency of the tissue constructs by increased supply of oxygen and nutrients to the cells compared to that of a porous scaffold. In this chapter major design parameters such as flow rate, shear stress, pressure drop and mass transfer rates were used to predict the optimal operating conditions of our modular constructs in a perfusion bioreactor. Using the calculated values, the system was operated and the metabolic performance of encapsulated hepatocytes was tested. The performance of the interconnected channels in our modular constructs was validated by comparing the metabolic data of the perfusion cultures to that of the standard sandwich cultures.

8.4 Experimental and design approach:

8.4.1 Design and fabrication of the bioreactor:

System description: Packed bed bioreactor system with spherical aggregates with following parameters: Dr = Diameter of the packed bed, Dp = Diameter of the aggregates/capsule, Lc= Length/Height of the construct, μ = Viscosity at 37^{o}C (Culture medium= 0.692*10-3 kg/m.s), ρ = Density at 37oC (Culture medium = 993 kg/m3), ε = Void fraction of the bed (0.4 - standard for bed with spherical particles). This may also be found experimentally by pressure drop calculations.

The following derivations are for a cylindrical packed bed chamber and can be used for rectangular chambers with similar cross section area with uniform flow.

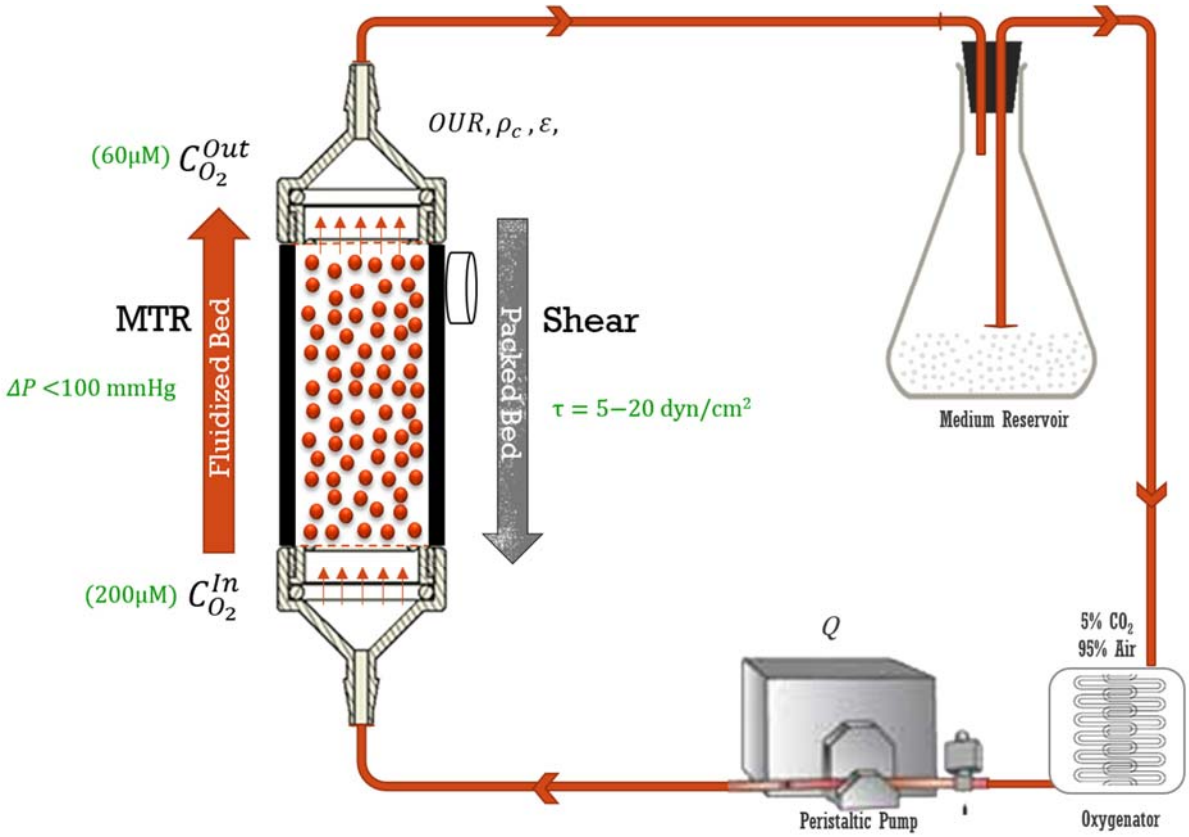

Figure 32: Schematic representation of our perfusion bioreactor

Design Constraints: Fluidized/Packed-bed perfusion culture

1. Shear Stress to maintain endothelial physiology: 5-20 dynes/cm2
2. Oxygen depletion to prevent hypoxia: >60μM dissolve O2 conc.
3. Pressure drop <100 mmHg to prevent bed compaction.
4. Maintain laminar flow to maintain endothelial quiescence: NRe<20

8.4.1 Modelling flow conditions

8.4.1.1 Flow characterization:

The Reynolds number for the flow inside the packed bed was used to determine the flow characteristics in our packed bed system.

$$N_{Re} = \frac{d_p \rho V'}{\mu(1-\varepsilon)} \quad (1)$$

Where, μ = Viscosity at 37°C (Culture medium= $0.692*10^{-3}$ kg/m.s), ρ = Density at 37°C (Culture medium = 993 kg/m^3), ε = Void fraction of the bed (0.4 - standard for bed with spherical particles). This may also be found experimentally by pressure drop calculations and V' = Superficial velocity = Total flow rate per unit cross-section area$\left(V' = \frac{4Q}{\pi D_r^2}\right)$.

$$N_{Re} = \frac{4\, d_p \rho\, Q}{\mu\, \pi\, {D_r}^2 (1-\varepsilon)} \quad (2)$$

Where, Q = flow rate in ml/min, D_r = diameter of the perfusion chamber or the modular construct. The Reynolds number for the flow with capsules of 500-1000μm in dia is calculated and found to be N_{Re} = 0.12 @ 20 dyn/cm^2 shear stress. For all the other conditions of shear < 20 dyn/cm^2 and dia <200μ the Reynolds number of the flow is below N_{Re} < 0.12. Hence, flow is considered laminar in all the following plots. Since, N_{Re} is very low, the convective terms are negligible and the shear stress is linearly related to the imposed inlet flow rate.

8.4.1.2 Shear stress

The flow of blood on the endothelial surface is generally considered as Newtonian except at very low shear rates (Barakat and Lieu 2003). The hemodynamic stress due to blood flow exposes the endothelial cells to shear stress (τ), hydrostatic pressure (p) and tensile stress (σ). Wall shear stress is the most important of the mechanical stress forces that is known to impact the endothelial physiology extensively (McCormick, Eskin et al. 2001). Some of the shear stress responsive phenomenon include angiogenesis, regulation of vascular tone, thrombosis and modulation of immune response (McCormick, Eskin et al. 2001, Ohura, Yamamoto et al. 2003). Depending on the diameter of the blood vessels, the endothelium experiences unidirectional shear stress in the range of 5-20 dyn/cm^2 due to blood flow. They express adaptive response to these hemodynamic stimulus in many ways such as by cell alignment, increasing mechanical stiffness, and expressing genes to promote anti- thrombogenicity. Hence, maintaining the shear stress in this range in our modular system can be beneficial to maintain the endothelial physiology. Therefore, we considered this limit as the set points for the endothelial cells in our modular constructs and analytically defined the other controllable parameters such as flow rate, module diameter and porosity. The equations for the analytical calculations are derived as follows.

Blake-Kozeny equation for laminar flow (Geankoplis 2003) through a porous scaffold with cylindrical interconnected channels is given by,

$$\Delta P = \frac{150\mu V' L_c (1-\varepsilon)^2}{{d_p}^2 \varepsilon^3} \quad (3)$$

Where, L_C = Length of the construct, void fractions less than 0.5, effective particle diameter d_p, and $N_{Re,p}$<10. In order to find the relaton between flow rate and shear stress, the pressure loss was

derivated as follows. pressure difference across a straight, cylindrical channel, of diameter D_p, was related to shear stress τ by:

$$\Delta P = \frac{4\tau L}{D_p} \quad (4)$$

The equation (4) was modified to account for the rhombohedral nature of the interconnected channels in our modular construct containing spherical modules (Niven 2002). Hence hydraulic radius R_H is considered for the non-circular conduits of our modular construct (Avgoustiniatos and Colton 1997). Hydraulic radius R_H, or characteristic dimension of the porous medium, is the ratio of the volume of voids (V_v) to their surface area (A_v).

$$D_p = \frac{V_v}{A_v} = \frac{V_v/V_T}{A_v/V_T} = \frac{\varepsilon d_p}{6(1-\varepsilon)} \quad (4)$$

Where, V_T the total volume of the packing, and d_p the diameter of a spherical modules. Clearly, represents R_H obtained by integrating the area and wetted perimeter over the length of the conduit.

V_v=V_T as the porosity, whilst A_v=V_T is the product of the surface area of a single particle, $A_p = \pi d_P^2$, multiplied by the number of particles per unit volume, $N = [(1 - V_v)/V_p]/V_T = 6(1 - \varepsilon) = \pi d_p^3$. This formulation assumes infinitesimal points of contact between solid particles, and the absence of dead pores which do not experience flow.

$$\Delta P = \frac{150\mu V' L_c (1-\varepsilon)^2}{{d_p}^2 \varepsilon^3} = \frac{4\tau L\ 6(1-\varepsilon)}{\varepsilon d_p} \quad (5)$$

$$\tau = \frac{6.25\ \mu V'(1-\varepsilon)}{d_p \varepsilon^2} \quad (6)$$

V' = Superficial velocity = Total flow rate per unit cross-section area$\left(V' = \frac{4Q}{\pi D_r^2}\right)$.

$$Q = \frac{\tau d_p \varepsilon^2 \pi {D_r}^2}{25\mu(1-\varepsilon)} \quad (7)$$

8.4.1.3 Mass transfer rates: Oxygen Uptake rates

Mass transfer rates of oxygen and its requirement by cells in a cylindrical modular construct is calculated by a simple mole balance on oxygen as follows. A steady-state mole balance on oxygen in the modular construct perfused with medium at a flow rate of Q, as it enters, leaves, and up taken in a differential cylindrical element dz of radius R and length Lc (along the z directions) is given by: [Rate in] – [Rate out] = [Rate of consumption of O2];

$$-Q \int_y^{y+\Delta y} \frac{dC_{O_2}}{dz} = OUR \rho_c (1-\varepsilon) A \quad (8)$$

Where, OUR= Oxygen uptake rate/ single cell, ρ_c = Density of cells per unit volume = Total number of cells/Volume of construct. Integrating equation (8) over the limits y and y+Δy gives

$$Q = \frac{OUR\ \rho_c (1-\varepsilon)\ \pi\ D_r^2\ L_c}{4\ (C_{O_2}^{In} - C_{O_2}^{Out})} \quad (9)$$

OUR = $4x10^{-16}$ mol/cells per s (Rotem, Toner et al. 1992). This serves as the upper limit for any cell type. C_{in} = 200μM (Dissolved oxygen concentrating in blood at the inlet), C_{out} = 65μM (Dissolved oxygen concentrating in blood at the outlet).

Table 3: Assumptions for the modelling

Parameters:	Value	Unit
Oxygen Uptake Rate (OUR)-Hepatocytes. V_m at $K_{0.5}$	$4*10^{-16}$	Mol/cell/s(Rotem, Toner et al. 1992)
Lowest Oxygen partial pressure in human body	58/65	mmHg/uM
Oxygen partial pressure in Air (21%-7.6mg/lit of water)	105/200	mmHg/uM
Void Fraction ε	0.4±0.1	No Unit
Medium Viscosity μ	0.007	dyn.s/cm^2

8.4.1.4 Mass Transfer Rate in Capsules:

The dimensionless concentration parameter called the Thiele modulus which is a measure of the rate of oxygen consumption relative to the rate of oxygen diffusion in the tissue matrix compartment is used to calculate the necrotic radius of our spherical aggregates. A modified form of Thiele modulus for a cell based system is defined previously (Avgoustiniatos and Colton 1997) as shown in equation (10). When the Thiele modulus for a spherical system is large, internal diffusion usually limits the overall rate of reaction; when it is small, the surface reaction is usually rate-limiting.

$$\phi_m{}^2 = \left(\frac{Vh^2}{\alpha D}\right)\frac{1}{\Delta P_V} \tag{10}$$

Dimensionless length

$$\xi = \frac{R_0}{R_s} = 0$$

ϕ_m -Thiele Modulus

ξ - Dimensionless length

R0- Radius

V- Rate of oxygen consumption per unit volume 3.2 (l.1)*10^{-8} mol/cm^3.s

h – Half thickness or the radius of the aggregate

α - Bunsen solubility coefficient of oxygen (=1*10^{-9} mol/cm^3.mmHg)

D – Diffusion coefficient of oxygen (=1.3(±0.2)*10^{-5} cm^2/s)

ΔP_v – Drop in oxygen partial pressure across the thickness r=vi

$$\phi_m{}^2 = \left(\frac{Vh^2}{\alpha D}\right)\frac{1}{\Delta P_V}$$

A- is a function of the permeabilities and thicknesses of the various layers.

For multiple layers:

For no necrotic core, the dimensionless length $\xi = \frac{R_0}{R_s} = 0$

$$\phi_m{}^2 = \left(\frac{6}{1+2A}\right)$$

$$\Delta h = d_{max} = \left[\left(\frac{\alpha D}{V}\right)\Delta P_V \frac{6}{1+2A}\right]^{1/2}$$

The effectiveness factor (η) is the ratio of the reaction rate to the rate of reaction in the absence of internal mass transfer limitations. Its magnitude ranges from 0 to 1, and it indicates the relative importance of diffusion and reaction limitations. The effectiveness factor was calculated for the first order kinetics as explained previously (Fogler 2005).

If ϕ>2 then

$$\eta = \frac{3}{\phi_m^2}[\phi_m - 1]$$

8.4.2 *Perfusion culture of encapsulated hepatocytes:*

Encapsulated primary rat hepatocytes (encapsulation density: $20x10^6$ cells/mL of CSA/CMC) were maintained in perfusion cultures under both packed bed and fluidized bed conditions as previously described (Matthew, Salley et al. 1993, Surapaneni, Pryor et al. 1997). For fluidized perfusion, non-fused capsules were fluidized by a continuous upward flow of the culture medium in a cylindrical chamber within a continuous circulation flow circuit. For the packed bed cultures, the capsules were fused in a cylindrical flow chamber as described above and subjected to a downward flow of the medium in a continuous circulation flow circuit. Medium exiting the culture chamber was oxygenated using a silicone tubing oxygenator (supplied with 95% air/5% CO_2) and recirculated using a peristaltic pump. The flow rates were adjusted to maintain physiological pressure differences (<100 mmHg) across the chamber (4-5 mL per minute). The perfusion system was maintained at 37°C for 1-2 weeks and medium was changed every 2-3 days. Medium samples were collected daily for evaluation of urea and albumin synthesis by the hepatocytes.

8.4.3 *Analysis of albumin and urea synthesis:*

Standard methods for measuring albumin and urea production rates were used to assess hepatocyte function. Culture medium collected from collagen sandwich cultures and perfusion bioreactor cultures at regular intervals was analyzed for rat serum albumin by ELISA with purified

rat albumin (Sigma) and a peroxidase conjugated anti-rat albumin antibody (Bethyl). Urea production was quantified using the diacetylmonoxime method as previously described (Wybenga, Di Giorgio et al. 1971). Standard curves for both quantification techniques were generated using purified rat albumin or urea dissolved in culture medium. Absorbances were measured with a Spectramax

8.5 Results

8.5.1 Design Parameters

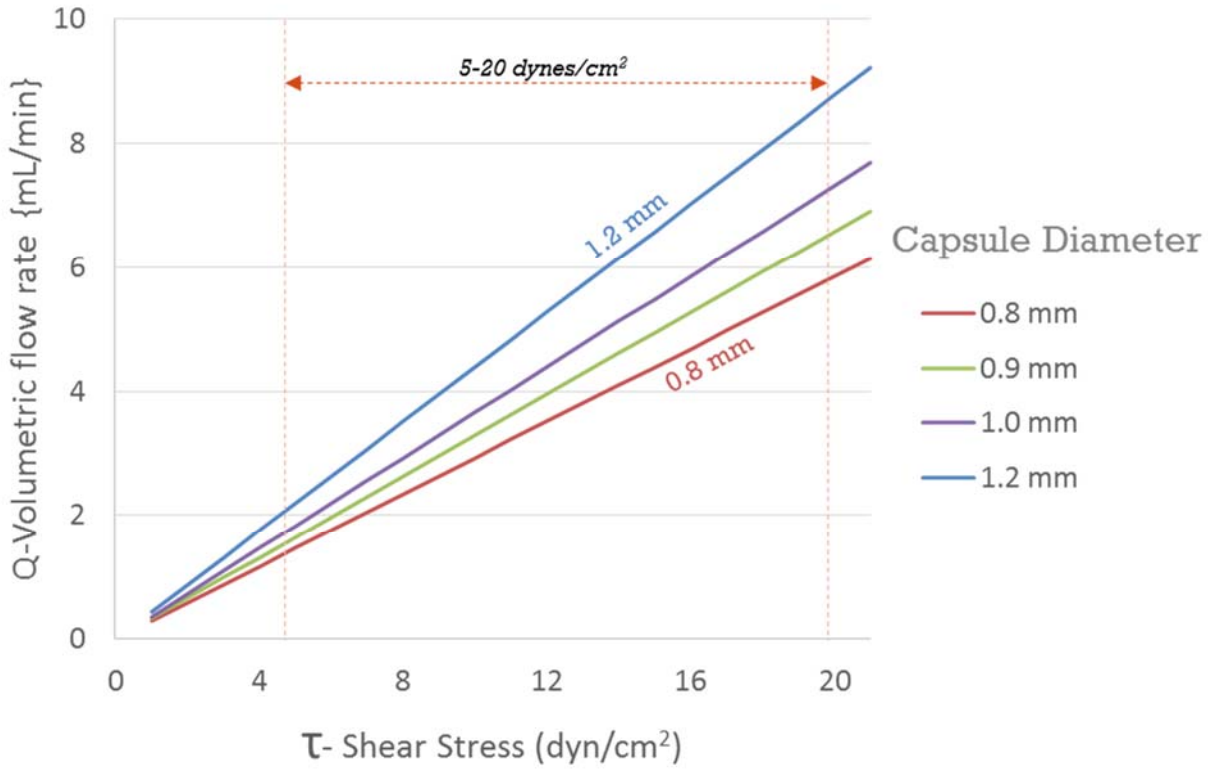

Figure 33: Flow rate required to impose a specific shear stress on the surface on the aggregated with various diameter (50-200 μ). Void fraction is kept constant at 0.4.

The Reynolds number for the flow with aggregates of 200μ in dia is NRe = 0.12 @ 20 dyn/cm2 shear stress. For all the other conditions of shear < 20 dyn/cm2 and dia <200μ the Reynolds number of the flow is below NRe < 0.12. Hence, flow is considered laminar in all the following plots. Fig.33 shows the flow rate required to impose a specific shear stress on the surface of the capsule with various diameter (50-200 μ). Void fraction is kept constant at 0.4.

8.5.2 Minimum flow rate to meet O2 need

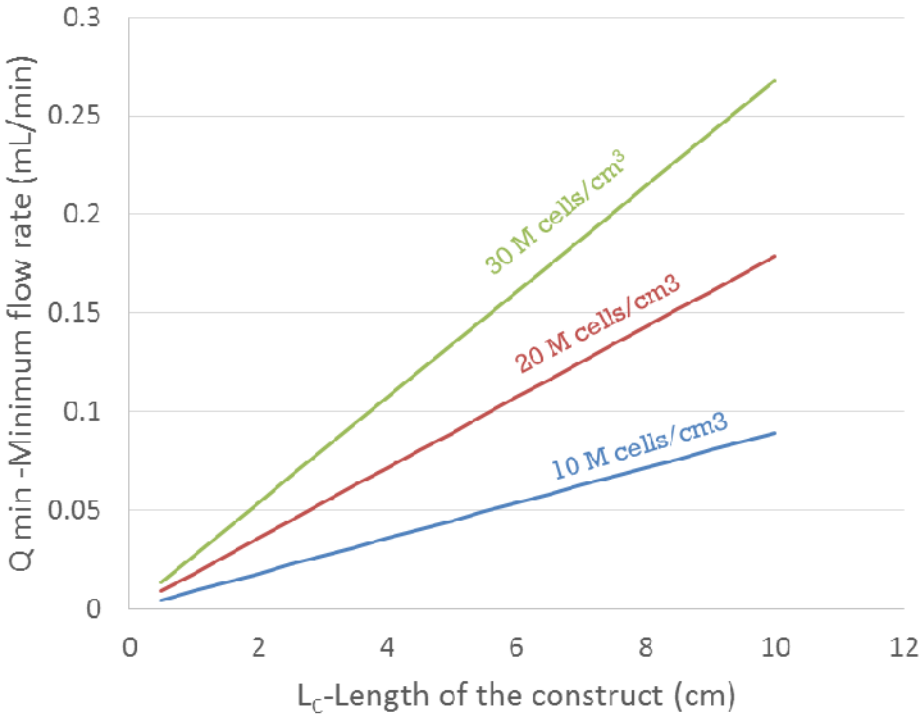

Figure 34: Change in minimum flow rate required to supply enough oxygen for constructs with different length.

Dr = Diameter of the packed bed (1mm), Dp = Diameter of the aggregates/capsule (100 μ), Lc= Length/Height of the construct, Cell density: 10, 25 and 50 Million cells/cm3. Assumptions: Upper limit of oxygen concentration: 135 μM, Lower limit of oxygen concentration: 65 μM (Outlet

concentration for the bioreactor). Oxygen uptake rate of hepatocyte = 4*10-16 mol/cell/s (1/2 VMax). Fig.34 shows the change in minimum flow rate required to supply enough oxygen for constructs with different length. The colored lines denotes three different constructs with different cell densities.

8.5.3 Mass Transfer within a Capsule

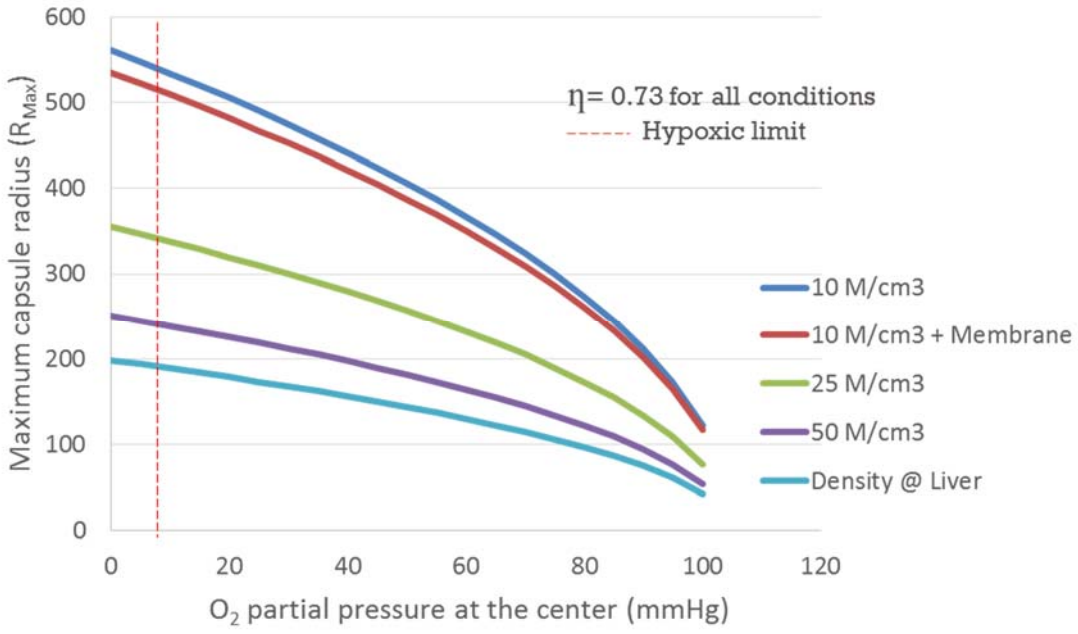

Figure 35: Mass Transfer within a Capsule. Thiele modulus analysis used to calculate maximum non-hypoxic capsule radius:

Thiele modulus analysis used to calculate maximum non-hypoxic capsule radius. The calculations shown in figure 35 shows that the higher cell densities reduce the maximum non-hypoxic capsule radius and capsule wall has minimal effect on the overall mass transfer. More importantly, capsule with 200μ radius can efficiently maintain hepatocytes at cell density of liver.

8.5.4 Bioreactor operation limits

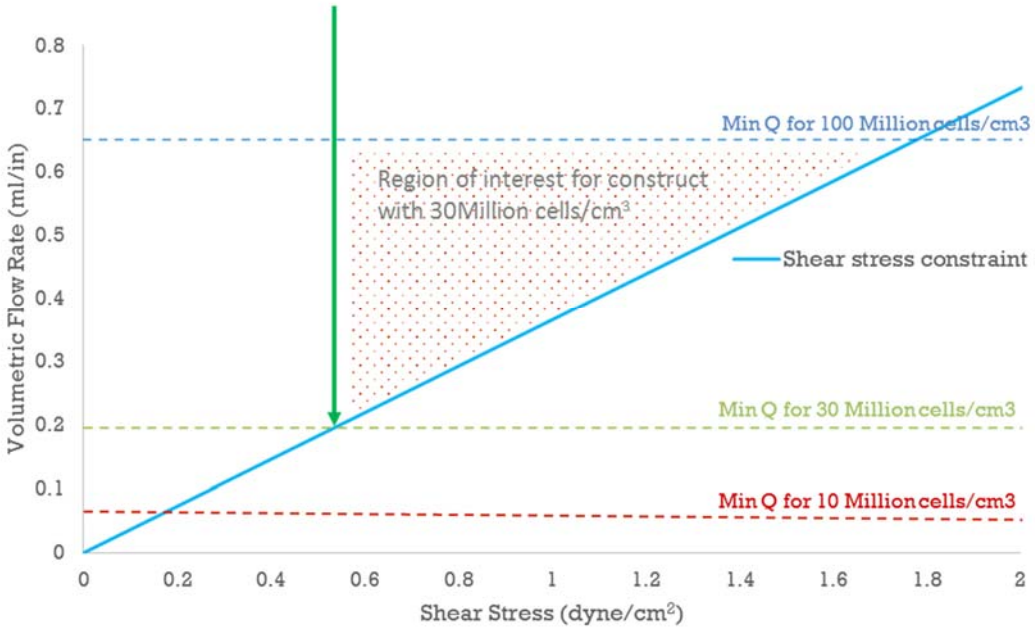

Figure 36: Shear stress range that ensures enough oxygen supply

The above calculations show that the flow will be laminar in the packed bed bioreactors at all ranges of physiological shear stress with capsule diameter less than 200 μ in diameter (arbitrary limit). The required operating flow rates (for a 5mm long construct and 1mm in dia) based on mass transfer limits are far below the flow rates required to satisfy physiological shear stress limits. The compaction characteristics of the capsules need to be tested experimentally to impose pressure drop constraints in the calculation. Overall, with flow rates at the physiological shear stress range, the bioreactor can maintain cell capsules with at least 15% liver cell density (50M cells/cm3) without any necrosis.

8.5.5 Perfusion culture dynamics

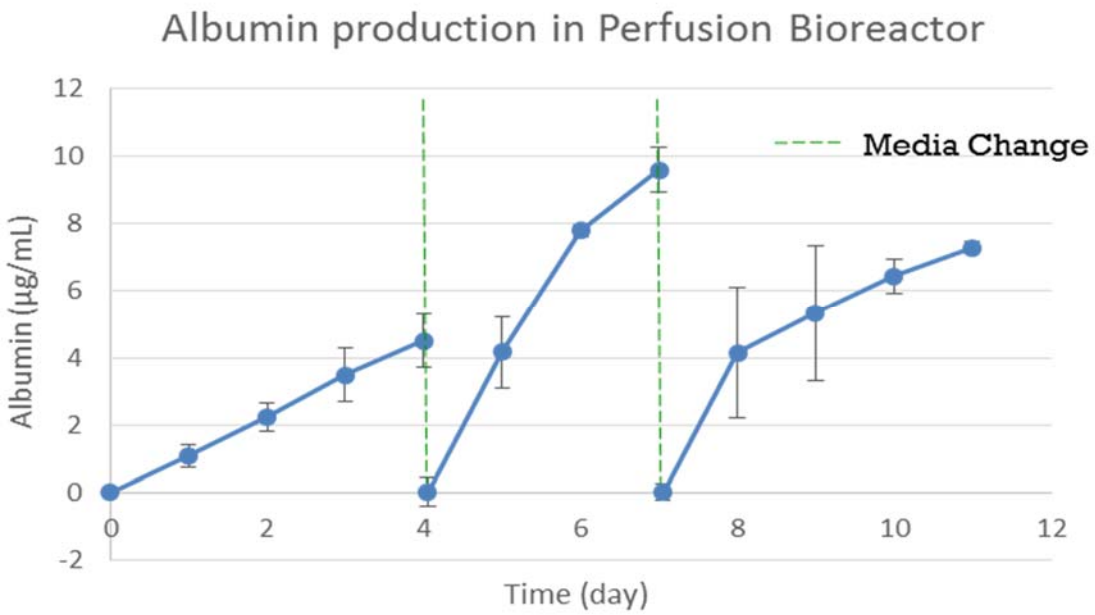

Figure 37: Perfusion culture dynamics of encapsulates hepatocytes.

There was a slow albumin production initially followed by an exponential increase and finally a lag phase. The initial lag in the albumin production can be attributed to the initial adaptation time required for the newly seeded cells in our GAG microcapsules. Once the cells overcome the initial shock, they show an exponential increase in the albumin production rates at the same time forms larger aggregates. The formation of larger aggregates introduces diffusion limitation in to the system that results in the decrease in the albumin production rates as seen in the figure 37.

8.5.6 Metabolic performance of hepatocytes in modular constructs

The metabolic performance of encapsulated primary rat hepatocytes maintained in perfusion culture conditions (Figure 38) was evaluated by measuring urea and albumin synthesis rates and comparing to rates of identical cells in standard collagen sandwich dish cultures.

Perfusion cultures maintained the functionality of encapsulated hepatocytes and healthy spheroids were seen in most capsules (Figure 38B). Albumin and urea synthesis rates in both types of perfusion cultures (Figure 39 C-F) approached those of the collagen sandwich cultures (Figure 39 A-B).

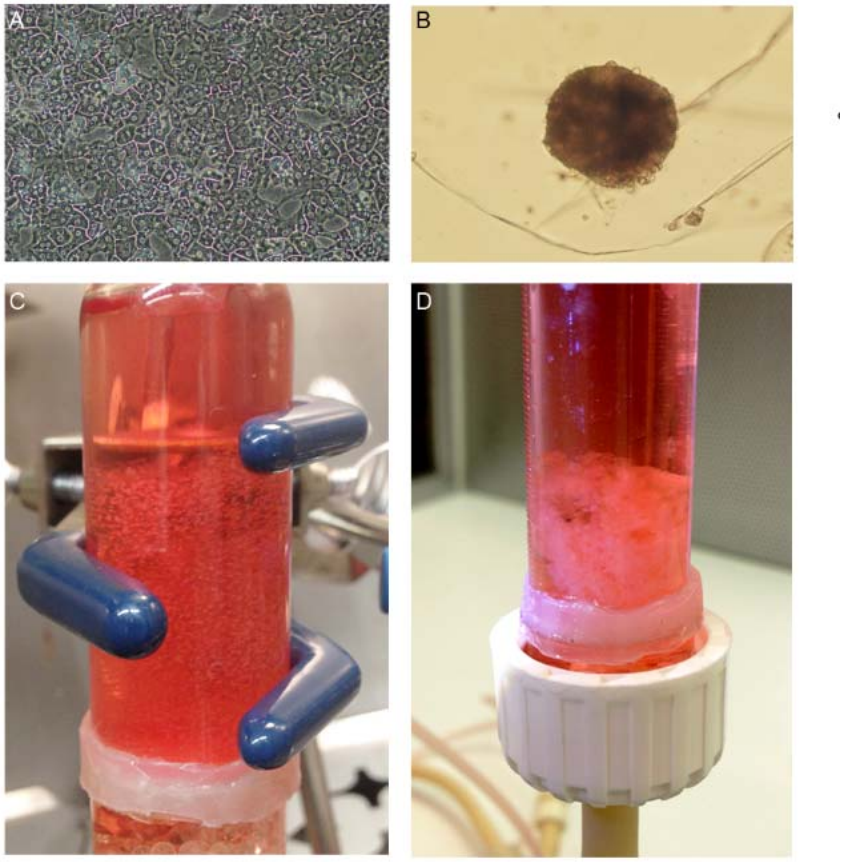

Figure 38: Primary rat hepatocytes were encapsulated in CSA/CMC capsules with a with 1 mg/ml collagen gel, at a density of $2x10^7$ cells/ml of CSA/CMC/collagen solution. (A) Control collagen sandwich dish culture. (B) Encapsulated hepatocytes aggregated into spheroids during culture as either (C) individual capsules in a fluidized bed bioreactor, or as a (D) fused modular construct in a packed bed bioreactor.

8.6 Summary and Discussion

The urea and albumin synthesis rates of the perfused cultures indicate that mass transfer rates were sufficient to maintain the encapsulated hepatocytes in our modular constructs. Thus, the interconnected endothelialized channels may provide a foundation for a vascular network and thereby accelerate the process of neovascularization by anastomosing with the host vasculature post-implantation. Thus, the fusion of the endothelialized capsules generated 3D constructs with an embedded network of interconnected channels that enabled long-term perfusion in-vitro.

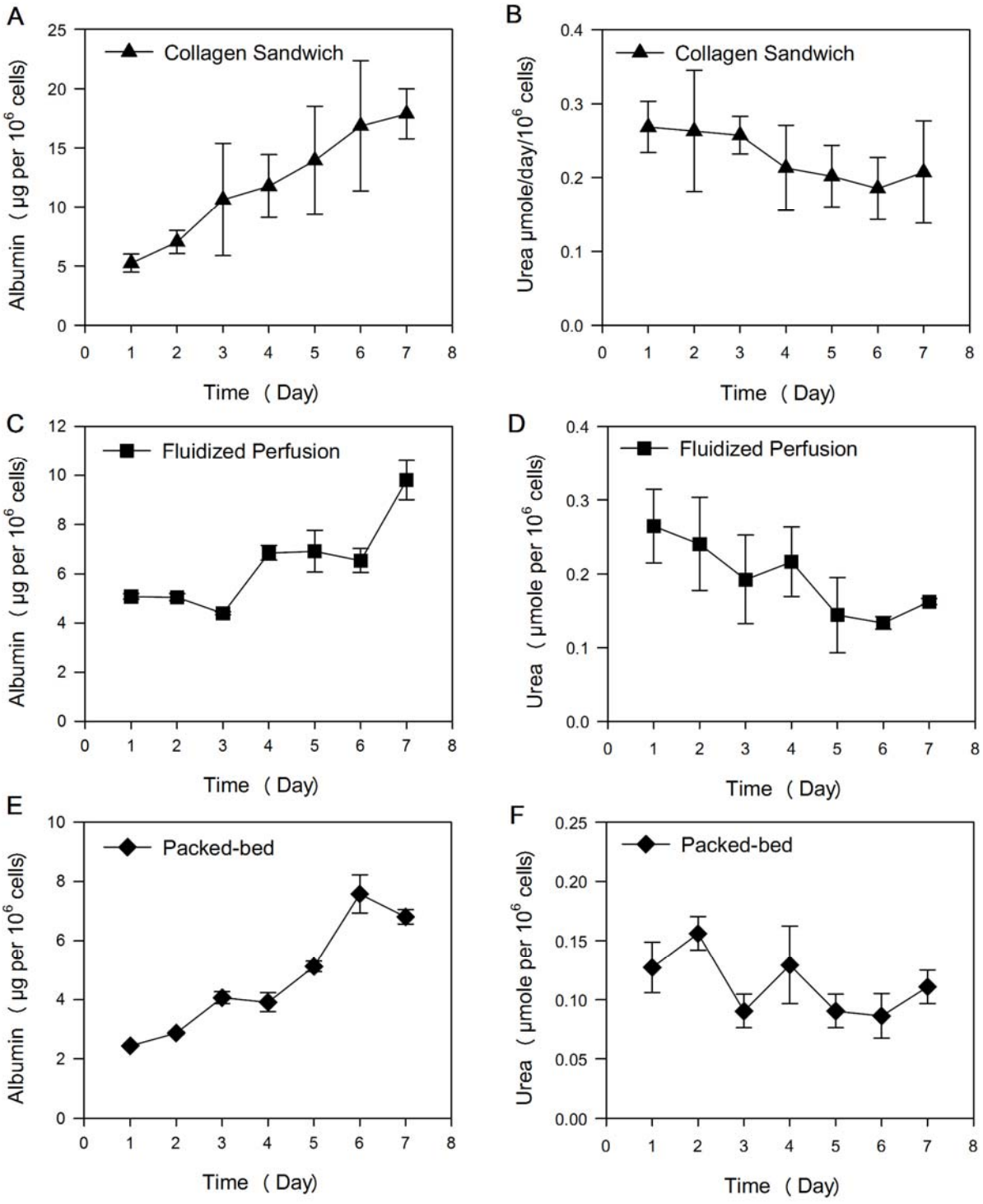

Figure 39: Albumin and urea synthesis rates of hepatocytes in encapsulated perfusion cultures.

(A-F) Albumin and urea synthesis rates by the hepatocytes in the three culture conditions. (A,B) Control collagen sandwich cultures. (C-F) Perfusion cultures. Error bars denote standard deviations from 3 replicate measurements.

CHAPTER: 9

ASSESSMENT OF VASCULARIZATION IN-VIVO

9.1 Introduction

In spite of the enormous scientific knowledge on biomaterials and tissue scaffolds, it is implausible to accurately predict the in vivo response to implanted tissue constructs based solely on in-vitro cultures techniques. Thus, it is widely recognized that in-vivo testing is necessary to investigate the biological responses such as neovascularization and angiogenesis of implantable material constructs as well as to identify wide range of host interactions with the implanted material. In our in-vivo study we tested the effectiveness of our method of modular fabrication by implanting small, multilayered tissues assembled using the method described in the previous chapters. The implanted tissue was imaged using magnetic resonance imaging (MRI) at 7 day intervals and was recovered at the end of week-3 and examined for material break down, formation of new blood vessels, and organization of the tissue cells.

9.2 Aim and rationale

Specific aim is to determine the effects of module endothelialization on vascularization of constructs in vivo. The objective of this specific aim is to investigate the rate and extent of vascularization of 3D constructs in a rat model by implanting them into subcutaneous pocket and doing histological analysis of the recovered explant at different time points. This will validate the feasibility of our technique for clinical applications. Our hypothesis that modules permeated by a network of interconnected, endothelial cell-lined channels can facilitate extensive vascularization and mass transport will also be tested in this animal study

9.3 Experimental approach

Small modular constructs of suitable dimensions made using our fabrication technique were implanted in subcutaneous pockets of SCID mice. Surgical implantation procedures include blunt dissection and direct injection of microcapsules into subcutaneous pockets. The surgical procedure were optimized in order to minimize incision related injuries and structural damage to the implanted modules.

9.4 Materials and Methods

Analysis criteria: Host cell infiltration, interactions between host-implant anastomoses, host immune response and apoptosis were evaluated quantitatively. Implant and surrounding tissue were recovered at different time points and following histological procedures and assays were performed: H&E, Masson's Trichrome, TUNEL, and Immunohistochemistry. Cell specific markers were used to identify cell type in the recovered explant. This will also enable us to quantify the extent of vascularization in the explant. If necessary GFP positive cells may be used in order to differentiate between host and implanted cells.

9.4.1 Subcutaneous implantation in mice

All the implantation surgeries were performed in a sterile hood located in one of the WSU animal care facility. The stainless steel surface of the hood was cleaned with Spor-Klenz™ sterilant and one mouse was anesthetized at a time using Isoflurane inhalant (1 – 3% (up to 5% for induction). A 2 cm^2 area of the dorsal skin (subcutaneous implants) was shaved. After shaving, the hood surface area was re-cleaned and sterilized with fabric sheet soaked in Spor-Klenz™. The shaved surgical site was prepared according to the Survival Surgery in Rodents SOP provided by

WSU DLAR. Mice was positioned on sterile dressing pads for the procedure. Puralube^{TM} was applied onto the eyes to prevent drying of conjunctive during the procedure. With round-tip forceps, dorsal skin was lifted at the center point between the hip joints. A 1.2-1.4 cm transverse incision was made in the dorsal skin using sterile instruments to make a subcutaneous pocket. Our modular scaffolds fabricated as previously described was inserted through this 1.2 cm incision, which was then closed using non-absorbable silk sutures followed by wound clips. The procedure was shown in the fig. 40.

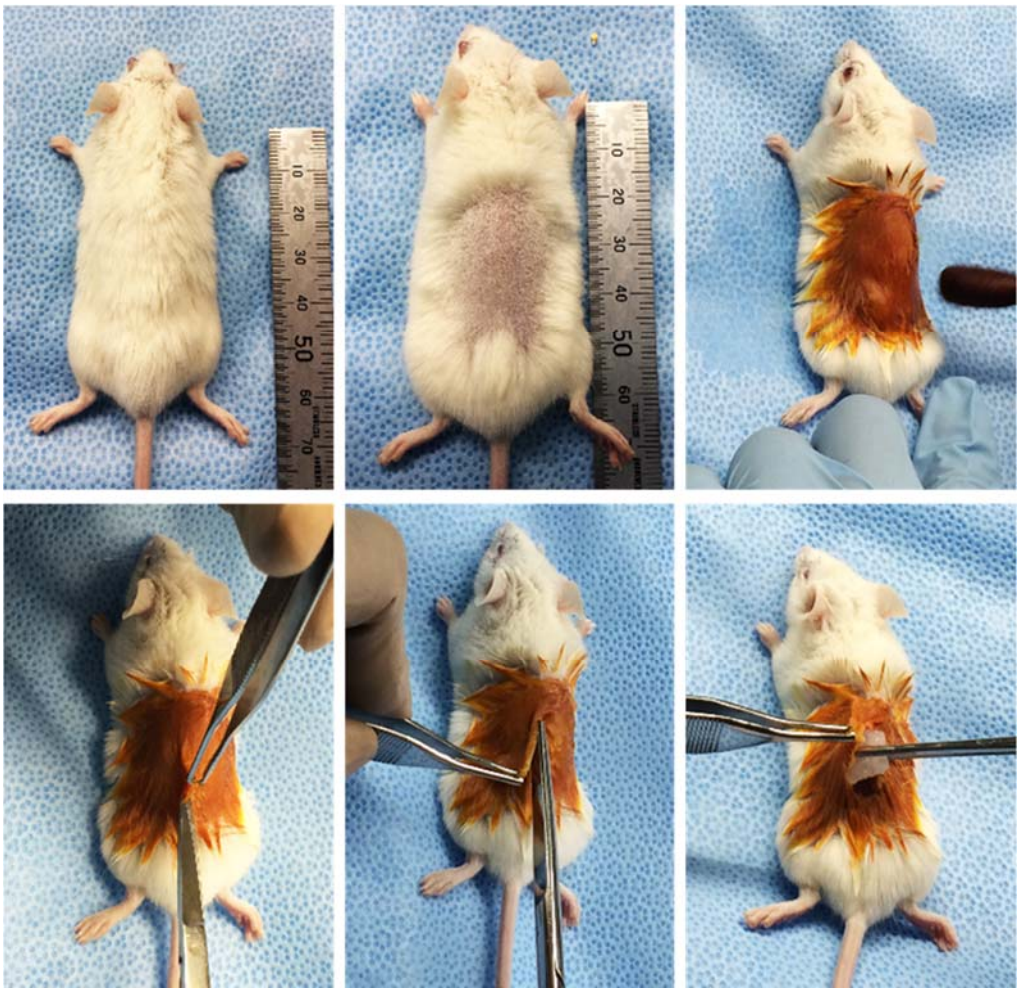

Figure 40: Subcutaneous implantation surgical procedure.

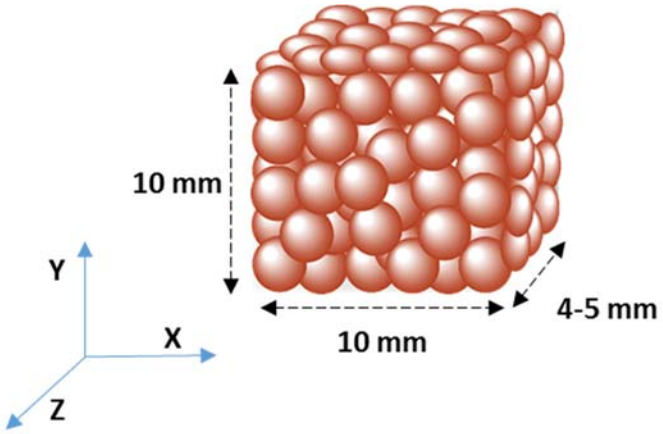

Figure 41: The dimension of the implanted modular construct.

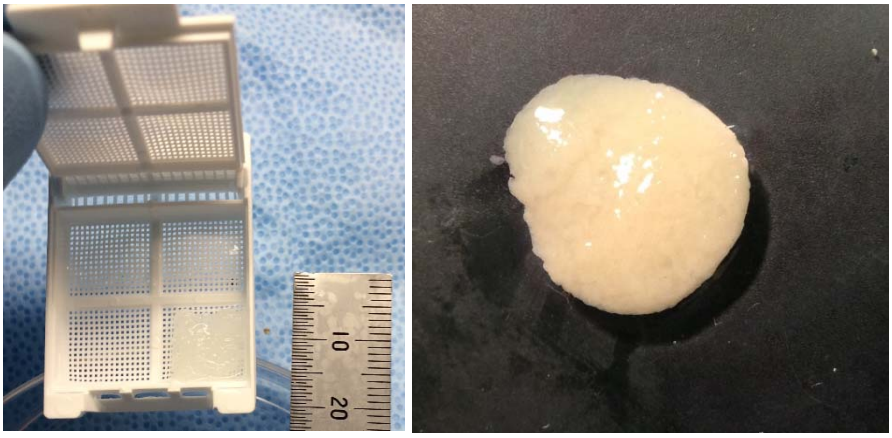

Figure 42: (A) Actual modular construct formed by perfusion method.(B) Fused hepatocyte capsules.

9.4.2 Dynamic Contrast Enhanced Magnetic Resonance Imaging:

MR Imaging:

Magnetic resonance imaging (MRI) is a versatile diagnostic technique that can be used non-invasively, to investigate morphological, metabolic and functional information of any organ or tissue in animal or human body. Here we employ MRI to study the developing vasculature in our

implanted modular scaffolds by administering a contrast agent. MR imaging is able to exploit the plasma flow, blood vessel morphology and distribution, and flow heterogeneity to investigate neovascularization in an implanted tissue scaffold. Neovascularization is a critical physiological process that determines the success of an implanted engineered tissue. Among the currently available noninvasive tools including computed tomography (CT), magnetic resonance imaging (MRI), positron emission tomography (PET) and single photon emission computed tomography (SPECT), MRI is probably the most potent method to characterize both morphological and functional aspects of vascular system (Oostendorp, Post et al. 2009). In addition, MRI is a more sensitive tool to investigate the growth of small blood vessels at various spatial-temporal scales (Padhani 2002).

Dynamic contrast-enhanced MRI:

Out of the different MRI techniques, the contrast enhanced methods are generally faster and show higher target-to-background contrast (Oostendorp, Post et al. 2009), which is particularly useful for imaging neovascularization. During the contrast-enhanced MRI, the blood plasma signal is selectively enhanced using a gadolinium chelate that shortens its T1 relaxation time (Prince 1994, Prince, Narasimham et al. 1995). Using dynamic contrast- enhanced MRI technique, physiological information of the implanted tissue including blood flow, blood vessel permeability and surface area of the capillaries can be obtained using T1 weighted MRI (Prince 1994). The kinetic profile of the gadolinium chelate is determined mainly by the following factors: active transport, blood plasma perfusion and passive diffusion out of the blood vessels into the extravascular-extracellular space (Prince 1994).

Three group of mice were imaged post-implantation at time points of 1, 2, and 3 weeks to evaluate the levels of vascularization and blood perfusion in the constructs. The scan was taken

one at a time and the animal was anesthetized by administration of inhalant isoflurane and kept warm on a warming pad. Once anesthetized, a 24G catheter with 27G needle was inserted into the tail vein (intravenous-IV) to administer the tracer intravenously. The tracer was also administered by intraperitoneal (IP) injection in many cases. After background imaging data are acquired, the tracer- Gd-DTPA dimeglumine (Magnevist) was administered as previously described (Orth, Bankson et al. 2007), while the animal was in the magnet 7T- MR scanner (Bruker BioSpin) and MRI data was acquired. The pharmaceutical grade tracer, Magnevist Injection, was supplied as sterile, 0.5 mmol/ml solution and was diluted with sterile saline for administration. The total anesthesia time was less than 1 hour per week. Since Gd-DTPA was exclusively eliminated in the urine with 90% clearance within 24 hours, there was no adverse effects on the animal after repeated injections on a weekly basis. To keep the tracer perfusion consistent between the IP and IV procedures, the concentration and the time delay for the scan was optimized using MRI images obtained with the first 2 to 4 animals. For IV procedures 0.3 mmol/kg of the tracer was administered and scans were obtained immediately. For IP procedure the dosage was doubled and the scans were obtained after 5 min delay. The following are the parameters of the MRI scans taken in 7T magnet: Repetition Time: 22s, Echo Time: 3.53s, Flip Angle: 30, Pixel Bandwidth: 260, Pixel Spacing: 0.125mm/0.125mm, Slice Thickness: 0.130mm.

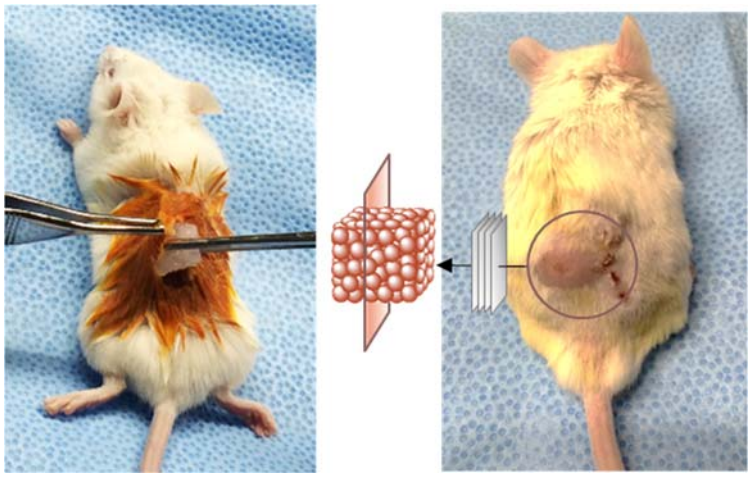

Figure 43: MRI scan. Stacked sagittal scans of the implanted constructs.

The Gd-DTPA concentration was calculated from the longitudinal relaxation time T1:

$$\frac{1}{T1(t)} = \frac{1}{T1(0)} + \alpha\, C(t)$$

$$\frac{1}{T1(t)} = \frac{-1}{TR} ln\left[1 - \frac{s(t)}{s(0)}\left(1 - e^{-\left(\frac{TR}{T1(0)}\right)}\right)\right]$$

$$[C] = \left(\frac{1}{\alpha}\right)\left\{\frac{-1}{T1(0)} - \frac{1}{TR} ln\left[1 - \frac{s(t)}{s(0)}\left(1 - e^{-\left(\frac{TR}{T1(0)}\right)}\right)\right]\right\}$$

c(t) is the tissue concentration of d-DTPA as a function of time

α = Longitudinal relativity [3-5 1/(smmol/L)]

T1(0) = Pre T1 value (ms)

T1(t) = Post Gd-DTPA (ms)

TE is the echo time

TR is the repetition times = 22ms

s(0) = Pre T1-weighted value

s(t) = Post T1-weighted value

TR = 2200 ms,

Post Gd-DTPA T1 = 2 s (Longitudinal relaxation time)

9.5 Results

9.5.1 Vascularization and blood perfusion in the constructs

The amount of blood perfusion in terms of blood volume per tissue volume was calculated by measuring the tracer intensity in the implanted tissue. To measure the intensity, SPIN software was used to analyze the obtained MRI scans. The implanted tissue in the images was first selected and the total intensity per unit pixel of that selected area was compared to that of the different groups after subtracting the pre scan values. An increase in the total blood volume to tissue volume was notice over the seven day time interval in all the test groups as shown in image below. Moreover, the total volume of the implanted construct also reduced over time due to the biodegradation of the materials by the host. At week-3 most of the material in the construct was degraded and the implant look completely vascularized as evident from the higher intensity of the tracer throughout the construct.

9.5.2 Effects of endothelialization on vascularization

Two groups of animals were included in our study to validate the rapid vascularization of our modular constructs. The first group received implants made out of empty capsules with no endothelial cells on the outside capsule wall. The second group of animals were implanted with implants made out of empty capsules with endothelial cells on the outside capsule wall. The

perfusion intensity of the tracer was compared between the groups. It was found that the implants with HUVECs on the outside wall showed higher level of enhancement by week-2 compares to that of the implants without the HUVECs as shown in the figure 45-47. Hence, the HUVECs seeded on the outside wall accelerated the process of neovascularization, thus supporting our central hypothesis.

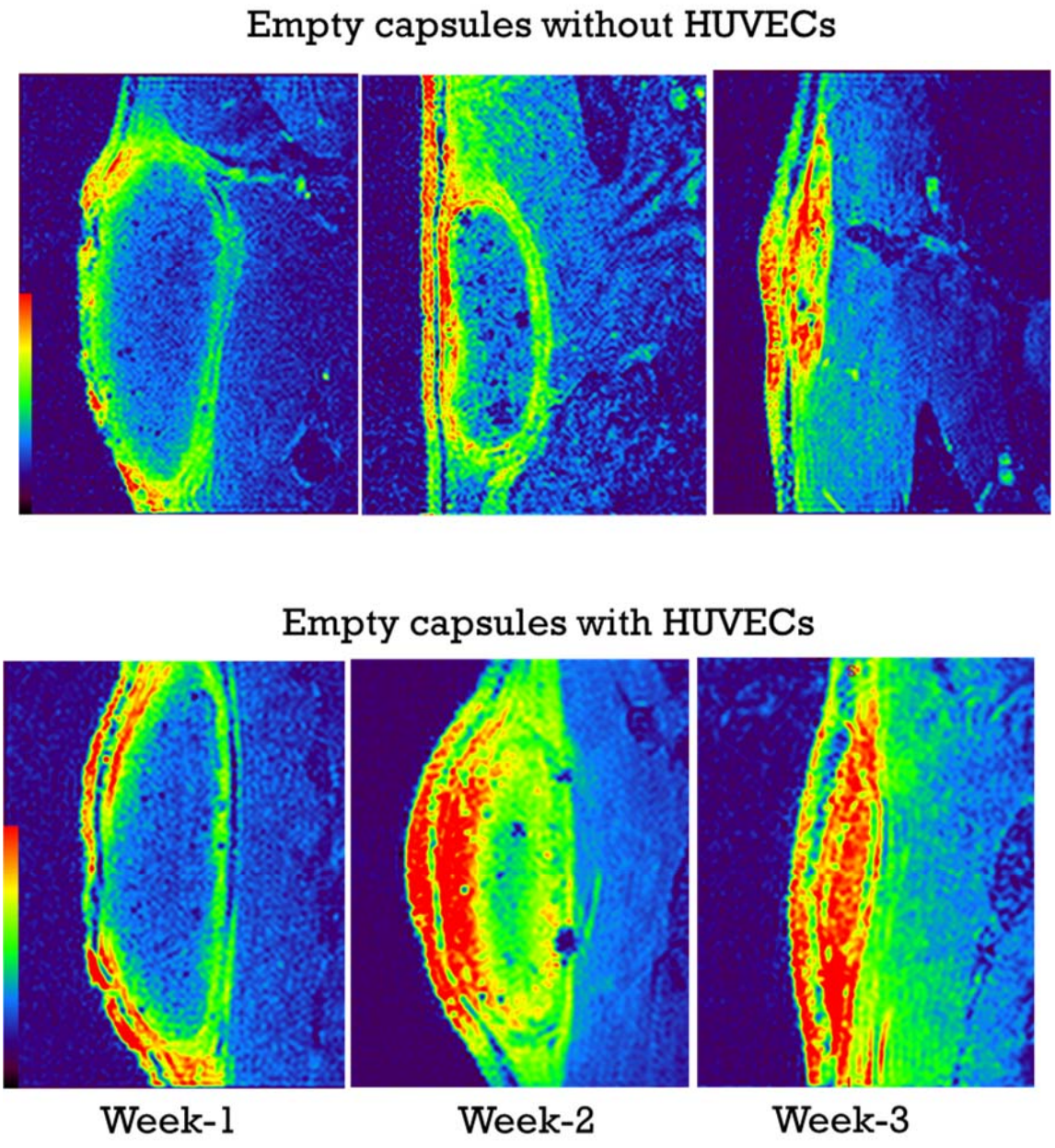

Figure 44: MRI scan. Stacked sagittal scans of the implanted constructs. Empty capsule constructs with and without HUVECs.

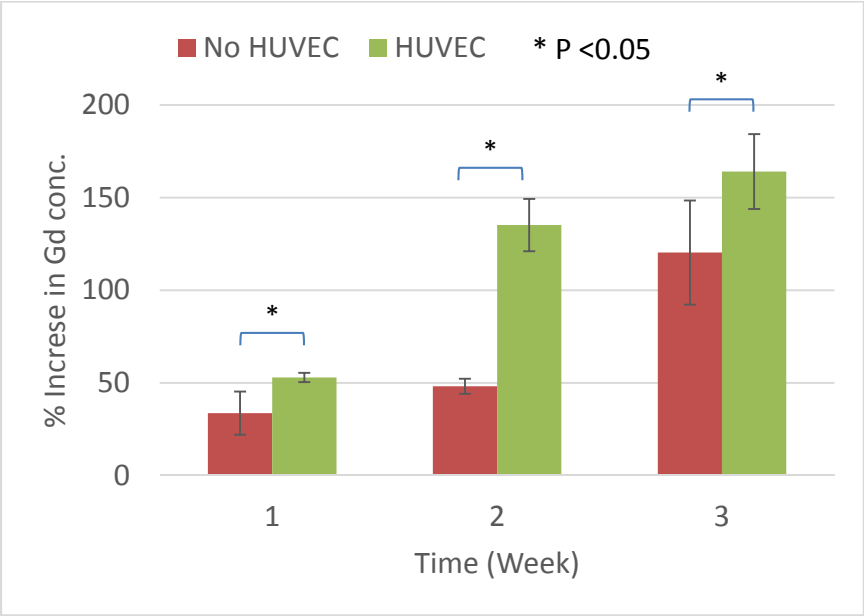

Figure 45: Percent increase in Gd-DTPA signal intensity. Increase in tracer concentration showing the effects of endothelialization on vascularization.

The concentration of Gd-DTPA in the extracellular-extravascular space after 5-8 min after administering intraperitoneally was calculated using the formula detailed in the previous section. The longitudinal relativity (α) for the our system was 5/(mmol/L/s) and the repetition time (TR) for the MRI scans was 22ms. The average signal intensity in the implanted tissue was calculated using SPIN image analysis. Figure 45 shows the percent increase in signal intensity post Gd-DTPA, in constructs seeded with and without endothelial cells on the outside. The results shows that the endothelialization of the capsules accelerated the vascularization of our modular constructs. Significant increase in the vascularization is seen at all-time points and a three fold increase is seen at week-2. This rapid vascularization thru endothelialization of the modular

construct can help retain cell viability and functionality of the parenchymal cells encapsulated in the capsules. This is crucial to improve the overall success rate of the implanted tissue as most of the implant necrosis happens during the first two weeks that ultimately leads to poor outcomes.

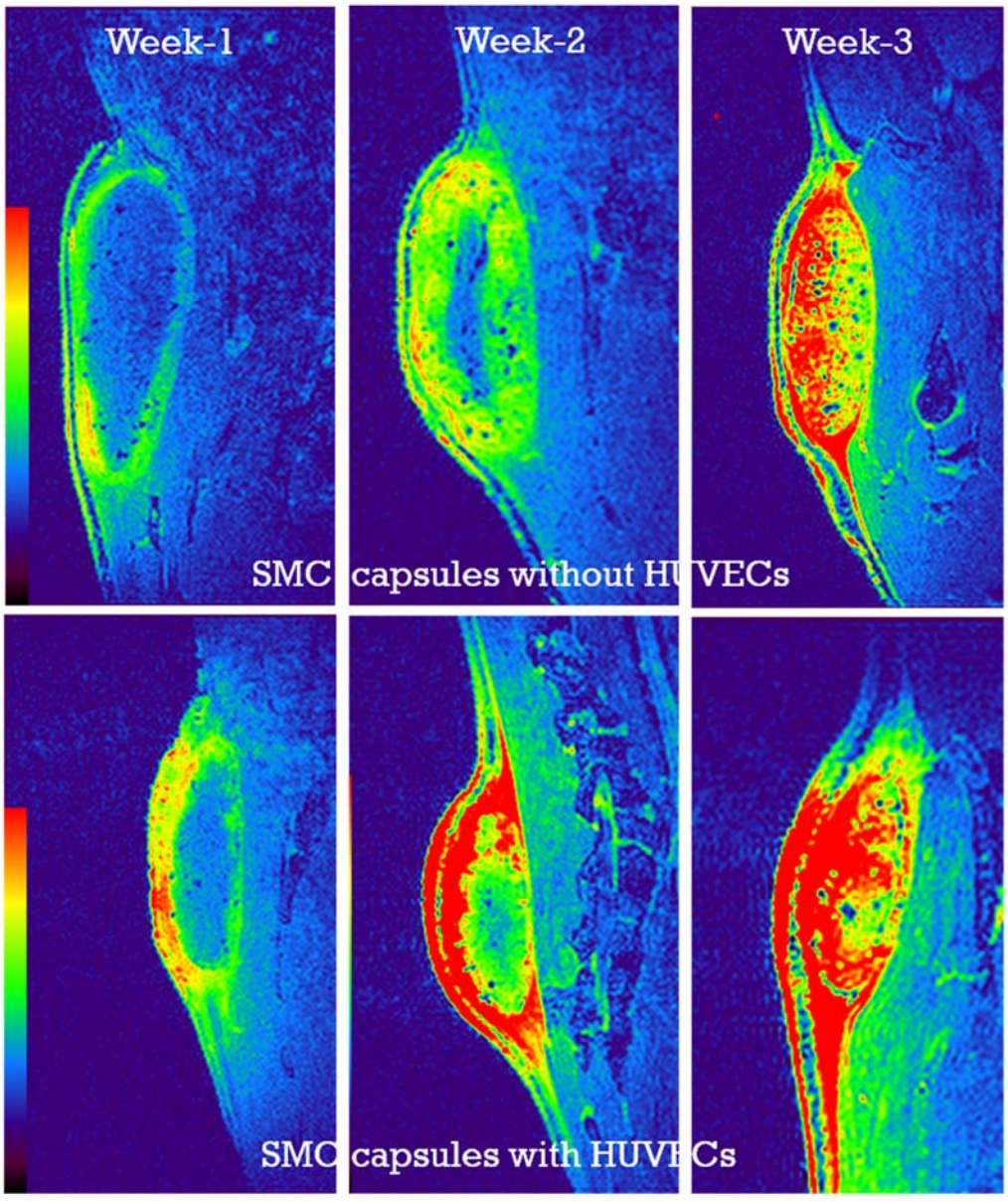

Figure 46: MRI scan. Stacked sagittal scans of the implanted constructs. SMC seeded capsule constructs with and without HUVECs.

Similar results were also seen when SMCs were encapsulated inside the capsules as shown in figure 46. Hence, the HUVECs seeded on the outside wall accelerated the process of neovascularization, thus supporting our central hypothesis. The The Gd-DTPA concentration was calculated using the above mentioned derivations and found to be 0.008 mmol/lit/min in the constructs with endothelial cells on the outside after two weeks and o.031mmol/lit/min in the constructs without the endothelial cells on the outside after two weeks post implantation.

9.6 Summary and Discussion

This is an important step in fabricating advanced tissue constructs as our technology can actually accelerate the vascularization process during the initial phases on the implantation in which the implant is more vulnerable to diffusion limitation and subsequent necrosis of the tissue. We have shown that our embedding a network of inter-connected endothelial cell lined channels in tissue constructs can accelerate the process of vascularization. The next step is to use a parenchymal cells such as smooth muscle cells or hepatocytes inside the capsules and test their performance enhancement in our modular scaffolds. In summary, our modular approach has the potential to allow rapid assembly of tissue constructs with clinically significant cell densities, uniform cell distribution, and endothelialized, perfusable channels. The total blood volume and the total surface area of the microvasculature in the implanted tissue can be determined from the concentration profiles of the Gd-DTPA calculated using T1 weighted images and T1 maps, which encompass our future direction.

CHAPTER: 10

Discussion and Future directions

Modularity is a phenomenon widely observed in nature, which enables biological systems to achieve precise control over organization and function in very compact spaces. The modularity of the kidney and its component nephrons are excellent examples of this concept. Adopting a similar approach in engineered organs has a number of advantages. The scalability of the modular strategy enables rapid fabrication of tissue constructs with greater control over their architecture. The major design challenges of a modular tissue construct include: limiting mass transfer distances, achieving high, tissue-like cell densities, and the ability to form interconnected, vascularizable channels. The GAG-based microcapsules described here allow efficient mass transfer, which is evident from the tissue-density cultures that were maintained for up to 45 days under static culture conditions. The diameter of the capsules can be easily controlled between 0.3 and 2.0 mm, and smaller diameters are achievable using more sophisticated droplet formation methods such as microfluidics. Capsule diameter imposes a natural upper limit on the maximum diffusion distances. The capsule system, in particular the hyaluronan-based capsules, supports direct encapsulation of cells at high, in vivo-like densities. In addition, the cell-contractable capsule formulations provide an additional mechanism for modulating cell density within either the capsules or the fused construct. Under random packing conditions, capsule fusion produced 3D structures with significant void space available for direct perfusion, accessory cell culture, or vascularization. The dimensions and architecture of the intercapsular voids can also be modulated by incorporating additional biomaterial components into fused capsule structures. Such accessory components include fibers, beads, films, tubes, etc. made from chitosan, chitosan-GAG complexes, or other degradable materials. The materials used in our modules are fully degradable,

and previous implantation results with similar materials indicate that in contrast to pure chitosan (VandeVord, Matthew et al. 2002), chitosan-GAG complexes (Chupa, Foster et al. 2000) degrade rapidly in vivo and stimulate rapid and extensive neovascularization due to GAG-mediated effects (West and Kumar 1989, Norrby 2006, Stringer 2006, Fuster and Wang 2010, Gaffney, Matou-Nasri et al. 2010). The high density trophoblast cultures were primarily intended to demonstrate the potential of the microcapsules with a highly proliferative human cell type. However, these cultures also provided direct evidence of both the degradability of the GAG-chitosan materials, and the ability of cells to invade the capsule wall. The trophoblast cell line maintains some characteristics of human trophoblasts, in particular the ability to tolerate hypoxic conditions and to invade tissue rapidly. Both characteristics are presumably related to its original, placenta-formation function (Chang and Vivian Yang 2013) and may be mediated by focal expression of MMPs, GAG lyases or other matrix degrading enzymes. Wall invasion and cell escape in these trophoblast cultures was evident after week 2 of culture and was clearly captured in histological sections (Figure 3C). This phenomenon strongly suggests that implanted capsules would present only a temporary barrier to integration of encapsulated cells with adjacent tissues. Coupled with the known pro-angiogenic effects of GAG-based materials (Black, Hudon et al. 1999, Ferretti, Boschi et al. 2003, Mathieu, Chevrier et al. 2013), these results further suggest that rapid vascularization is a likely outcome after transplantation of capsule-based constructs

Beyond modular assembly, the ability to incorporate clinically significant cell numbers into an implantable construct of feasible size is an additional challenge. We have shown that cells and matrix can be efficiently packed inside capsules of a non-diffusion limited size (Figures 8, 13). Our liver organoid prototype had a cell density of $50x10^6$ cells/cm^3 (Figure 13A). This is 40-60% of the hepatocyte cell density of liver tissue. From a practical standpoint, the cell densities achieved

in our systems are adequate for liver tissue engineering, as it has been demonstrated that with good blood chemistry, ~10% of total liver mass can support survival in rats (Arkadopoulos, Lilja et al. 1998, Kobayashi, Miyazaki et al. 2000) and humans (Bilir, Guinette et al. 2000). It should be noted that maintaining high cell densities inside capsules presents particular diffusion challenges in the case of highly metabolic cells such as primary hepatocytes. Thus, we have also shown that the cell density can be scaled down to compensate for such high metabolic requirements (Figure 13 C-D). In principle, diffusion challenges can be minimized by limiting the maximum capsule diameter to ensure an adequate supply of nutrients and oxygen to all regions of the cell mass. Diffusion inside capsules can be further modulated by controlling the extent of cell distribution and aggregation. In particular, co-encapsulating hydrogel components (e.g. collagen gels) or microcarriers provides a mechanism for tuning the interior microenvironment as well as the architecture of the cell mass. Such hydrogel materials can benignly interfere or directly compete with large scale cell aggregation, and thus serve to promote formation of multiple smaller or looser cell aggregates.

The encapsulation method also allows incorporation of microcarriers of various biomaterials. As with hydrogels, these microcarriers can produce additional adhesion ligand signaling, organizational barriers or mechanical enhancement. Our results show that gelatin coated dextran microcarriers significantly enhanced the growth and viability of encapsulated smooth muscle cells. These and other cell-adhesive microparticles can also be used to alter the physical properties of the fused capsule construct. It should also be noted that inclusion of microcarriers resulted in capsules with reduced osmotic swelling and substantially reduced internal volumes. This was particularly noteworthy in the case of CSA/CMC capsules which swelled more than HA capsules. We postulate that the increased swelling in the CSA/CMC system was due to higher interior osmotic pressures resulting from combined effects of a higher mass concentration, and

lower molecular mass of the interior polymer solution compared to HA capsules. Inclusion of a high volume fraction of microcarriers within a capsule-forming CSA/CMC droplet reduced both the volume of CSA/CMC solution inside the capsule and also the residual concentration of this solution after capsule membrane formation. This lower final concentration (caused by incorporation of polymer into the capsule membrane) produced a lower osmotic pressure and resulted in contraction of the capsule membrane around the cell+microcarrier mass. In general, the inclusion of microparticles provides a wide range of options for tuning the cellular organization and overall mechanical properties of modular constructs.

Fused capsule modules yielded 3D constructs with inter-capsular spaces that are perfusable in vitro and vascularizable in vivo. The urea and albumin synthesis rates of the perfused cultures indicate that mass transfer rates were sufficient to maintain the encapsulated hepatocytes in our modular constructs. In addition, the interconnected endothelilized channels may provide a foundation for a vascular network and thereby accelerate the process of neovascularization by anastomosing with the host vasculature post-implantation. At the very least, intercapsular endothelial cells are likely to participate in vessel formation between fused capsules. However, the kinetics of this process, and the relative degrees of transplanted vs. host cell organization in the final structure remain to be characterized through animal studies.

Our results also suggest that the capsule membrane can facilitate paracrine signaling as seen by the increase in SMC proliferation during coculture with endothelial cells. This suggests that various other interacting cell types can be cultured in this modular system with a degree of material-based control over cell organization while still allowing substantial paracrine signaling. Several coculture systems have previously been shown to improve morphology and function of engineered tissues including liver (Parekkadan, van Poll et al. 2007, Yagi, Parekkadan et al. 2009,

Kasuya, Sudo et al. 2011, Kim, Ohashi et al. 2012, No da, Lee et al. 2012), bone (Sun, Qu et al. 2007, Tao, Sun et al. 2009, Steiner, Lampert et al. 2012{Tao, 2009 #415) and cartilage (Bian, Zhai et al. 2011, Qing, Wei-ding et al. 2011, Meretoja, Dahlin et al. 2013). Our results suggest that similar trophic effects can be achieved with ease in capsule-based modular scaffolds, with added the added benefit of control over cell arrangement and distribution.

Unlike traditional scaffolds, porosity can be either maintained evenly throughout the modular capsule scaffolds or different layers with different capsule sizes and hence different porosity can be easily implemented. GAG-chitosan surfaces can support cell adhesion and proliferation, partly due to GAG-mediated binding of matrix proteins and growth factors (Chupa, Foster et al. 2000, Uygun, Stojsih et al. 2009). External cell adhesion can further be enhanced by directly incorporating cell-adhesive proteins such as collagen into the capsule wall by either blending with the polycationic solution or direct application to external capsule surfaces.

In conclusion, we have demonstrated the formation and use of GAG-based microcapsules to generate a variety of tunable, intracapsular microenvironments. These capsules have been shown suitable for fabrication of porous, 3D constructs that have the potential to mimic native tissue architecture with high cell densities, vascular and parenchymal cell types, and perfusable, endothelium-lined channels. This capsule-based modular tissue assembly approach is a promising strategy that provides a wide range of options for the efficient assembly of three-dimensional, engineered tissues.

REFERENCES

Arkadopoulos, N., H. Lilja, K. S. Suh, A. A. Demetriou and J. Rozga (1998). "Intrasplenic transplantation of allogeneic hepatocytes prolongs survival in anhepatic rats." Hepatology **28**(5): 1365-1370.

Avgoustiniatos, E. S. and C. K. Colton (1997). "Effect of external oxygen mass transfer resistances on viability of immunoisolated tissue." Ann N Y Acad Sci **831**: 145-167.

Barakat, A. I. and D. K. Lieu (2003). "Differential responsiveness of vascular endothelial cells to different types of fluid mechanical shear stress." Cell Biochemistry and Biophysics **38**(3): 323-343.

Bencherif, S. A., A. Srinivasan, F. Horkay, J. O. Hollinger, K. Matyjaszewski and N. R. Washburn (2008). "Influence of the degree of methacrylation on hyaluronic acid hydrogels properties." Biomaterials **29**(12): 1739-1749.

Bian, L., D. Y. Zhai, R. L. Mauck and J. A. Burdick (2011). "Coculture of human mesenchymal stem cells and articular chondrocytes reduces hypertrophy and enhances functional properties of engineered cartilage." Tissue Eng Part A **17**(7-8): 1137-1145.

Bilir, B. M., D. Guinette, F. Karrer, D. A. Kumpe, J. Krysl, J. Stephens, L. McGavran, A. Ostrowska and J. Durham (2000). "Hepatocyte transplantation in acute liver failure." Liver Transpl **6**(1): 32-40.

Black, A. F., V. Hudon, O. Damour, L. Germain and F. A. Auger (1999). "A novel approach for studying angiogenesis: a human skin equivalent with a capillary-like network." Cell Biol Toxicol **15**(2): 81-90.

Butcher, J. T. and R. M. Nerem (2004). "Porcine aortic valve interstitial cells in three-dimensional culture: comparison of phenotype with aortic smooth muscle cells." J Heart Valve Dis **13**(3): 478-485; discussion 485-476.

Carmeliet, P. and R. K. Jain (2000). "Angiogenesis in cancer and other diseases." Nature **407**(6801): 249-257.

Carmeliet, P. and R. K. Jain (2000). "Angiogenesis in cancer and other diseases." Nature **407**(6801): 249-257.

Chang, S. C. and W. C. Vivian Yang (2013). "Hyperglycemia induces altered expressions of angiogenesis associated molecules in the trophoblast." Evid Based Complement Alternat Med **2013**: 457971.

Chiu, L. L. Y. and M. Radisic (2010). "Scaffolds with covalently immobilized VEGF and Angiopoietin-1 for vascularization of engineered tissues." Biomaterials **31**(2): 226-241.

Christen, T., M. L. Bochaton-Piallat, P. Neuville, S. Rensen, M. Redard, G. van Eys and G. Gabbiani (1999). "Cultured porcine coronary artery smooth muscle cells. A new model with advanced differentiation." Circ Res **85**(1): 99-107.

Chupa, J. M., A. M. Foster, S. R. Sumner, S. V. Madihally and H. W. T. Matthew (2000). "Vascular cell responses to polysaccharide materials:: in vitro and in vivo evaluations." Biomaterials **21**(22): 2315-2322.

Couchman, J. R. and C. A. Pataki (2012). "An Introduction to Proteoglycans and Their Localization." Journal of Histochemistry & Cytochemistry **60**(12): 885-897.

Crooks, C. A., J. A. Douglas, R. L. Broughton and M. V. Sefton (1990). "Microencapsulation of mammalian cells in a HEMA-MMA copolymer: effects on capsule morphology and permeability." J Biomed Mater Res **24**(9): 1241-1262.

Cucina, A., V. Borrelli, B. Randone, P. Coluccia, P. Sapienza and A. Cavallaro (2003). "Vascular endothelial growth factor increases the migration and proliferation of smooth muscle cells through the mediation of growth factors released by endothelial cells." Journal of Surgical Research **109**(1): 16-23.

Cunha, C., S. Panseri and S. Antonini (2010). "Emerging nanotechnology approaches in tissue engineering for peripheral nerve regeneration." Nanomedicine.

Cunha, C., S. Panseri and S. Antonini (2011). "Emerging nanotechnology approaches in tissue engineering for peripheral nerve regeneration." Nanomedicine **7**(1): 50-59.

Du, Y., E. Lo, S. Ali and A. Khademhosseini (2008). "Directed assembly of cell-laden microgels for fabrication of 3D tissue constructs." Proc Natl Acad Sci U S A **105**(28): 9522-9527.

Dunn, J. C., R. G. Tompkins and M. L. Yarmush (1991). "Long-term in vitro function of adult hepatocytes in a collagen sandwich configuration." Biotechnol Prog **7**(3): 237-245.

Dunn, J. C., M. L. Yarmush, H. G. Koebe and R. G. Tompkins (1989). "Hepatocyte function and extracellular matrix geometry: long-term culture in a sandwich configuration." FASEB J **3**(2): 174-177.

Fedorovich, N. E., J. R. De Wijn, A. J. Verbout, J. Alblas and W. J. Dhert (2008). "Three-d imensional fiber deposition of cell-laden, viable, patterned constructs for bone tissue printing." Tissue Eng Part A **14**(1): 127-133.

Ferdous, Z. and K. J. Grande-Allen (2007). "Utility and control of proteoglycans in tissue engineering." Tissue Eng **13**(8): 1893-1904.

Ferretti, A., E. Boschi, A. Stefani, S. Spiga, M. Romanelli, M. Lemmi, A. Giovannetti, B. Longoni and F. Mosca (2003). "Angiogenesis and nerve regeneration in a model of human skin equivalent transplant." Life Sci **73**(15): 1985-1994.

Fogler, S. (2005). Elements of Chemical Reaction Engineering (4th Edition), Prentice Hall**:** 814-832.

Fuster, M. M. and L. Wang (2010). "Endothelial heparan sulfate in angiogenesis." Prog Mol Biol Transl Sci **93**: 179-212.

Gaffney, J., S. Matou-Nasri, M. Grau-Olivares and M. Slevin (2010). "Therapeutic applications of hyaluronan." Mol Biosyst **6**(3): 437-443.

Gallagher, S. R. and P. R. Desjardins (2001). Quantitation of DNA and RNA with Absorption and Fluorescence Spectroscopy. Current Protocols in Protein Science, John Wiley & Sons, Inc.**:** A.4K.1–A.4K.21.

Gandhi, N. S. and R. L. Mancera (2008). "The structure of glycosaminoglycans and their interactions with proteins." Chem Biol Drug Des **72**(6): 455-482.

Geankoplis, C. J. (2003). Transport processes and separation process principles : (includes unit operations). Upper Saddle River, NJ, Prentice Hall Professional Technical Reference**:** 121-136.

Germain, L., P. Carrier, F. A. Auger, C. Salesse and S. L. Guerin (2000). "Can we produce a human corneal equivalent by tissue engineering?" Prog Retin Eye Res **19**(5): 497-527.

Graham, C. H., T. S. Hawley, R. G. Hawley, J. R. MacDougall, R. S. Kerbel, N. Khoo and P. K. Lala (1993). "Establishment and characterization of first trimester human trophoblast cells with extended lifespan." Exp Cell Res **206**(2): 204-211.

Hahn, M. S., L. J. Taite, J. J. Moon, M. C. Rowland, K. A. Ruffino and J. L. West (2006). "Photolithographic patterning of polyethylene glycol hydrogels." Biomaterials **27**(12): 2519-2524.

Hammouche, S., D. Hammouche and M. McNicholas (2012). "Biodegradable bone regeneration synthetic scaffolds: in tissue engineering." Curr Stem Cell Res Ther **7**(2): 134-142.

Hunt, N. and L. Grover (2010). "Cell encapsulation using biopolymer gels for regenerative medicine." Biotechnology Letters **32**(6): 733-742.

Iozzo, R. V. (2005). "Basement membrane proteoglycans: From cellar to ceiling." Nat Rev Mol Cell Biol **6**(8): 646-656.

Jain, M., Q. He, W. S. Lee, S. Kashiki, L. C. Foster, J. C. Tsai, M. E. Lee and E. Haber (1996). "Role of CD44 in the reaction of vascular smooth muscle cells to arterial wall injury." J Clin Invest **97**(3): 596-603.

Jain, R. K. (2003). "Molecular regulation of vessel maturation." Nat Med **9**(6): 685-693.

Jones, E. and X. Yang (2011). "Mesenchymal stem cells and bone regeneration: Current status." Injury **42**(6): 562-568.

Kasuya, J., R. Sudo, T. Mitaka, M. Ikeda and K. Tanishita (2011). "Hepatic stellate cell-mediated three-dimensional hepatocyte and endothelial cell triculture model." Tissue Eng Part A **17**(3-4): 361-370.

Kim, K., K. Ohashi, R. Utoh, K. Kano and T. Okano (2012). "Preserved liver-specific functions of hepatocytes in 3D co-culture with endothelial cell sheets." Biomaterials **33**(5): 1406-1413.

Kobayashi, N., M. Miyazaki, K. Fukaya, Y. Inoue, M. Sakaguchi, T. Uemura, H. Noguchi, A. Kondo, N. Tanaka and M. Namba (2000). "Transplantation of highly differentiated immortalized human hepatocytes to treat acute liver failure." Transplantation **69**(2): 202-207.

Kolset, S. O., K. Prydz and G. Pejler (2004). "Intracellular proteoglycans." Biochemical Journal **379**: 217-227.

L'Heureux, N., T. N. McAllister and L. M. de la Fuente (2007). "Tissue-engineered blood vessel for adult arterial revascularization." N Engl J Med **357**(14): 1451-1453.

L'heureux, N., S. Paquet, R. Labbe, L. Germain and F. A. Auger (1998). "A completely biological tissue-engineered human blood vessel." FASEB J. **12**(1): 47-56.

Langer, R. (2000). "Tissue engineering." Mol Ther **1**(1): 12-15.

Langer, R. and J. P. Vacanti (1993). "Tissue engineering." Science **260**(5110): 920-926.

LaPorta, T. F., A. Richter, N. A. Sgaglione and D. A. Grande (2012). "Clinical relevance of scaffolds for cartilage engineering." Orthop Clin North Am **43**(2): 245-254, vi.

Lawrence, B. D., J. K. Marchant, M. A. Pindrus, F. G. Omenetto and D. L. Kaplan (2009). "Silk film biomaterials for cornea tissue engineering." Biomaterials **30**(7): 1299-1308.

Leslie-Barbick, J. E., J. J. Moon and J. L. West (2009). "Covalently-Immobilized Vascular Endothelial Growth Factor Promotes Endothelial Cell Tubulogenesis in Poly(ethylene

glycol) Diacrylate Hydrogels." Journal of Biomaterials Science, Polymer Edition **20**(12): 1763-1779.

Leung, B. M. and M. V. Sefton (2010). "A modular approach to cardiac tissue engineering." Tissue Eng Part A **16**(10): 3207-3218.

Lin, S. V. and H. W. Matthew (2002). Microencapsulation methods: Glycosaminoglycans and Chitosan. Methods of Tissue Engineering. A. Atala and R. Lanza**:** 815-823.

Lin, X. and N. Perrimon (2002). "Developmental roles of heparan sulfate proteoglycans in *Drosophila*." Glycoconj J **19**(4): 363-368.

Lindahl, U. and M. Hook (1978). "Glycosaminoglycans and Their Binding to Biological Macromolecules." Annual Review of Biochemistry **47**(1): 385-417.

Livoti, C. M. and J. R. Morgan (2010). "Self-assembly and tissue fusion of toroid-shaped minimal building units." Tissue Eng Part A **16**(6): 2051-2061.

MacNeil, S. (2007). "Progress and opportunities for tissue-engineered skin." Nature **445**(7130): 874-880.

Mathieu, C., A. Chevrier, V. Lascau-Coman, G. E. Rivard and C. D. Hoemann (2013). "Stereological analysis of subchondral angiogenesis induced by chitosan and coagulation factors in microdrilled articular cartilage defects." Osteoarthritis Cartilage **21**(6): 849-859.

Matthew, H. W., S. O. Salley, W. D. Peterson and M. D. Klein (1993). "Complex coacervate microcapsules for mammalian cell culture and artificial organ development." Biotechnol Prog **9**(5): 510-519.

Matthew, H. W. T., J. Sternberg, P. Stefanovich, J. R. Morgan, M. Toner, R. G. Tompkins and M. L. Yarmush (1996). "Effects of plasma exposure on cultured hepatocytes: Implications for bioartificial liver support." Biotechnology and Bioengineering **51**(1): 100-111.

McCormick, S. M., S. G. Eskin, L. V. McIntire, C. L. Teng, C.-M. Lu, C. G. Russell and K. K. Chittur (2001). "DNA microarray reveals changes in gene expression of shear stressed human umbilical vein endothelial cells." Proceedings of the National Academy of Sciences **98**(16): 8955-8960.

McGuigan, A. P. and M. V. Sefton (2006). "Vascularized organoid engineered by modular assembly enables blood perfusion." Proc Natl Acad Sci U S A **103**(31): 11461-11466.

Meretoja, V. V., R. L. Dahlin, S. Wright, F. K. Kasper and A. G. Mikos (2013). "The effect of hypoxia on the chondrogenic differentiation of co-cultured articular chondrocytes and mesenchymal stem cells in scaffolds." Biomaterials **34**(17): 4266-4273.

Mironov, V., T. Boland, T. Trusk, G. Forgacs and R. R. Markwald (2003). "Organ printing: computer-aided jet-based 3D tissue engineering." Trends Biotechnol **21**(4): 157-161.

Miyagi, Y., L. L. Y. Chiu, M. Cimini, R. D. Weisel, M. Radisic and R.-K. Li (2011). "Biodegradable collagen patch with covalently immobilized VEGF for myocardial repair." Biomaterials **32**(5): 1280-1290.

Naito, H., I. Melnychenko, M. Didie, K. Schneiderbanger, P. Schubert, S. Rosenkranz, T. Eschenhagen and W. H. Zimmermann (2006). "Optimizing engineered heart tissue for therapeutic applications as surrogate heart muscle." Circulation **114**: I72-I78.

Nelson, C. M. and C. S. Chen (2003). "VE-cadherin simultaneously stimulates and inhibits cell proliferation by altering cytoskeletal structure and tension." Journal of Cell Science **116**(17): 3571-3581.

Nichol, J. W. and A. Khademhosseini (2009). "Modular Tissue Engineering: Engineering Biological Tissues from the Bottom Up." Soft Matter **5**(7): 1312-1319.

Nillesen, S. T. M., P. J. Geutjes, R. Wismans, J. Schalkwijk, W. F. Daamen and T. H. van Kuppevelt (2007). "Increased angiogenesis and blood vessel maturation in acellular collagen–heparin scaffolds containing both FGF2 and VEGF." Biomaterials **28**(6): 1123-1131.

Niven, R. K. (2002). "Physical insight into the Ergun and Wen & Yu equations for fluid flow in packed and fluidised beds." Chemical Engineering Science **57**(3): 527-534.

No da, Y., S. A. Lee, Y. Y. Choi, D. Park, J. Y. Jang, D. S. Kim and S. H. Lee (2012). "Functional 3D human primary hepatocyte spheroids made by co-culturing hepatocytes from partial hepatectomy specimens and human adipose-derived stem cells." PLoS One **7**(12): e50723.

Norrby, K. (2006). "Low-molecular-weight heparins and angiogenesis." APMIS **114**(2): 79-102.

Ohura, N., K. Yamamoto, S. Ichioka, T. Sokabe, H. Nakatsuka, A. Baba, M. Shibata, T. Nakatsuka, K. Harii, Y. Wada, T. Kohro, T. Kodama and J. Ando (2003). "Global Analysis of Shear Stress-Responsive Genes in Vascular Endothelial Cells." Journal of Atherosclerosis and Thrombosis **10**(5): 304-313.

Oostendorp, M., M. J. Post and W. H. Backes (2009). "Vessel growth and function: depiction with contrast-enhanced MR imaging." Radiology **251**(2): 317-335.

Orth, R. C., J. Bankson, R. Price and E. F. Jackson (2007). "Comparison of single- and dual-tracer pharmacokinetic modeling of dynamic contrast-enhanced MRI data using low, medium, and high molecular weight contrast agents." Magnetic Resonance in Medicine **58**(4): 705-716.

Padhani, A. R. (2002). "Dynamic contrast-enhanced MRI in clinical oncology: current status and future directions." J Magn Reson Imaging **16**(4): 407-422.

Paquet, C., D. Larouche, F. Bisson, S. Proulx, C. Simard-Bisson, M. Gaudreault, H. Robitaille, P. Carrier, I. Martel, L. Duranceau, F. A. Auger, J. Fradette, S. L. Guerin and L. Germain (2010). "Tissue engineering of skin and cornea Development of new models for in vitro studies." Aging, Cancer, and Age-Related Diseases: Common Mechanism? **1197**: 166-177.

Paquet, C., D. Larouche, F. Bisson, S. Proulx, C. Simard-Bisson, M. Gaudreault, H. Robitaille, P. Carrier, I. Martel, L. Duranceau, F. A. Auger, J. Fradette, S. L. Guerin and L. Germain (2010). "Tissue engineering of skin and cornea: Development of new models for in vitro studies." Ann N Y Acad Sci **1197**: 166-177.

Parekkadan, B., D. van Poll, Z. Megeed, N. Kobayashi, A. W. Tilles, F. Berthiaume and M. L. Yarmush (2007). "Immunomodulation of activated hepatic stellate cells by mesenchymal stem cells." Biochem Biophys Res Commun **363**(2): 247-252.

Prince, M. R. (1994). "Gadolinium-enhanced MR aortography." Radiology **191**(1): 155-164.

Prince, M. R., D. L. Narasimham, J. C. Stanley, T. L. Chenevert, D. M. Williams, M. V. Marx and K. J. Cho (1995). "Breath-hold gadolinium-enhanced MR angiography of the abdominal aorta and its major branches." Radiology **197**(3): 785-792.

Qing, C., C. Wei-ding and F. Wei-min (2011). "Co-culture of chondrocytes and bone marrow mesenchymal stem cells in vitro enhances the expression of cartilaginous extracellular matrix components." Braz J Med Biol Res **44**(4): 303-310.

Ravi, S. and E. L. Chaikof (2010). "Biomaterials for vascular tissue engineering." Regen Med **5**(1): 107-120.

Rotem, A., M. Toner, R. G. Tompkins and M. L. Yarmush (1992). "Oxygen uptake rates in cultured rat hepatocytes." Biotechnol Bioeng **40**(10): 1286-1291.

Sasisekharan, R., R. Raman and V. Prabhakar (2006). "Glycomics approach to structure-function relationships of glycosaminoglycans." Annu Rev Biomed Eng **8**: 181-231.

See, E. Y., S. L. Toh and J. C. Goh (2010). "Multilineage potential of bone-marrow-derived mesenchymal stem cell cell sheets: implications for tissue engineering." Tissue Eng Part A **16**(4): 1421-1431.

Seglen, P. O. (1979). "Hepatocyte suspensions and cultures as tools in experimental carcinogenesis." J Toxicol Environ Health **5**(2-3): 551-560.

Shi, C., Y. Zhu, X. Ran, M. Wang, Y. Su and T. Cheng (2006). "Therapeutic Potential of Chitosan and Its Derivatives in Regenerative Medicine." Journal of Surgical Research **133**(2): 185-192.

Steiner, D., F. Lampert, G. B. Stark and G. Finkenzeller (2012). "Effects of endothelial cells on proliferation and survival of human mesenchymal stem cells and primary osteoblasts." J Orthop Res **30**(10): 1682-1689.

Stringer, S. E. (2006). "The role of heparan sulphate proteoglycans in angiogenesis." Biochem Soc Trans **34**(Pt 3): 451-453.

Sun, H., Z. Qu, Y. Guo, G. Zang and B. Yang (2007). "In vitro and in vivo effects of rat kidney vascular endothelial cells on osteogenesis of rat bone marrow mesenchymal stem cells growing on polylactide-glycoli acid (PLGA) scaffolds." Biomed Eng Online **6**: 41.

Surapaneni, S., T. Pryor, M. D. Klein and H. W. Matthew (1997). "Rapid hepatocyte spheroid formation: optimization and long-term function in perfused microcapsules." ASAIO J **43**(5): M848-853.

Tao, J., Y. Sun, Q. G. Wang and C. W. Liu (2009). "Induced endothelial cells enhance osteogenesis and vascularization of mesenchymal stem cells." Cells Tissues Organs **190**(4): 185-193.

Theocharis, D. A., S. S. Skandalis, A. V. Noulas, N. Papageorgakopoulou, A. D. Theocharis and N. K. Karamanos (2008). "Hyaluronan and chondroitin sulfate proteoglycans in the supramolecular organization of the mammalian vitreous body." Connect Tissue Res **49**(3): 124-128.

Tiruvannamalai-Annamalai, R., D. R. Armant and H. W. Matthew (2014). "A glycosaminoglycan based, modular tissue scaffold system for rapid assembly of perfusable, high cell density, engineered tissues." PLoS One **9**(1): e84287.

Tiruvannamalai-Annamalai, R., D. R. Armant and H. W. T. Matthew (2014). "A Glycosaminoglycan Based, Modular Tissue Scaffold System for Rapid Assembly of Perfusable, High Cell Density, Engineered Tissues." PLoS ONE **9**(1): e84287.

Uygun, B. E., S. E. Stojsih and H. W. Matthew (2009). "Effects of immobilized glycosaminoglycans on the proliferation and differentiation of mesenchymal stem cells." Tissue Eng Part A **15**(11): 3499-3512.

VandeVord, P. J., H. W. Matthew, S. P. DeSilva, L. Mayton, B. Wu and P. H. Wooley (2002). "Evaluation of the biocompatibility of a chitosan scaffold in mice." J Biomed Mater Res **59**(3): 585-590.

Villalona, G. A., B. Udelsman, D. R. Duncan, E. McGillicuddy, R. F. Sawh-Martinez, N. Hibino, C. Painter, T. Mirensky, B. Erickson, T. Shinoka and C. K. Breuer (2010). "Cell-seeding techniques in vascular tissue engineering." Tissue Eng Part B Rev **16**(3): 341-350.

Vinatier, C., C. Bouffi, C. Merceron, J. Gordeladze, J. M. Brondello, C. Jorgensen, P. Weiss, J. Guicheux and D. Noel (2009). "Cartilage tissue engineering: towards a biomaterial-assisted mesenchymal stem cell therapy." Curr Stem Cell Res Ther **4**(4): 318-329.

Wang, Z. H., X. J. He, Z. Q. Yang and J. B. Tu (2010). "Cartilage tissue engineering with demineralized bone matrix gelatin and fibrin glue hybrid scaffold: an in vitro study." Artif Organs **34**(2): 161-166.

West, D. C. and S. Kumar (1989). "Hyaluronan and angiogenesis." Ciba Found Symp **143**: 187-201; discussion 201-187, 281-185.

Wu, P. K. and B. R. Ringeisen (2010). "Development of human umbilical vein endothelial cell (HUVEC) and human umbilical vein smooth muscle cell (HUVSMC) branch/stem structures on hydrogel layers via biological laser printing (BioLP)." Biofabrication **2**(1): -

Wybenga, D. R., J. Di Giorgio and V. J. Pileggi (1971). "Manual and Automated Methods for Urea Nitrogen Measurement in Whole Serum." Clinical Chemistry **17**(9): 891-895.

Yagi, H., B. Parekkadan, K. Suganuma, A. Soto-Gutierrez, R. G. Tompkins, A. W. Tilles and M. L. Yarmush (2009). "Long-term superior performance of a stem cell/hepatocyte device for the treatment of acute liver failure." Tissue Eng Part A **15**(11): 3377-3388.

Yang, B., Z. Yin, J. Cao, Z. Shi, Z. Zhang, H. Song, F. Liu and B. Caterson (2010). "In vitro cartilage tissue engineering using cancellous bone matrix gelatin as a biodegradable scaffold." Biomed Mater **5**(4): 045003.

Zhang, G. and L. J. Suggs (2007). "Matrices and scaffolds for drug delivery in vascular tissue engineering." Adv Drug Deliv Rev **59**(4-5): 360-373.

Zhang, Y., J. R. Venugopal, A. El-Turki, S. Ramakrishna, B. Su and C. T. Lim (2008). "Electrospun biomimetic nanocomposite nanofibers of hydroxyapatite/chitosan for bone tissue engineering." Biomaterials **29**(32): 4314-4322.

Zhu, Y., Y. Cao, J. Pan and Y. Liu (2010). "Macro-alignment of electrospun fibers for vascular tissue engineering." J Biomed Mater Res B Appl Biomater **92**(2): 508-516.

ABSTRACT

A BOTTOM-UP ASSEMBLY OF VASCULARIZED BIOARTIFICIAL CONSTRUCTS USING ECM BASED MICROSCALE MODULES

by:

RAMKUMAR TIRUVANNAMALAI ANNAMALAI

August 2014

Advisor: Dr. Howard Matthew

Major: Biomedical Engineering

Degree: Doctor of Philosophy

Tissue engineering aims to create functional biological tissues to treat diseases and damaged organs. A primary goal is to fabricate a 3D construct that can promote cell-cell interaction, extra cellular matrix (ECM) deposition and tissue level organization. Accomplishing these prerequisites with the currently available conventional scaffolds and fabrication techniques still remains a challenge. To reproduce the full functionality there is a need to engineer tissue constructs that mimic the innate architecture and complexity of natural tissues. The limited ability to vascularize and perfuse thick, cell-laden tissue constructs has hindered efforts to engineer complex tissues and organs, including liver, heart and kidney. The emerging field of modular tissue engineering aims to address this limitation by fabricating constructs from the bottom up, with the objective of recreating native tissue architecture and promoting extensive vascularization.

Here, we report the elements of a simple yet efficient method for fabricating vascularized tissue constructs by fusing biodegradable microcapsules with tunable interior environments. Parenchymal cells of various types, (i.e. trophoblasts, vascular smooth muscle cells, hepatocytes) were suspended in glycosaminoglycan (GAG) solutions (4%/1.5% chondroitin

sulfate/carboxymethyl cellulose, or 1.5 wt% hyaluronan) and encapsulated by forming chitosan-GAG polyelectrolyte complex membranes around droplets of the cell suspension. The interior capsule environment could be further tuned by blending collagen with or suspending microcarriers in the GAG solution. These capsule modules were seeded externally with vascular endothelial cells (VEC), and subsequently fused into tissue constructs possessing VEC-lined, inter-capsule channels. The microcapsules supported high density growth achieving clinically significant cell densities. Fusion of the endothelialized capsules generated 3D constructs with an embedded network of interconnected channels that enabled long-term perfusion in-vitro and accelerated neovascularization in-vivo. A prototype, engineered liver tissue, formed by fusion of hepatocyte-containing capsules exhibited urea synthesis rates and albumin synthesis rates comparable to standard collagen sandwich hepatocyte cultures. Our modular approach has the potential to allow rapid assembly of liver constructs with clinically significant cell densities, uniform cell distribution, and endothelialized, perfusable channels.

AUTOBIOGRAPHICAL STATEMENT

Academic Background:

- **Master of Science in Biomedical Engineering** , Fall 2007 – 09 **GPA 3.9/4.0**
  Wayne State University, Detroit, MI
  Advisor: *Professor Howard W.T. Matthew*
- **Bachelor of Technology in Biotechnology**, 2003 – 07 **80%**
  Bharathidasan University, Trichy, India (1st class/Distinction)

Honors/Awards:

- *Thomas C. Rumble Fellowship*, 2011-2012, Wayne State University, USA
- *Travel Award*: 2010, 2012 : Biomedical Engineering National Society (BMES), USA
- *Travel Award*: 2010,-13 : Wayne State University, Detroit, Michigan, USA

Publications in Peer Reviewed Journals:

1. *A glycosaminoglycan based, modular tissue scaffold system for rapid assembly of perfusable, high cell density, engineered tissues*, **T-Annamalai R,** Armant & Matthew, PLoS One, 2014. **9**(1):p. e84287

Publications to be submitted:

2. *Design and characterization of dynamic environment imposed to a three-dimensional engineered modular liver orgonoid in a perfusion bioreactor system.* **T-Annamalai, R**. and Matthew, H.W.T., To be Submitted to "PLoS ONE"
3. *Role of Glycosaminoglycans in Stem Cell Maintenance, Expansion and Differentiation*. **T-Annamalai, R.** and Matthew, H.W.T., submitted to "*ISRN Biomedical Engineering*"

National Affiliations:

- Biomedical Engineering Society (BMES)
- Society for Biomaterials (SFB)
- American Institute of Chemical Engineers (AIChE)
- Tissue Engineering and Regenerative Medicine (TERMIS)